

EPA-600/3-76-035

April 1976

THE GENERAL MOTORS/ENVIRONMENTAL PROTECTION AGENCY  
SULFATE DISPERSION EXPERIMENT

Selected EPA Research Papers

Edited by

R. K. Stevens

P. J. Lamothe

W. E. Wilson

J. L. Durham

T. G. Dzubay

Atmospheric Chemistry and Physics Division  
Environmental Sciences Research Laboratory  
Research Triangle Park, North Carolina 27711

U.S. ENVIRONMENTAL PROTECTION AGENCY  
OFFICE OF RESEARCH AND DEVELOPMENT  
ENVIRONMENTAL SCIENCES RESEARCH LABORATORY  
RESEARCH TRIANGLE PARK, NORTH CAROLINA 27711

## DISCLAIMER

This report has been reviewed by the Environmental Sciences Research Laboratory, U.S. Environmental Protection Agency, and approved for publication. Approval does not signify that the contents necessarily reflect the views and policies of the U.S. Environmental Protection Agency, nor does mention of trade names or commercial products constitute endorsement or recommendation for use.

## PREFACE

A. Paul Altshuller\*

An invitation was given to the U. S. Environmental Protection Agency (EPA) by General Motors (GM) to participate in a test track study at the GM Proving Ground to measure the effect on air quality of emissions from a fleet of catalyst equipped vehicles under controlled experimental conditions. These experiments would permit concentration levels to be measured which would not be attained for many years with actual vehicle populations on roadways. After discussions of experimental design, EPA investigators agreed to participate. The EPA participation was provided by the Environmental Sciences Research Laboratory, Research Triangle Park, North Carolina, using in-house, contractor, and grantee capabilities.

The test track facilities and drivers were provided by GM. The test fleet consisted of 352 low-mileage 1975 and 1976 catalyst equipped vehicles with air pumps provided by manufacturers. The roadway test section used was the 10-km north-south straightway. During October 1975 for about two hours a day, 350 vehicles were operated in packs on four lanes at a speed of 50 miles per hour. This mode of operation was equivalent to a traffic density of 5,460 vehicles an hour. The fuel used contained 0.03 weight percent sulfur. Eight vehicles were equipped by GM to emit sulfur hexafluoride as a tracer. A vehicle was equipped by EPA to measure particle sizes, sulfate, and sulfuric acid on the test track.

---

\*The author is Director of the Environmental Sciences Research Laboratory, U. S. Environmental Protection Agency, Research Triangle Park, North Carolina.

EPA investigators made measurements for sulfates, sulfuric acid, sulfur dioxide, ammonia, ammonium, and particle size at towers and in mobile laboratories at several distances just off the test track. GM investigators made measurements for sulfates, sulfur hexafluoride, and for meteorological parameters from towers in the median of the roadway and at various distances out to 113 m off the roadway. Vertical profile measurements also were made by both GM and EPA investigators from these towers.

The following conclusions can be drawn to date from the analysis of these experiments.

1. The particulate sulfur flow rate measured from the vehicle fleet was computed to correspond to about 12 percent of the fuel sulfur being emitted as particulate sulfur. A separate estimate by GM gave the average sulfate emission rate as 0.037 g/mile.
2. Most of the aerosol mass emitted from the air injection catalyst equipped vehicles was in the form of ultrafine sulfur aerosol in the size range between 0.01 and 0.1  $\mu\text{m}$ .
3. During the background measurements before and after operation of the vehicle fleet, this ultrafine sulfur-containing aerosol was almost completely absent. Instead the sulfur-containing aerosol was in the usual urban-regional fine aerosol range of 0.1 to 1  $\mu\text{m}$  particle sizes. This "aged" sulfur-containing aerosol was not acid, so it was probably in the form of neutralized ammonium sulfate.
4. The rate at which the ultrafine aerosols grew towards the size range of "aged" aerosols was very rapid. When the wind was across the test track (shorter aging time) most of the aerosol from the vehicles measured 30 m off the test track was ultrafine aerosol. When the wind blew down the test track (longer aging time) one-third to one-half of the aerosol shifted into the "aged" 0.1 to 1  $\mu\text{m}$  range.
5. Sulfuric acid was measured inside the equipped vehicle running on the test track. More than two-thirds of the sulfate emitted by the vehicles was measured as sulfuric acid 20 m off the test track.

6. One set of ammonium-to-sulfate ratios appeared to indicate substantial neutralization. However, the ratio corresponds to complete neutralization at all measurement points rather than being consistent with gradual neutralization. The ammonia measured was hardly sufficient to permit neutralization, particularly very rapid neutralization at the sampling site. This result appears to be associated with neutralization occurring from neutralization occurring as an artifact during sampling and storage and not during transport of sulfuric acid from the vehicles on the test track to the sampling sites. Other measurements of acidity and sulfuric acid indicate the presence of sulfuric acid off the roadway, but suggest partial or complete neutralization at 100 meters downwind.

7. Computations by the HIWAY model were compared with the sulfate concentrations reported by GM investigators. The computed values were in good agreement with the experimental values when the wind was nearly perpendicular to the roadway under unstable meteorological conditions and at wind speeds at or above 1 m/sec. The tracer data indicates the HIWAY model tends to overestimate by a factor of 2 to 3 for E and F stability conditions, and by a factor of nearly 2 for the parallel wind case.

8. Neither the off-roadway sulfate measurements nor the model results are likely to be accurate in predicting the commuter exposure during the parallel wind case.

## TABLE OF CONTENTS

	Page
Chemical Characterization of Aerosols Present During the General Motors Sulfate Dispersion Experiment . . . . .	1
P. J. Lamothe, T. G. Dzubay, R. K. Stevens	
Aerosol Size Distributions and Concentrations Measured During the General Motors Proving Ground Sulfate Study . . . . .	29
K. T. Whitby, D. B. Kittelson, B. K. Cantrell, N. J. Barsic, D. F. Dolan, L. D. Tarvestad, D. J. Nieken, J. L. Wolf, J. R. Wood	
Particulate Sulfur Emission Rate from a Simulated Freeway. . . . .	81
E. S. Macias, R. A. Fletcher, J. D. Husar, R. B. Husar	
Comparisons of Dispersion Model Estimates with Measured Sulfate Concentrations. . . . .	103
W. B. Petersen	
APPENDIX	
Chemical Speciation of Sulfate Emissions from Catalyst Equipped Automobiles under Ambient Conditions . . . . .	131
R. L. Tanner, L. Newman	

CHEMICAL CHARACTERIZATION OF AEROSOLS  
PRESENT DURING THE GENERAL MOTORS  
SULFATE DISPERSION EXPERIMENT

Paul J. Lamothe, Thomas G. Dzubay, Robert K. Stevens\*

ABSTRACT

*A study was conducted during October 1975 at General Motors Milford Proving Ground to measure the chemical properties of sulfate emissions from a fleet of catalyst equipped vehicles under controlled highway driving conditions. Aerosol samples were collected with dichotomous samplers and were analyzed by both X-ray fluorescence spectrometry and wet chemical procedures for strong acid, ammonium and sulfate content. In addition sulfuric acid, ammonia and SO<sub>2</sub> measurements were obtained during the study.*

*The peak sulfate concentrations ranged from 2.4 to 5.7  $\mu\text{g}/\text{m}^3$  above background and the sulfuric acid concentrations ranged from 1.1 to 5.4  $\mu\text{g}/\text{m}^3$ . Because significant amounts of sulfuric acid were measured at 20m downwind of the roadway, it can be assumed that the product of the ammonia concentration and transport time from the roadway to the monitor was insufficient to cause complete neutralization of the sulfuric acid.*

INTRODUCTION

To meet Federal and state emission standards, automobile manufacturers have incorporated catalytic converters in vehicle exhaust systems to reduce hydrocarbon and carbon monoxide emissions to acceptable levels. However, gasolines contain trace amounts of sulfur (typically 0.03% by weight) which are converted to SO<sub>2</sub> during the combustion process.

---

\*The authors are with the U. S. Environmental Protection Agency, Environmental Sciences Research Laboratory, Research Triangle Park, North Carolina 27711.

A portion of the  $\text{SO}_2$  is subsequently oxidized to sulfur trioxide by the catalytic converter and, ultimately, sulfuric acid aerosols result from the reaction of  $\text{SO}_3$  with water vapor. Several reports in the literature (refs. 1,2) have documented this combustion process and identified the emission products.

Very little information is available on the chemical and physical properties of sulfuric acid emitted from cars under actual highway conditions; likewise, there is no available information on how the  $\text{H}_2\text{SO}_4$  from the catalyst equipped cars is dispersed in the atmosphere.

In April 1975, General Motors proposed a study to measure sulfate exposures utilizing a fleet of catalyst equipped motor vehicles in controlled simulated highway driving conditions and under as many different meteorological situations as possible. At the request of General Motors, E.P.A. consented to participate in the study which was conducted at the G.M. Milford Proving Ground.

The study was conducted during October 1975 because several days with temperature inversions and low wind speeds were predicted for the test track site.

E.P.A.'s participation included:

1. operating eight dichotomous samplers upwind and downwind of the test track.
2. making sulfuric acid measurements inside one of the test vehicles, and
3. obtaining  $\text{H}_2\text{SO}_4$ , ammonia and  $\text{SO}_2$  measurements 20 meters downwind of the test track.

Samples collected with dichotomous sampler were analyzed by X-ray fluorescence spectrometry for elemental composition, and by the Brosset et al. (ref. 3) procedure for strong acid, ammonium, and sulfate content. A prototype sulfuric acid monitor, based on the low temperature volatilization technique described by Mudgett, et al. (ref. 4) was employed to obtain hourly measurements.

This report describes the results of these experiments and their relationship to data gathered by other investigators participating in the study.



## EXPERIMENTAL

### A. Test Conditions

The study was conducted during October 1975 at the General Motors Milford Proving Ground's 10km N-S straightaway. The test fleet consisted of 350 vehicles equipped with catalytic converters and air pumps. None of the converters used in the study had logged more than 10,000km (6,000 miles). During the two-hour experimental runs, the vehicles traveled at approximately 80kph (50 miles/hr), producing a traffic density of 5460 vehicles/hour. The gasoline used by the cars was unleaded and was blended to contain 0.03% sulfur by weight.

### B. Sampling

Airborne particulate samples were collected using 8 dichotomous samplers situated across the roadway as shown in figure 1. Each dichotomous sampler collects particles in two size ranges using the principle of virtual impaction. In this device, the air is sampled through an inlet at a height of 1.2m above the ground, passes through a jet and is deflected around a coarse particle receptor. Coarse particles ( $>3.5\mu\text{m}$ ), which are unable to follow the curving air stream, enter the coarse receptor and are collected on a  $1\mu\text{m}$  pore size Teflon (Fluoropore) filter. Fine particles ( $<3.5\mu\text{m}$ ) which move with the air stream are collected on a second Teflon filter. The flow rate through the fine particle filter is 13.7 l/min. The use of filters in a virtual impactor eliminates the particle bounce problem associated with the collection surfaces of a conventional impactor. A complete description of the dichotomous sampler has been reported by Stevens and Dzuby (ref. 5).

Samples were collected for 2 hours during the experiments on 10/1, 10/2, 10/3, 10/6, 10/8, 10/10, and 10/13 and were analyzed for

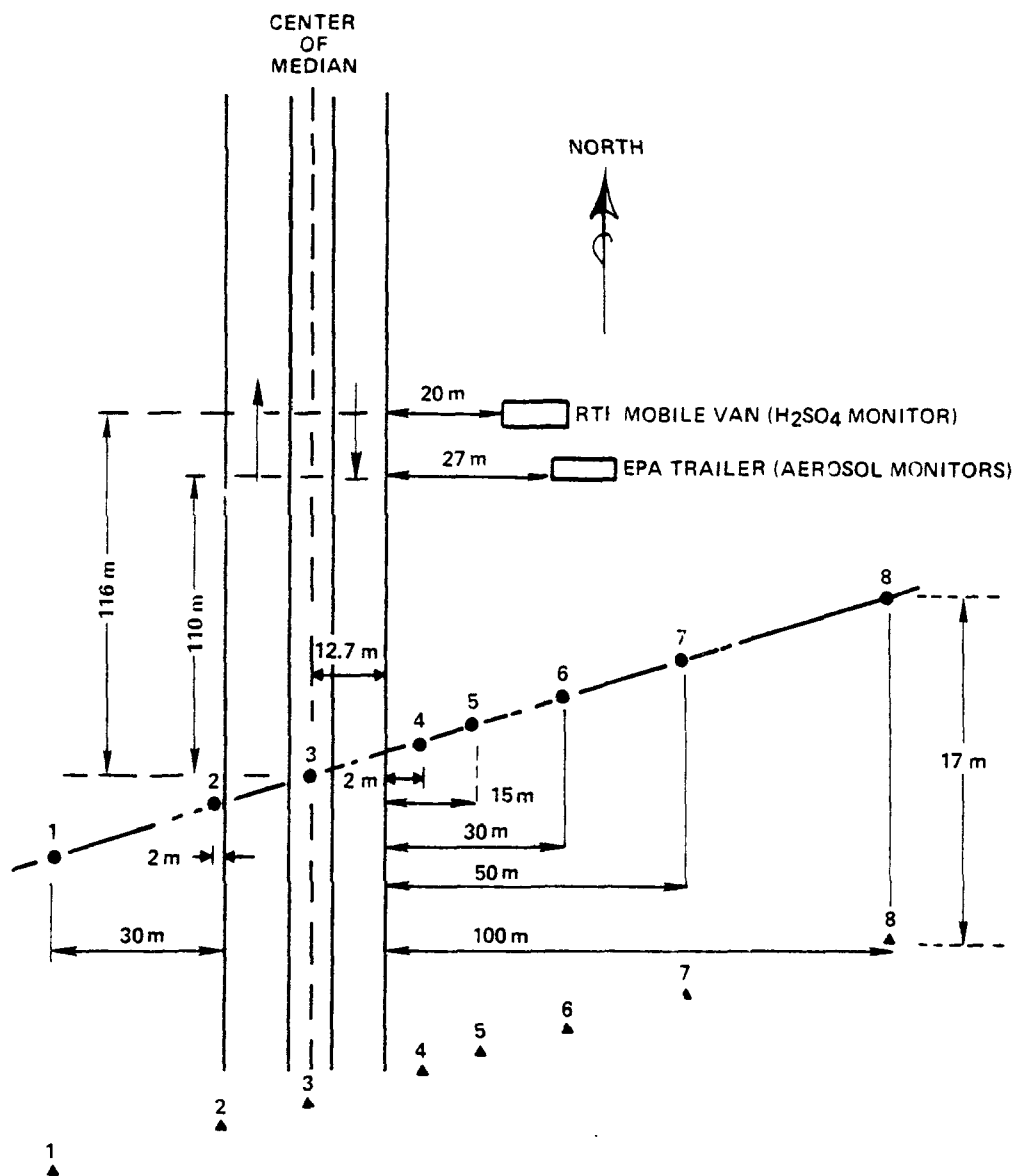


Figure 1 Location of EPA dichotomous samplers (circles), General Motors sampling towers (triangles), and mobile laboratories at General Motors Milford Proving Ground, October 1975.

total acidity, ammonium, soluble sulfate, and elemental composition as described below. In addition to the samples collected during the experimental runs, background samples were collected on 10/2, 10/3, 10/4, 10/8, 10/10 and 10/13. In an attempt to prevent neutralization of the collected sulfuric acid by ambient  $\text{NH}_3$ , all filter samples were stored in a desiccator containing  $\text{H}_3\text{PO}_3$  crystals.

Sulfuric acid ( $\text{H}_2\text{SO}_4$ ), ammonia ( $\text{NH}_3$ ) and sulfur dioxide ( $\text{SO}_2$ ) measurements were obtained using instruments located inside a mobile laboratory provided by Research Triangle Institute (figure 1). For the measurements, ambient air was drawn through a glass manifold system at 1,500 l/min with an inlet 20m east of the roadway at a vertical height of 3.3m.

Filter samples were also collected inside the passenger compartment of one of the cars in the test fleet (G.M. car 24-7). Samples were collected only during the two-hour driving cycles on the test track. The filter sampler in the car employed the use of a diffusion denuder to remove  $\text{NH}_3$  from the ambient aerosol prior to filter collection. The diffusion denuder consists of six pieces of glass tubing (6mm o.d. x 30cm long), mounted side by side in a lucite block, 5cm in length, having a common outlet leading to the filter holder. The inside walls of each section of glass tubing were coated with  $\text{H}_3\text{PO}_3$ , which is a highly effective absorbent for  $\text{NH}_3$ . Ambient air was drawn through the denuder and filter at a flow rate of 3.0 liters per minute using a vacuum pump and critical orifice. Under these conditions, the denuder is capable of reducing ammonia concentrations by a factor of 100, while passing particles having diameters of  $0.01\mu\text{m}$  and above.

#### C. Wet Chemical Procedures

Samples collected with dichotomous samplers were analyzed for strong acid ( $\text{H}^+$ ), ammonium ion ( $\text{NH}_4^+$ ), and soluble sulfate ( $\text{SO}_4^{=}$ ) in three successive steps by wet-chemical procedures similar to those developed by Dr. Cyrill Brosset at IVL, Swedish Water and Air Pollution Research Laboratory, Gothenburg, Sweden (ref. 3).

The procedure used here deviates from the Swedish procedure only in the filter extraction method. Gentle stirring has been replaced by ultrasonic action to insure quantitative extraction of the sample from the filter. Filter samples were placed sample-side-down into 6ml of extracting solution ( $5 \times 10^{-5} \text{M HClO}_4$ ), contained in a 30ml polypropylene bottle. The hydrophobic filter was submerged using a Teflon fork constructed from Teflon tubing, and subjected to ultrasonic action for twenty minutes using an electronic nebulizer (Mistogen Equipment Co., Oakland, Cal.).

A 5ml aliquot of extracted sample was first analyzed for  $\text{H}^+$  content by a Gran's (ref. 6) function potentiometric titration method. An antilog amplifier was used in conjunction with an electrometer and pH electrodes to produce a linear plot of  $\text{H}^+$  concentration versus NaOH titrant volume. Although the Gran function contains an additional titrant volume term, a simple antilog amplifier is sufficient to produce linearity because the titrant volume never exceeded a few percent of the sample volume.

The titrated sample was then diluted with 5ml of extracting solution, made basic with NaOH to convert ammonium ion to ammonia and analyzed for ammonia concentration using an ion-selective electrode (Orion Research Model 95-10). This electrode is a gas-detecting electrode and is consequently not affected by anions, cations and other dissolved species other than those which form complexes with ammonia. The electrode which was used gave a nerstian response to ammonia for concentrations between  $10^{-2} \text{M}$  and  $10^{-6} \text{M}$ .

Following the ammonium ion determination, the sample was passed through a column containing Dowex 50W-X8, 50-100 mesh ion exchange resin. A 3ml aliquot of the ion-exchanged sample was collected and subjected to sulfate analysis by the spectrophotometric-thorin method. This method is based on a single spectrophotometric determination of the loss of a known amount of barium-thorin complex caused by the precipitation of barium by sulfate in the sample. Since barium forms a complex with thorin which has a higher absorptivity than thorin at

520nm, it was possible to determine the amount of complex left in the solution and, therefore, how much sulfate was precipitated. Isopropanol was used in the method to reduce both the dissociation of the barium-thorin complex and the solubility product constant of barium sulfate.

An automatic pipetting system was used to simultaneously dispense measured volumes of barium ion, thorin and sample solutions to an optical absorption cell. The transmission was read and converted to absorbance from which the sulfate concentration in the sample was determined from a calibration curve.

From repetitive analyses of blank filters, the minimum detectable limits for  $H^+$  (as  $H_2SO_4$ ),  $NH_4^+$  and  $SO_4^{=}$  were determined to be 2, 0.1 and 3.5  $\mu g$  per filter, respectively.

#### D. X-ray Fluorescence Analysis

Measurement of the trace element composition was made using an energy dispersive X-ray fluorescence (XRF) spectrometer (refs. 7,8). In this device, an X-ray beam excites a secondary fluorescer which in turn excites the sample with its nearly monochromatic characteristic X-rays (ref. 7). Elements in the sample with atomic numbers in the ranges 13-20 and 19-38 were analyzed using titanium and molybdenum secondary fluorescers, respectively. This range of elements includes sulfur, which was analyzed using the titanium fluorescer. In addition, lead was analyzed using the molybdenum fluorescer.

The fluorescent X-ray lines emitted by the sample were detected using a lithium drifted silicon detector with electronic collimation to enhance the signal above background (ref. 7). Because of a very compact geometrical arrangement between X-ray tube, fluorescer, sample and detector, an adequate count rate was obtained with X-ray tube power dissipation of less than 15w. The total irradiation time for each sample using both fluorescers was 10 minutes. A minicomputer was used to control the operation of the X-ray spectrometer allowing the samples to be analyzed in batches of 20 without operator intervention.

The elemental concentrations were determined by the minicomputer. For the analysis, it was assumed that an observed X-ray spectrum was

a superposition of the characteristic X-ray spectra for each individual element in the sample. Individual spectra of 30 pure element standards were accumulated and stored in the computer memory. These individual spectra as well as a stored clean filter background spectrum were compared with the unknown aerosol spectrum using a stripping procedure to determine the concentration of each element (ref. 7). By making a judicious choice of the order in which the elements were stripped, the problem of interfering  $K\alpha$  and  $K\beta$  X-ray lines was largely eliminated. Although there is a potential interference between the M X-rays from lead and the K X-rays from sulfur, it was insignificant in this study because of the low lead concentrations. Nonetheless, a correction for the interference was made on the basis of the lead concentration measures for the sample using the interference-free  $L\beta$  X-ray from lead and the X-ray ratio of intensities for the lead M and  $L\beta$  X-rays. The ratio was determined using a thin lead film.

The analyzer was calibrated using thin single-element concentration standards according to a procedure developed by Giaque et al. (ref. 9). These standards consisted of vacuum evaporated foils obtained from Micromatter Co. (Seattle, Wash.). The elemental deposits were uniform across the 37mm diameter of each standard and ranged in mass per unit area from 10-150  $\mu\text{g}/\text{cm}^2$ . They were known to an accuracy of  $\pm 10\%$  or better. For airborne particles uniformly deposited onto the membrane filters, the concentration (in  $\mu\text{g}/\text{cm}^2$ ) of a specific element on the filter was determined by comparison of the observed count rate with that of the known foil of the same element.

From these considerations, it is estimated that for elements well above the detection limit, the 1- $\sigma$  accuracy for X-ray analysis of elements with atomic numbers above 20 (Ti and heavier) is  $\pm 10\%$ . For the lighter elements, the energies of the characteristic X-rays are sufficiently low that self-absorption can take place within the larger collected particles and within the filter media for fine particles that penetrate into the filter. Self-absorption corrections were made, using a procedure developed by Dzubay and Nelson (ref. 10).

For sulfur, almost all of the mass appears in the fine particle range. Hence, attenuation effects within the individual particles are negligible (ref. 10). A correction factor of  $0.85 \pm 0.10$  was used to account for a slight penetration of the aerosol into the filter and the associated attenuation of the outgoing sulfur X-rays. The overall  $2\sigma$  accuracy for measuring sulfur is estimated to be  $\pm 15\%$ .

#### E. Sulfuric Acid Monitor

The sulfuric acid monitor (figure 2) used during the G.M. Sulfate Dispersion Experiment was fabricated for EPA by Cabot Corporation (Billerica, Mass.). The monitoring method involves filter collection of ambient particulate matter followed by separation of the sulfuric acid from the other sulfur containing particles by low temperature ( $130^\circ\text{C}$ ) volatilization. The amount of sulfuric acid volatilized is determined using a Meloy flame photometric sulfur gas analyzer.

The monitor is a combination sampler/analyzer; therefore, two filters are in active use by the monitor at all times. Ambient air flows through one of the filters to collect the particulate matter and simultaneously, dry air heated to  $130^\circ\text{C}$  flows through the other filter to volatilize the sulfuric acid collected during the previous cycle. The instrument has been designed to mechanically move the filters back and forth between the ambient and dry air flows, rather than use valves for switching the air flows between filters. Moving the filters eliminates the need for both passing ambient air as well as clean air through the same parts of the apparatus and having aerosol-laden ambient air pass through a valve on the way to the filter.

Fluoropore ( $0.5\ \mu\text{m}$  pore size) filters were chosen for use in the monitor because they have been found to have greater than 99% collection efficiency for particles ranging from  $0.03$  to  $1\ \mu\text{m}$  in diameter (ref. 11). Also, Fluoropore filters were the most inert to sulfuric acid of all the filter substrates tested.

# SULFURIC ACID MONITOR

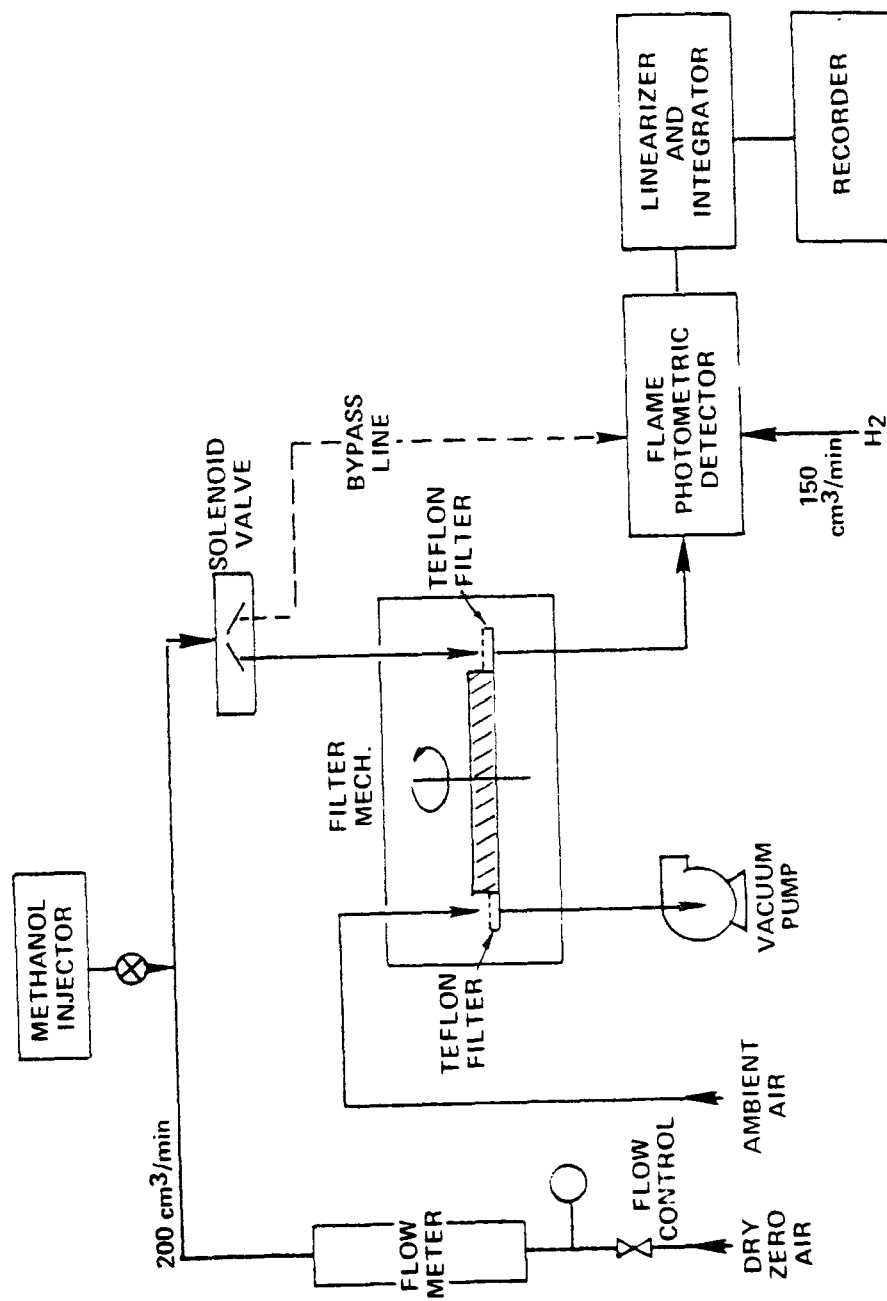


Figure 2 Schematic Diagram of Sulfuric Acid Monitor



Ammonium sulfate aerosols ( $0.07\text{ }\mu\text{m}$  mean diameter) do not cause interferences at volatilization temperatures below  $140^{\circ}\text{C}$  (ref. 12). The detection limit of the monitor is  $0.8\text{ }\mu\text{g H}_2\text{SO}_4/\text{m}^3$  for a one hour sample collection period, and the precision of the method is  $\pm 20\%$ .

#### F. Ammonia Monitor

The monitor used to measure atmospheric ammonia ( $\text{NH}_3$ ) concentrations was a Thermo Electron model 14T analyzer. This monitor uses as its measurement technique a combination of the chemiluminescent  $\text{NO}-\text{O}_3$  reaction and three reaction chambers in combination with one photomultiplier tube and two thermal converters.

The sample stream is split into three portions as it enters the analyzer. One portion goes to the  $\text{NO}$  reaction chamber where it mixes with ozone for a direct  $\text{NO}$  measurement. A second portion of the sample passes through a low temperature ( $250^{\circ}\text{C}$ ) molybdenum converter, where  $\text{NO}_2$  is converted to  $\text{NO}$ , into the second reaction chamber for a measurement of  $\text{NO}_x$  ( $\text{NO} + \text{NO}_2$ ). A third portion of the sample passes through a high temperature ( $800^{\circ}\text{C}$ ) stainless steel converter, which converts  $\text{NO}_2$  and  $\text{NH}_3$  to  $\text{NO}$ , into the third reaction chamber for a "total nitrogen" measurement ( $\text{NO} + \text{NO}_2 + \text{NH}_3$ ). The use of a spinning chopper wheel allows a single photomultiplier tube to sequentially measure the chemiluminescence produced in each chamber.

The monitor determines the ammonia concentration by electronically subtracting the  $\text{NO}_x$  signal from the "total nitrogen" signal. Periodically the sample stream is allowed to flow through a  $50\text{cm} \times 0.50\text{m}$   $\text{H}_3\text{PO}_3$  coated glass tube. This tube removes the  $\text{NH}_3$  but not the  $\text{NO}_x$ ; therefore, the  $\text{NO}_x$  signal should be equal to the  $\text{NO}_x + \text{NH}_3$  signal when the tube is in stream. If the  $\text{NO}_x + \text{NH}_3$  signal is larger than the  $\text{NO}_x$ , some species other than  $\text{NH}_3$  is producing an anomalous response. During these studies, no evidence of an interference of this type was observed.

The analyzer exhibits a linear response for ammonia concentrations ranging from 2ppb to 1000ppb. The minimum detectable limit of the monitor is 2ppb  $\text{NH}_3$  when the  $\text{NO}_x$  concentration is below 50ppb.

During periods of higher  $\text{NO}_x$  concentrations, the detection limit for ammonia is 5ppb.

#### G. Sulfur Dioxide (total Sulfur) Monitor

A flame photometric sulfur gas analyzer (Melo Model SA 185) was used for the measurements of gaseous sulfur ( $\text{SO}_2$ ). A continuous measurement of sulfur concentration is possible with the monitor since the sample is brought through a filter directly to the detector where it burns in a hydrogen rich flame. Light emitted from the chemiluminescent sulfur reaction passes through a 394nm interference filter into a photomultiplier tube. The dynamic range of this monitor usually ranges from 10 to 1000ppb; however, during this study, the instrument was calibrated to give a 100ppb full scale response. This special calibration was performed to achieve a 2ppb detection limit for the monitor.

### RESULTS

The results of the X-ray fluorescence (XRF) analyses are shown in tables 1 and 2. Table 1 shows the elemental analyses of the 4 and 24-hour background runs to indicate which chemical elements were present in this geographic location. Table 2 shows the sulfate concentrations deduced from the XRF analyses assuming that all of the observed particulate sulfur is in the form of sulfate. For the background runs, there is agreement among the amounts of sulfur collected in each of the eight dichotomous samplers. According to table 2, the standard deviation for the background sulfur values never exceeds 15% and is generally 10% or less.

As an independent test of the XRF measure for sulfate, five of the fine particle filter samples were analyzed during a barium chloranilate procedure, and the results are shown in table 3. The two methods agree well, except at low sulfate concentrations where small deviations in the experimental values produce large percentage deviations.

Table 1. Elemental Concentrations in Nanograms per m<sup>3</sup> for  
Background Runs determined by X-ray Fluorescence  
Analysis of Dichotomous Sample<sup>a,b</sup>.

Date	Start Time	Duration Minutes	Size Range	Si	S	Cl	Ca	Fe	Ni	Zn	Br	Pb
10/2/75	1030	240	Fine coarse	<350 <350	495 <140	<120 <120	<140 <140	<70 <70	<43 <43	<30 <30	<25 <25	<50 <50
10/3/75	1030	220	Fine coarse	<400 <400	650 <100	<130 <130	<150 <150	<70 <70	<43 <43	<30 <30	<25 <25	<50 <50
10/4/75	1400	1400 <sup>a</sup>	Fine coarse	275 1740	2500 130	<20 <20	180 1400	200 420	<7 <7	43 <6	69 10	330 <8
10/8/75	1015	240	Fine coarse	800 3000	3900 250	<120 <120	170 1500	460 980	<43 <43	190 <30	120 20	380 <50
10/10/75	1030	1440 <sup>a</sup>	Fine coarse	215 510	1000 50	<20 <20	92 450	77 95	<7 <7	23 <5	35 4	110 <8
10/13/75	1015	240	Fine coarse	<500 <600	2500 <100	<120 <120	<160 210	<80 <80	<43 <43	<30 <30	22 <25	<50 <50

<sup>a</sup>In comparison with the 4-hour runs, the detection limits for the 24-hour runs are reduced by a factor of 6.

<sup>b</sup>For the two 24-hour background runs, the following elements were below the indicated detection limits for both the fine and coarse particles:

P	Ti	V	Cr	Mn	Co	Cu	As	Se	Rb	Sr	Pt	Hg
<50	<30	<20	<15	<15	<9	<20	<20	<5	<4	<7	<10	<9

Table 2. Concentration of Sulfate Deduced From X-Ray Fluorescence Analysis of Dichotomous Samples at Various Site Locations. The Site Locations are Identified in Figure 1.

Date	Start Hours	Nominal Duration Min.	Wind Direction	Status <sup>a</sup>	fine particle sulfate at each site, $\mu\text{g}/\text{m}^3$										coarse particles	
					1	2	3	4	5	6	7	8	Ave. <sup>b</sup>	o <sup>b</sup>	All Sites, $\mu\text{g}/\text{m}^3$	
10/1/75	1340	120	285°	CR	2.1	2.3	3.5	4.5	(1.6)	3.2	2.9	2.6			<0.5	
10/2/75	0745	120	330°	CR	0.5	1.4	2.8	3.6	2.6	1.6	1.2	1.0			<0.4	
10/2/75	1030	240	335°	BG	1.5	1.5	1.4	1.5	1.9	1.4	1.6	1.3	1.5	0.2	<0.3	
10/3/75	0745	120	223°	CR	2.5	2.6	5.2	6.9	5.7	5.0	4.1	3.4			<0.4	
10/3/75	1030	220	230°	BG	2.0	2.0	2.1	2.2	2.0	2.0	2.0	2.0	2.0	0.1	<0.3	
10/4/75	1400	1440		BG	7.8	7.8	7.2	7.2	6.5	6.9	7.6	7.0	7.3	0.4	<0.4	
10/6/75	0745	120	250°	CR	9.7	11.2	12.8	14.9	13.5	12.4	12.2	11.6			<0.6	
10/8/75	0745	120	69°	CR	12.0	14.9	13.2	10.7	10.1	9.9		10.1			<0.6	
10/8/75	1015	240	80°	BG	11.7	12.9	13.1	12.3	12.4	12.5		12.8	12.5	0.5	<0.8	
10/10/75	0745	120	245°	CR	15.5	16.0	20.0	21.2	17.7	15.7		15.9			<0.5	
10/10/75	1030	1440	210°	BG	3.0	3.0	2.8	2.9						2.9	<0.3	
10/13/75	0745	120	195°	CR	8.2	8.4	11.3	13.5	10.4	10.1	9.4	8.5			<0.6	
10/13/75	1015	240	220°	BG	7.6	8.7	8.4	9.4					8.5	0.8	<0.4	

<sup>a</sup>Status: CR-catalyst run; BG-background

<sup>b</sup>Mean and standard deviation for fine particles in background runs.

<sup>c</sup>Void because of gross inconsistency with other sites.

Table 3. Comparison Between EPA Sulfate Measurements using X-Ray Fluorescence and Barium Chloranilate Methods

SAMPLE	TYPE	DATE	START TIME	DURATION MINUTES	a XRF S <sub>2</sub> $\mu\text{g}/\text{cm}^2$	b XRF SO <sub>4</sub> $\mu\text{g}$	c BCA SO <sub>4</sub> $\mu\text{g}$	d BCA XRF
8201	background	10/2/75	1030	240	0.25	5.0	7.8	1.56
9401	background	10/4/75	1400	1440	7.81	155	141	0.91
801	catalyst run	10/8/75	0745	116	0.97	19.2	17.9	0.93
9801	background	10/8/75	1015	244	1.90	37.7	34.2	0.91
7301	background	10/13/75	1015	240	1.26	24.9	24.8	1.00

<sup>a</sup>Flow rate =  $13.7 \pm 0.3$  L/min; deposit area =  $6.6 \text{ cm}^2$ .

<sup>b</sup>Calibrated using Micromatter CuS foil and assuming an attenuation factor of 0.85 for the aerosol in the filter.

<sup>c</sup>XRF sulfate is assumed to be total sulfur multiplied by 3.

<sup>d</sup>Analysis by Dr. S. Tejada

Table 4. Colorimetric Determination of Soluble Sulfate Ion ( $\text{SO}_4^{2-}$ )  
by the Spectrophotometric-Thorin Method.

DATE	START HOURS	DURATION MINUTES	STATUS <sup>a</sup>	FINE PARTICLE SULFATE AT EACH SITE, $\mu\text{g}/\text{m}^3$							
				1	2	3	4	5	6	7	8
10/3/75	0745	120	CR	4.0 $\pm$ .6	3.6 $\pm$ .6	5.7 $\pm$ .6	5.8 $\pm$ .6	6.0 $\pm$ .6	6.2 $\pm$ .6	5.6 $\pm$ .6	4.9 $\pm$ .6
10/3/75	1030	240	BG	1.6 $\pm$ .3	1.3 $\pm$ .3	2.8 $\pm$ .3	2.3 $\pm$ .3	2.1 $\pm$ .3	2.0 $\pm$ .3	2.1 $\pm$ .3	2.2 $\pm$ .3
10/4/75	1400	1440	BG	ND <sup>b</sup>	7.1 $\pm$ .2	7.1 $\pm$ .2	6.6 $\pm$ .2	7.3 $\pm$ .2	6.5 $\pm$ .2	6.3 $\pm$ .2	6.9 $\pm$ .2
10/6/75	0745	120	CR	9.8 $\pm$ .6	11.2 $\pm$ .6	12.9 $\pm$ .6	14.7 $\pm$ .6	13.4 $\pm$ .6	12.6 $\pm$ .6	12.1 $\pm$ .6	11.6 $\pm$ .6
10/8/75	0745	120	CR	ND	14.3 $\pm$ .6	13.2 $\pm$ .6	10.4 $\pm$ .6	10.2 $\pm$ .6	9.8 $\pm$ .6	ND	12.2 $\pm$ .6
10/10/75	0745	120	CR	14.9 $\pm$ .6	15.1 $\pm$ .6	19.0 $\pm$ .6	19.4 $\pm$ .6	18.4 $\pm$ .6	16.6 $\pm$ .6	ND	16.6 $\pm$ .6
10/10/75	1030	1440	BG	2.6 $\pm$ .2	2.7 $\pm$ .2	2.7 $\pm$ .2	2.7 $\pm$ .2	ND	ND	ND	ND
10/13/75	0745	120	CR	8.8 $\pm$ .6	8.6 $\pm$ .6	11.6 $\pm$ .6	12.4 $\pm$ .6	11.0 $\pm$ .6	11.2 $\pm$ .6	11.2 $\pm$ .6	9.5 $\pm$ .6
10/13/75	1015	240	BG	ND	8.4 $\pm$ .3	8.6 $\pm$ .3	9.0 $\pm$ .3	ND	ND	ND	ND

<sup>a</sup>CR - Catalyst Run; BG = Background

<sup>b</sup>ND - No Data Available

Table 5. Potentiometric Determination of Ammonium Ion ( $\text{NH}_4^+$ ) using the Orion 95-10 Ion Selectric Electrode.

DATE	START HOURS	DURATION MINUTES	STATUS <sup>a</sup>	FINE PARTICLE $\text{NH}_4^+$ AT EACH SITE, $\mu\text{g}/\text{m}^3$							
				1	2	3	4	5	6	7	8
10/3/75	0745	120	CR	0.70 $\pm$ .03	0.74 $\pm$ .02	1.67 $\pm$ .07	2.00 $\pm$ .08	1.80 $\pm$ .07	1.61 $\pm$ .06	1.32 $\pm$ .05	1.10 $\pm$ .04
10/3/75	1030	240	BG	0.51 $\pm$ .02	0.57 $\pm$ .02	0.58 $\pm$ .02	0.54 $\pm$ .02	0.47 $\pm$ .02	0.50 $\pm$ .02	0.52 $\pm$ .02	0.59 $\pm$ .02
10/4/75	1400	1440	BG	ND <sup>b</sup>	2.38 $\pm$ .09	2.27 $\pm$ .09	2.13 $\pm$ .09	2.05 $\pm$ .08	2.08 $\pm$ .08	2.32 $\pm$ .09	2.40 $\pm$ .09
10/6/75	0745	120	CR	2.5 $\pm$ .1	3.0 $\pm$ .1	3.8 $\pm$ .1	4.5 $\pm$ .2	4.0 $\pm$ .2	3.6 $\pm$ .1	3.3 $\pm$ .1	3.1 $\pm$ .1
10/8/75	0745	120	CR	ND	4.1 $\pm$ .2	3.8 $\pm$ .1	2.8 $\pm$ .1	2.6 $\pm$ .1	2.6 $\pm$ .1	ND	2.6 $\pm$ .1
10/10/75	0745	120	CR	4.5 $\pm$ .2	4.2 $\pm$ .2	5.6 $\pm$ .2	6.1 $\pm$ .2	5.6 $\pm$ .2	4.8 $\pm$ .2	ND	5.0 $\pm$ .2
10/10/75	1030	1440	BG	0.83 $\pm$ .03	0.87 $\pm$ .03	0.91 $\pm$ .03	0.86 $\pm$ .03	ND	ND	ND	ND
10/13/75	0745	120	CR	2.4 $\pm$ .1	2.6 $\pm$ .1	3.5 $\pm$ .1	3.8 $\pm$ .1	3.3 $\pm$ .1	3.0 $\pm$ .1	2.9 $\pm$ .1	2.7 $\pm$ .1
10/13/75	1015	240	BG	2.6 $\pm$ .1	2.7 $\pm$ .1	2.8 $\pm$ .1	ND	ND	ND	ND	ND

<sup>a</sup>CR - Catalyst Run; BG = Background

<sup>b</sup>ND = No Data Available

Table 6. Ammonia, Sulfur Dioxide and Sulfuric Acid Data Obtained In The Research Triangle Institute Mobile Laboratory Located 20m East of the Roadway.

Date	Time	Wind Direction	Wind Speed KM/HR	NH <sub>3</sub> µg/m <sup>3</sup>	SO <sub>2</sub> µg/m <sup>3</sup>	(ppb)	H <sub>2</sub> SO <sub>4</sub> Ambient Air µg/m <sup>3</sup>	H <sub>2</sub> SO <sub>4</sub> Car Sample µg/m <sup>3</sup>
10/1/75	11:00-13:00			ND <sup>a</sup>	ND		<0.4	
"	13:40-15:40	285°	15	ND	7.9	(3)	1.9+0.4	2.1+0.4
"	16:40			ND	<5.2	(<2)	ND	
10/2/75	6:30-7:30			1.4	ND	(2)	<0.8	
"	7:40-9:40	330°	13	1.4	ND	(2)	1.1+0.2	1.2+0.2
"	13:00-14:00			1.4	ND	(2)	<0.8	
10/3/75	6:30-7:30			1.4	ND	(2)	<0.8	
"	7:40-9:40	222°	8	2.1	5.2	(3)	2.7+0.5	3.3+0.7
"	13:00-14:00			2.1	<5.2	(3)	<0.8	
10/6/75	6:30-7:30			2.1	<5.2	(3)	ND	
"	7:40-9:40	250°	6	2.8	7.9	(4)	ND	ND
"	13:00-14:00			2.1	<5.2	(3)	ND	
10/8/75	6:30-7:30			1.4	5.2	(2)	<0.8	
"	7:40-9:40	69°	9	<3.5	141.6	(<5)	<0.8	2.5+0.5
"	13:00-14:00			1.4	15.7	(2)	<0.8	
10/10/75	6:30-7:30			1.4	<5.2	(2)	<0.8	
"	7:40-9:40	245°	6	<3.5	7.3	(<5)	5.4+1.1	2.9+0.6
"	13:00-14:00			<1.4	<5.2	(<2)	<0.8	
10/13/75	6:30-7:30			ND	5.2	(2)	<0.8	ND
"	7:40-9:40	195°	12	<3.5	10.5	(<5)	2.4+0.5	
"	13:00-14:00			<1.4	15.7	(<2)	<0.8	

<sup>a</sup>ND = No Data Available



For both background and catalyst runs, results for sulfate and ammonium analysis of the dichotomous samples were given in tables 4 and 5. For the catalyst runs, figures 3-5 show a comparison of the XRF and Thorin sulfate in the fine particle fraction ( $<3.5\mu\text{m}$ ) from the dichotomous samplers at various locations across the roadway. Figures 3-5 also show the sulfate determinations made by General Motors personnel for their sampler located 0.5m above the ground. The G.M. samplers collect a total aerosol sample without size fractionation, and the G.M. samples were analyzed for safety by a barium chloronilate procedure.

Table 6 shows the  $\text{NH}_3$  and  $\text{SO}_2$  gas and the  $\text{H}_2\text{SO}_4$  data obtained at the RTI van. It also shows the  $\text{H}_2\text{SO}_4$  data for the car operated on the test track.

#### DISCUSSION

From the XRF data in tables 1 and 2, one can conclude that of the elements with atomic numbers above 12, sulfur is the element in greatest abundance in the fine particle fraction for both the catalyst and background runs. Typically, at least 90% of the sulfur occurs in the fine particle fraction. For the fine particle fraction, there is considerable agreement between sulfate deduced from the XRF analysis and the sulfate measurements by the Thorin method as shown in figures 3-5. For each run, the sulfate concentration peaked at the downwind edge of the roadway.

The sulfate deduced from the XRF analysis of the fine particle fraction is compared with the total sulfate measured by General Motors personnel in figures 3-5. Agreement is greater for the far upwind and downwind sites, where background sulfate predominates, than near the roadway where the automotive component predominates. Figures 3-5 also show that the peak sulfate concentrations observed by G.M. always exceed those observed by EPA.

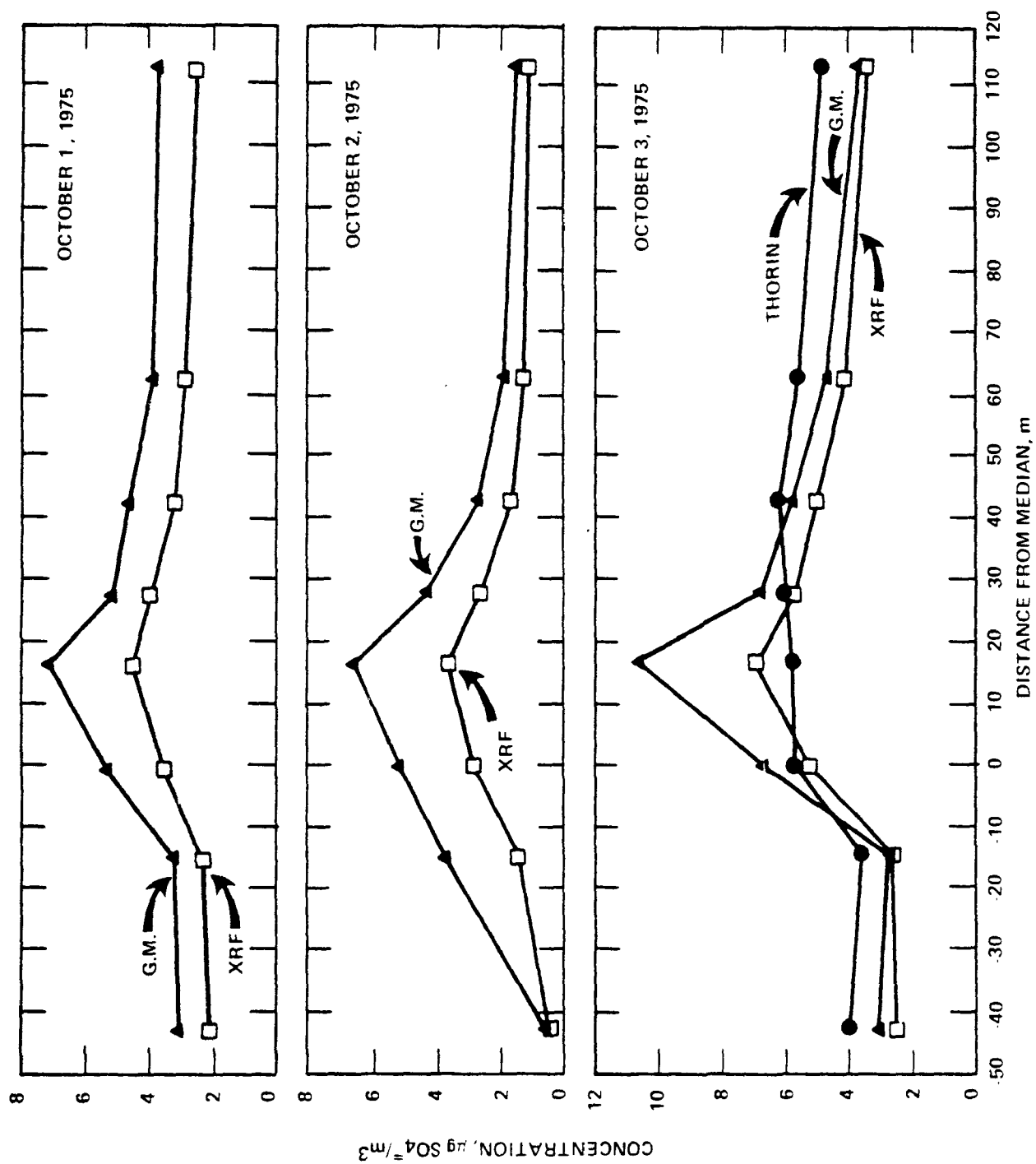


Figure 3 Sulfate concentrations measured on October 1, 2 and 3, 1975 at General Motors Milford Proving Ground.

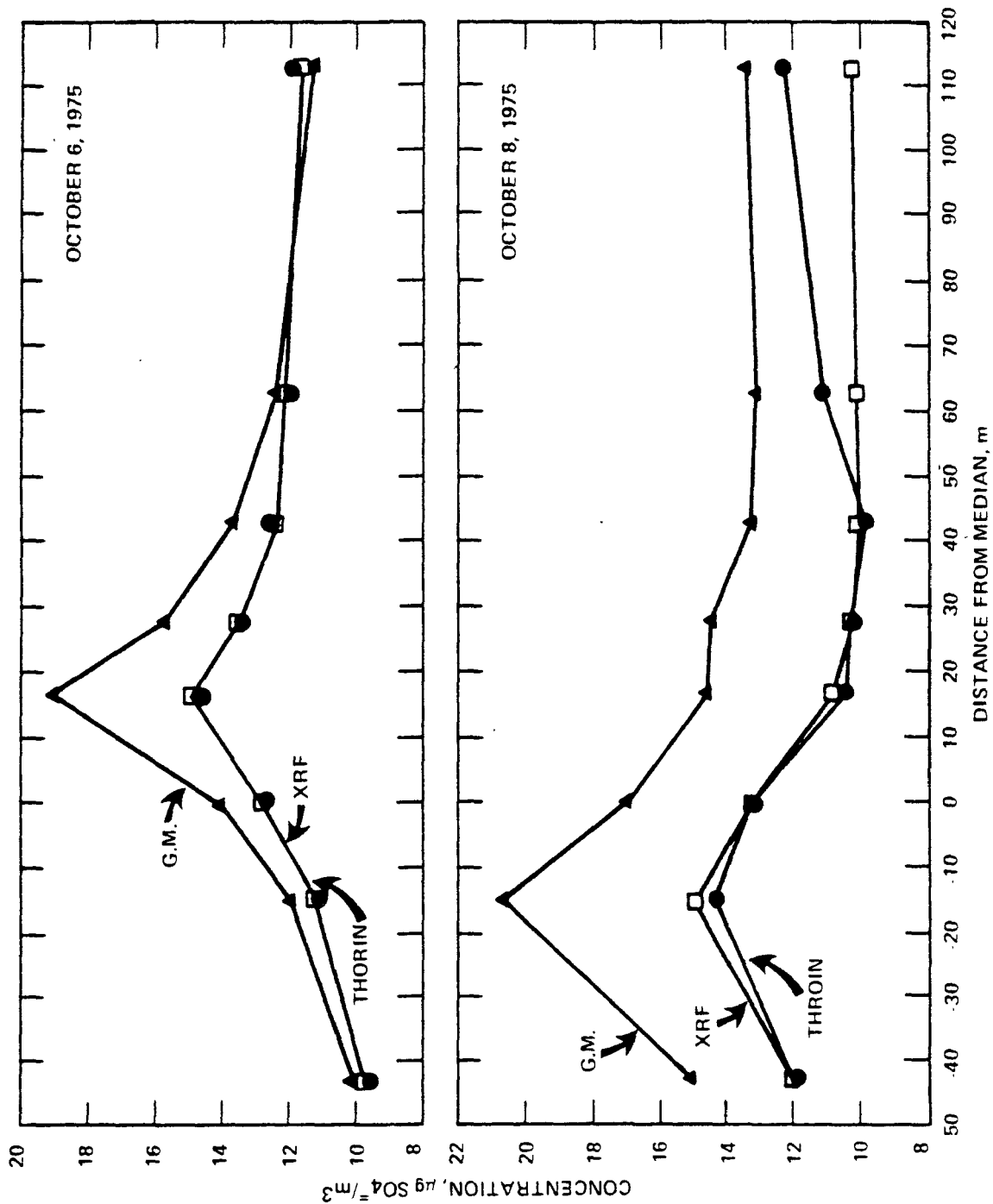


Figure 4 Sulfate concentrations measured on October 6 and 8, 1975 at General Motors Milford Proving Ground.

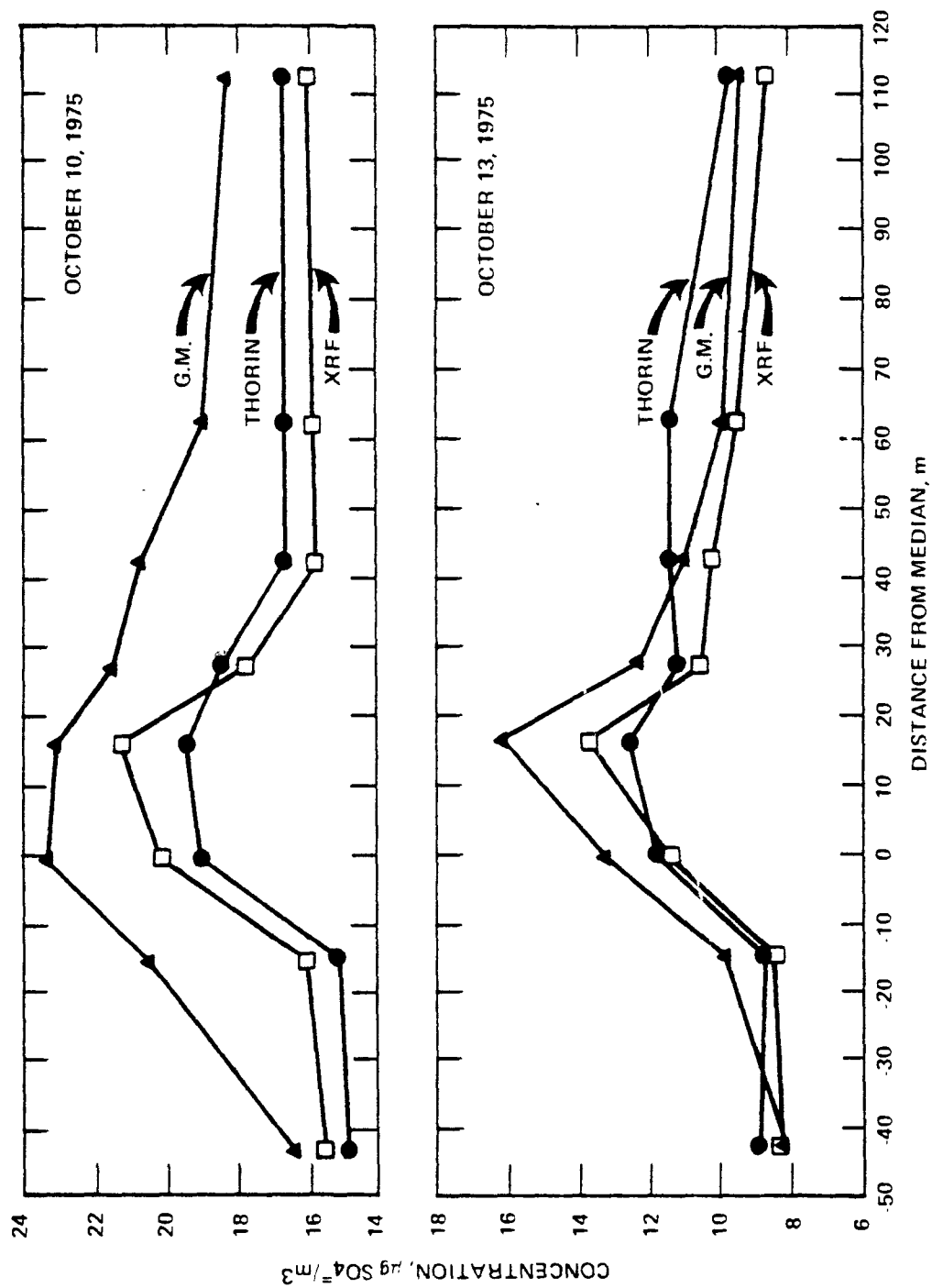


Figure 5 Sulfate concentrations measured on October 10 and 13, 1975 at General Motors Milford Proving Ground.

Differences in sampler locations and the handling of samples could account for the above discrepancies. First of all, the inlets for the G.M. samplers were at a height of 0.5m, which is closer to the height of the exhaust pipes than the 1.2m height of the inlets of the EPA dichotomous samplers. Secondly, the storage of the EPA samples in the ammonia free atmosphere of the desiccator containing  $\text{H}_3\text{PO}_3$  may have enhanced losses of collected sulfuric acid by volatilization. This contention is supported by recent observations made by Cabot Corporation (ref. 12) which indicates 20% losses of sulfuric acid from filter samples stored for one month in a nitrogen atmosphere at room temperature. The Cabot samples were prepared by collecting a laboratory generated sulfuric acid aerosol having a mean diameter of  $0.07\ \mu\text{m}$ . Since the data obtained by the University of Minnesota personnel indicated that the aerosols produced by the vehicles during this study had diameters between  $0.02$  and  $0.03\ \mu\text{m}$ , the sulfuric acid volatility problem was potentially more severe than the Cabot results indicate. It is unlikely that the higher sulfate concentrations observed by G.M. are associated with the fact that the G.M. sampler did not discriminate between fine and coarse particles, since less than 10% of the total particulate sulfate is associated with particles greater than  $3.5\ \mu\text{m}$  in diameter.

The particulate ammonium data, given in table 5, indicate an apparent downwind increase in ammonium concentration. These increases could result from  $\text{H}_2\text{SO}_4 - \text{NH}_3$  reactions occurring both prior to and during the sample collections. Moreover, the possibility of neutralization reactions occurring after the samples were collected cannot be unequivocally ruled out because the samples were exposed to laboratory air for periods up to 48 hours during XRF analyses.

The downwind increases in  $\text{NH}_4^+$  concentrations above background ( $\Delta\text{NH}_4^+$ ) relative to the downwind increases in  $\text{SO}_4^{=}$  ( $\Delta\text{SO}_4^{=}$ ) indicate that the sulfate present on the fine particle filters was in the form of  $(\text{NH}_4)_2\text{SO}_4$ . However, the  $\Delta\text{NH}_4^+/\Delta\text{SO}_4^{=}$  ratios do not vary as a function of downwind distance from the roadway. If sulfuric acid aerosols emitted

by the vehicles were neutralized by ambient  $\text{NH}_3$ , one would expect to observe increases in the  $\Delta\text{NH}_4^+/\Delta\text{SO}_4^-$  ratio at increasing distances from the roadway. The lack of variation in  $\Delta\text{NH}_4^+/\Delta\text{SO}_4^-$  ratio is a further indication of filter sample degradations caused by  $\text{H}_2\text{SO}_4$  volatilization and/or neutralization during sampling and storage.

Sulfuric acid, ammonia and sulfur dioxide data are given in table 6. The  $\text{SO}_2$  results indicate that during the driving cycles, the vehicles added less than  $8 \mu\text{g}/\text{m}^3$  (3 ppb) of  $\text{SO}_2$  to the background at 20m downwind. The highest concentration of  $\text{SO}_2$  observed during the study occurred on 10/8/75 when the wind was out of the East (Detroit). Occasional spikes of  $\text{SO}_2$  as high as  $78 \mu\text{g}/\text{m}^3$  (30 ppb) were recorded during periods when cars were idling on the track.

Ambient air sulfuric acid concentrations ranged from  $1.1 \pm 0.2$  to  $5.4 \pm 1.1 \mu\text{g}/\text{m}^3$  on those days when the wind was out of the West (10/1, 10/2, 10/3, 10/10, 10/13). It should be noted in table 6 that the highest  $\text{H}_2\text{SO}_4$  concentration occurred on 10/10 when the wind speed was relatively low.

Sulfuric acid determinations made from samples collected inside the car ranged from  $1.2 \pm 0.2$  to  $3 \pm 0.7 \mu\text{g}/\text{m}^3$ . These samples were collected under normal driving conditions, usually with car windows rolled up and heater on. To preclude the possibility of interferences from tobacco smoke, a nonsmoking driver was selected for these tests.

Comparisons of the EPA sulfuric acid data, obtained 20m east of the roadway at a height of 3.3m, and the G.M. sulfate data are presented in table 7. The sulfate data in table 7 is the average of the four 1/2 hour measurements obtained by G.M. at a site 15m east of the roadway at a height of 3.5m. The  $\Delta\text{SO}_4^-$  values were obtained by subtracting the upwind background sulfate concentrations from the 15m downwind data. The data in table 7 shows that for four out of five days, more than 70% of the sulfate emitted by the vehicles was in the form of  $\text{H}_2\text{SO}_4$  at 20m downwind. It is felt that the anomalously high result ( $\text{H}_2\text{SO}_4/\text{SO}_4^-$ ) obtained for 10/10/75 was due to the  $\pm 20\%$ .

Table 7. Comparison of Sulfuric Acid and Sulfate Results.

Date	Wind Direction	Wind Speed km/h	Background Sulfate <sup>a</sup> μg/m <sup>3</sup>	Downwind Sulfate <sup>b</sup> μg/m <sup>3</sup>	$\Delta\text{SO}_4^=$ μg/m <sup>3</sup>	$\text{H}_2\text{SO}_4^c/\Delta\text{SO}_4^=$
10/1/75	285 <sup>0</sup>	15	2.75	4.51	1.76	1.08
10/2/75	330 <sup>0</sup>	13	0.59	3.49	2.90	0.38
10/3/75	335 <sup>0</sup>	8	2.27	5.53	3.26	0.83
10/10/75	245 <sup>0</sup>	6	17.19	20.65	3.46	1.56
10/13/75	195 <sup>0</sup>	12	7.55	10.85	3.30	0.73

<sup>a</sup>Background sulfate values are averages of four 1/2 hour measurements obtained by G.M. 30m West of the roadway at a height of 3.5m.

<sup>b</sup>Downwind sulfate values are averages of four 1/2 hour measurements obtained by G.M. 15m East of the roadway at a height of 3.5m.

<sup>c</sup>The  $\text{H}_2\text{SO}_4$  values are from the ambient air data in Table 6.

experimental uncertainty in the  $\text{H}_2\text{SO}_4$  value and differences in the sulfate concentration between the two sites.

It was intended that the strong acid titration procedure would provide an independent measurement to be compared with the results obtained using the Sulfuric Acid Monitor. However, these acid titration measurements exhibited an unexpectedly large amount of variability which rendered the measurements useless for determining the acid properties of the aerosol in the present study. For the background runs when the cars were not on the roadway the standard deviation of the strong acid determinations was  $6.7 \mu\text{g}$  of  $\text{H}_2\text{SO}_4$  per filter. This corresponds to a  $2\sigma$  detection limit of  $8.2 \mu\text{g}$  of  $\text{H}_2\text{SO}_4$  per  $\text{m}^3$  for a two hour sampling period at a flow rate of  $13.71/\text{min}$ . The strong acid titration data were inconclusive because the limit of detection for the titration measurements was larger than the highest value measured by the Sulfuric Acid Monitor.

## CONCLUSIONS

From the data presented in this paper, the following conclusions are drawn:

1. More than 90% of the total particulate sulfur mass, present in both background and vehicle aerosols, is associated with particles less than  $3.5 \mu\text{m}$  in diameter.
2. Sulfuric acid was not detected during any of the background measurements, but was always detected whenever the catalyst equipped vehicles were operating on the roadway upwind of the sulfuric acid monitor. On four of the five days when sulfuric acid was detected, more than 70% of the sulfate emitted by the vehicles was in the form of  $\text{H}_2\text{SO}_4$  at 20m downwind of the roadway.
3. For the samples collected while the vehicles were operating on the roadway, sulfur was the only element which had concentrations detectable above the background. There was no detectable change from the background concentrations for silicon, calcium, iron, bromine, lead and other elements as analyzed by X-ray fluorescence.



4. Because significant amounts of sulfuric acid were measured at 20m downwind of the roadway, it can be assumed that the product of the ammonia concentration and transport time from the roadway to the monitor was insufficient to cause complete neutralization of the sulfuric acid.

#### ACKNOWLEDGMENTS

The authors are grateful to General Motors Corporation for their hospitality during the experiment, and to S. Cadle and J. Heuss of the G.M. Research Staff for providing the preliminary data. We are indebted to C. Kistler, S. Scott, W. Shepherd, J. Stikeleather and S. Tejada for performing the wet chemical analyses, and to R. Baumgardner for obtaining the ammonia and sulfur dioxide measurements. Comments on our data provided by R. Hammerle and W. Pierson are also gratefully acknowledged.

#### REFERENCES

1. R. L. Bradow and J. B. Moran, "Sulfate Emissions from Catalyst Cars - a Review," SAE Paper No. 750090, Detroit, Michigan (Feb. 1975).
2. W. R. Pierson, R. H. Hammerle and J. T. Kimmer, "Sulfuric Acid Aerosol Emissions from Catalyst-Equipped Engines," SAE Paper No. 740287, Detroit, Michigan (Feb. 1974).
3. C. Brosset, C. Askne and M. Ferm, IVL Publication No. B-157, Gothenburg (1973).
4. P. S. Mudgett, L. W. Richards and J. R. Roehrig, in "Analytical Methods Applied to Air Pollution Measurement," R. K. Stevens and W. F. Herget, Eds., Ann Arbor Science Publ., Inc., pp 85-105 (1974).
5. R. K. Stevens and T. G. Dzubay, *IEEE Trans. Nucl. Sci.*, NS-22, 849 (1975).
6. G. Gran, *Analyst*, 661 (1952).
7. F. S. Goulding and J. M. Jaklevic, "X-Ray Fluorescence Spectrometer for Airborne Particulate Monitoring," EPA Report No. R2-73-182 (April 1973).

8. T. G. Dzubay and R. K. Stevens, "Ambient Air Analysis with Dichotomous Sampler and X-Ray Fluorescence Spectrometer," *Environ. Sci. & Technol.*, 9, 663 (1975).
9. R. D. Giauque, F. S. Goulding, J. M. Jaklevic, and R. H. Pehl, *Anal. Chem.*, 45, 671 (1973).
10. T. G. Dzubay and R. O. Nelson, in "Advances in X-Ray Analysis," Vol. 18, p. 619, W. L. Pickels, C. S. Barrett, C. O. Ruud, Eds., 1974.
11. B.Y.H. Liu and K. W. Lee, "Efficiency of Membrane and Nuclepore Filters for Submicrometers Aerosols," *Environ. Sci. & Technol.*, (1976) (In Press).
12. P. Fowler, "Second Stage Development of An Automated Field Sulfuric Acid Sampler and Analyzer," Technical Narrative No. 7, EPA Contract 68-02-2338, Feb. 1976.

AEROSOL SIZE DISTRIBUTIONS AND CONCENTRATIONS MEASURED  
DURING THE GENERAL MOTORS PROVING GROUNDS SULFATE STUDY

K. T. Whitby, D. B. Kittelson, B. K. Cantrell,  
N. J. Barsic, D. F. Dolan, L. D. Tarvestad  
D. J. Nieken, J. L. Wolf, and J. R. Wood\*

*Abstract*

*In October 1975, General Motors (GM) and the Environmental Protection Agency (EPA) conducted a freeway simulation study at the GM Milford Proving Ground, using only catalytic converter equipped cars. During the study, nearly 900 aerosol size distribution measurements were made, both on the test track and close by. At the same time, sulfate measurements were also being made by other experimental teams.*

*Background aerosol volume size distributions measured during the test show three distinct modes with mean sizes of approximately 0.03, 0.24 and 6.0  $\mu\text{m}$ . Aerosol distributions measured during the run, both on and off the track, also exhibit three modes. Those at 0.24 and 6.0 remain essentially unchanged while the smaller mode contains much more volume than the background aerosol, and now has a mean size of about 0.02  $\mu\text{m}$ . The exact amount of the increase in volume of the smallest mode is greatly dependent on meteorological parameters. This was seen to vary from about 20  $\mu\text{m}^3/\text{cm}^3$ , when the wind direction was parallel to the track, to 2  $\mu\text{m}^3/\text{cm}^3$ , when the wind blew across the track. On days when the wind was parallel to the track, approximately 1/3 to 1/2 of the increase in volume during the test runs over background appeared in the 0.24  $\mu\text{m}$  mode. No*

---

\*The authors are with the Particle Technology Laboratory, Mechanical Engineering Department, University of Minnesota, Minneapolis, Minnesota.

significant increase for the 0.24  $\mu\text{m}$  mode was noted when the wind blew across the track. Together, these facts would indicate that the primary aerosol volume emission of the catalytic converter equipped cars is of a mean size of 0.02 $\mu\text{m}$ . We can also conclude that the increase in volume in the size 0.1 to 1  $\mu\text{m}$  is primarily caused by coagulation of the small diameter aerosol, and that this occurs in the atmosphere after emission and dilution of the tailpipe.

#### SUMMARY

In October 1975, GM and the Environmental Protection Agency conducted a freeway simulation study at the GM proving ground. Only catalytic converter equipped cars were used in order to provide base line data for modeling future freeway conditions. Particular effort was directed towards estimating sulfate content of the aerosols produced. During the study, the University of Minnesota Particle Technology Laboratory, under EPA sponsorship and in collaboration with EPA personnel, made measurements of *in situ* aerosol size distributions and concentrations at the test track site using the large EPA mobile laboratory and a specially equipped automobile prepared by the University. Approximately 450 size distributions were measured with the EPA trailer and 450 with the car.

The most significant results and conclusions from the University of Minnesota portion of the work are presented in this report. Because of the short time available for data analysis, it has not been possible to make intercomparisons with other investigators' results or to investigate the more subtle aspects of our own data.

1. Difference distributions calculated by taking the difference between the average size distributions during the test and the average of the background distributions before and after the test, suggest that most of the aerosol volume (and hence mass) is emitted in the size range smaller and 0.1  $\mu\text{m}$ .

The geometric mean diameter by volume of this nuclei mode aerosol is about  $0.02\text{ }\mu\text{m}$ . Figure 4 compares with the background the size distribution of aerosol measured during the test period of GM run 15. It is clear that the size distribution of the accumulation mode (center mode) and coarse particle mode (right hand mode) have not changed significantly. It is also clear that the nuclei mode (left hand mode) is contributed almost entirely by the cars on the roadway.

Figure 10 shows car difference distributions calculated for a typical day having a cross wind (GM 10), and for the day having the highest concentration (GM 12) when the wind was exactly parallel to the roadway. This figure shows that when the wind is across the roadway (short aging time) most of the aerosol contributed by the cars is smaller than  $0.1\text{ }\mu\text{m}$ . When the wind is along the roadway (long aging time) coagulation transfers 1/3 to 1/2 of the aerosol to the mode in the  $0.1$  to  $1\text{ }\mu\text{m}$  size range. Therefore, under the conditions of the test, most of the aerosol growth from the  $0.01$  to  $0.1$  size range to the  $0.1$  to  $1\text{ }\mu\text{m}$  range occurs in the atmosphere after emission and dilution at the tail pipe.

2. The highest contributions observed on the track by the car and at the trailer were during GM Run #12 on October 23 when the average wind direction during the run was  $181^\circ$  or the wind was blowing almost directly down the track. The pertinent aerosol volumes are given in table 1.

3. Although it is not possible to calculate comparable averages over all of the data for the trailer and the car, the arithmetic average over the 12 GM runs for which data can be averaged for the trailer gives means of  $1.49$  and  $0.63\text{ }\mu\text{m}^3/\text{cm}^3$  for  $\Delta\text{VAN}$  and  $\Delta\text{VAC}$  respectively or a total fine particle contribution of  $2.12$ . A somewhat comparable average for  $\Delta\text{VAN}$  for the car is  $7.00\text{ }\mu\text{m}^3/\text{cm}^3$ .

4. When the wind was blowing almost directly across the track, values of VAN measured in the car were significantly higher on the downwind side. For example, for GM Run #4, wind W-SW, the average

values on the downwind leg near the track were  $VAN = 10.1$ , compared to an upwind value of  $4.32 \mu\text{m}^3/\text{cm}^3$ .

5. The geometric mean diameter by volume for the aerosol as emitted by the cars is about  $0.02 \mu\text{m}$ . When the wind was directly parallel to the roadway as it was for GM 12, coagulation increased the mean size to about  $0.04$  and significant mass was transferred to the accumulation mode.

Table 1  
Typical and High Average Aerosol Volumes  
Measured by the Car and EPA Trailer.

Measurement	Background		Test		Difference		
	$VAN^a$	$VAC^b$	$VAN$	$VAC$	$\Delta VAN$	$\Delta AFP^c$	$VFP^c$
Trailer GM 7	.07	10.2	1.96	10.4	1.88	0.2	2.08
Car GM 7	.05	8.43	4.56	9.79	4.51	1.36	5.87
Trailer GM 12	.10	17.2	2.35	18.3	2.25	1.10	3.35
Car GM 12	.15	12.2	22.9	26.6	22.7	14.4	37.1

<sup>a</sup>Volume in the Aitken Nuclei mode,  $\mu\text{m}^3/\text{cm}^3$

<sup>b</sup>Volume in accumulation mode,  $\mu\text{m}^3/\text{cm}^3$

<sup>c</sup>Fine particle volume =  $\Delta VFP = \Delta VAN + \Delta VAC$ ,  $\mu\text{m}^3/\text{cm}^3$

Note that the total fine particle volume (VFP) contribution for GMP #12 is  $3.35 \mu\text{m}^3/\text{cm}^3$  at the trailer and  $37.1 \mu\text{m}^3/\text{cm}^3$  as measured by the car on the inside lane. Run 7, which is probably more typical, is shown for comparison. During Run 7, the wind was from the southwest, at  $197^\circ$ .

## INTRODUCTION

This is a report describing the origin, degree of participation, and most important results from the participation of the University of Minnesota's Particle Technology Laboratory in the EPA/General Motors proving ground study of sulfate aerosols during October 1975 at the General Motors Milford Test Track.

The origin and original purpose of the project is described in General Motors Research Publication GMR-1967 (ref. 1). We were invited by EPA to participate in order to use the University of Minnesota's and EPA's aerosol size distribution measuring equipment to measure size distributions on the test track and near the track.

To make measurements on the track, we installed the aerosol analyzing equipment that has been used aboard an aircraft for plume studies in St. Louis in a 1975 Ford four-door sedan. Basically, this car system consisted of an automated bag sampler, a condensation nuclei counter, an electrical aerosol analyzer, an optical particle counter, and an automatic sulfur sampler (refs. 2,3). With this system, *in situ* aerosol size distributions from .0075 to about 6 microns could be measured, and filtered samples could be acquired on glass fiber filter media for subsequent analysis by Husar at Washington University.

The large EPA mobile laboratory was also operated jointly by EPA and University of Minnesota personnel about 30m east of the test track. Its *in situ* aerosol analyzing system, some gas analyzers, and filter samplers, were operated. The EPA laboratory acquired data during all of the GM runs; however, the car began taking data with GM PG Run #4.

#### LABORATORY VEHICLES USED IN THE GENERAL MOTORS SULFATE DISPERSION EXPERIMENT

##### A. Instrumented Automobile

The automobile used for this study was a 1975 Ford Custom 500 four-door sedan with a catalytic converter equipped 351 CID engine. Original seats were removed from the car and replaced by two bucket seats: one for the driver and one in the right rear for an observer. This provided space for the instruments in the right front and the sample bag assembly in the left rear, as shown in figure 1.

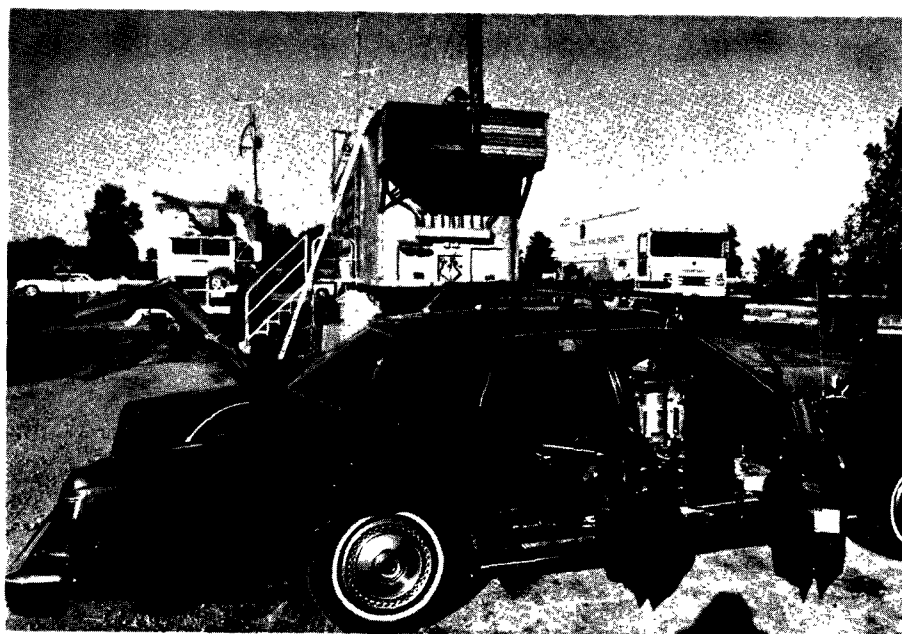


Figure 1 EPA trailer (center background) and special aerosol measurement car at the experimental site during the GMPG experiment. Note the sampling inlets projecting from the top of the car.

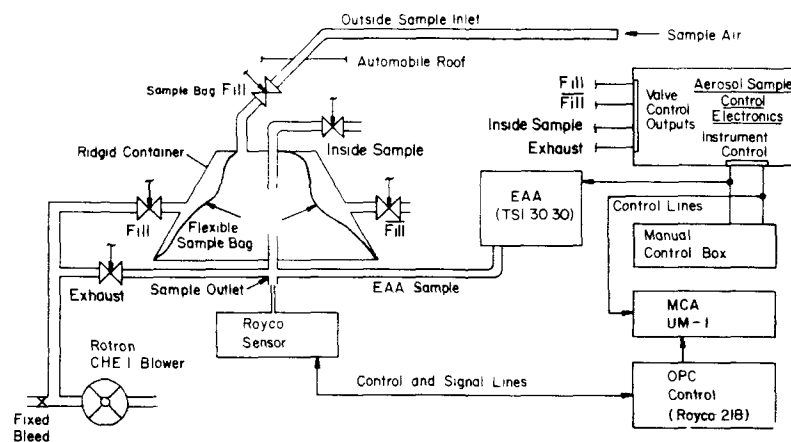


Electrical power for the instrumentation was supplied by two heavy-duty twelve-volt batteries connected parallel to a twelve-volt D.C. to 110-volt A.C. inverter. Motorized valve power was supplied as 24 volts D.C. by two heavy-duty twelve-volt batteries connected in series. A ninety-amp alternator (factory option) was installed to provide power for all system vacuum pumps. The vacuum pumps were placed in the trunk compartment with the exception of the internal sample pumps in the CNC and OPC. A Rotron CHE 1 blower was used to evacuate and fill the sample bag. Gast Model 343 D.C. pumps were used for the EAA (two pumps in parallel) and for the three filter samplers.

#### B. Instrumentation

The aerosol instrumentation package used, figure 2, was basically that used in an aircraft in the 1974 and 1975 St. Louis Urban Plume Study. This package provides aerosol size distribution measurement capabilities in the range of 0.01 to 5  $\mu\text{m}$ , using an Electrical Aerosol Analyzer (EAA) (Thermo Systems Model 3030) for the .01 to 1  $\mu\text{m}$  range and a modified Royco 218 for the 0.5 to 5  $\mu\text{m}$  range. An Environment One, Model Rich 100 counter was used to measure Aitken nuclei.

Two filter collection systems were incorporated into the car to collect aerosol samples for sulfate particulate mass fraction determination. These filter systems were also used in the 1975 St. Louis Plume Study. One system used comprised four 25mm Millipore type AH filter holders containing a media consisting of glass fiber with cellulose backing (Pallflex E70/2075 W, manufactured by Pallflex Products Corp.). These were used to collect separate integrated filter samples of air from outside and inside the car. The other system used is an automated sulfate filter sampler developed by Husar (ref. 2,3), Washington University, St. Louis. This device, utilizing the Pallflex filter media, was used primarily to sample outside air. A third filter sampling system was used occasionally to collect samples for acid sulfate aerosol analysis by Research Triangle Institute (RTI).



Portable Aerosol Analysis System Used In Ford Custom 500, Detroit (1975)

Figure 2 Schematic of the aerosol sampling system used in the aerosol measurement car. The system consists of an automatic bag sampler, TSI electrical aerosol analyzer, Royco 218 optical particle counter, Environment One condensation nuclei counter, Husar TWO MASS sulfate sampler and an integrating filter sampler.

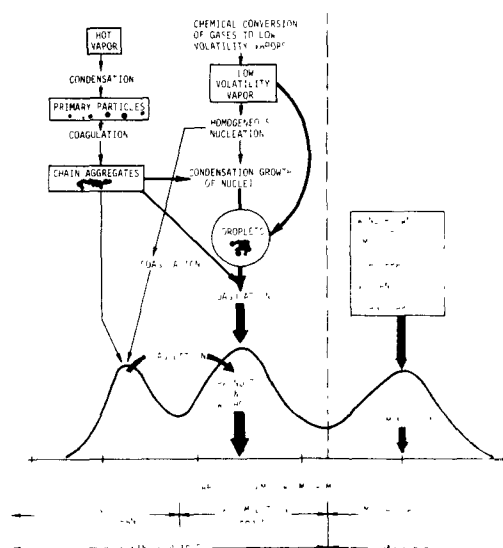


Figure 3 Schematic of a trimodal atmospheric aerosol size distribution showing the principal modes, main sources of mass for each mode, and the principal processes involved in inserting mass and removing mass from each mode.

### C. System Operation

The EAA and OPC require 150 and 60 seconds respectively to complete a measurement cycle. With this long a cycle time, direct sampling of a rapidly changing aerosol such as is produced by a fleet of automobiles on a roadway would yield erratic results. To minimize this problem, a system was designed which rapidly takes a sample (18 sec) into a sampling chamber inside the car as the car passes through the region of interest. The size analysis instruments then sample directly from the static air volume in the sampling chamber while executing their analysis cycles. The sample thus represents the characteristics of the atmosphere sampled along about a 0.5km portion of the test track. The two-chamber sampling system shown in figure 3 was designed to allow sampling at any speed.

Operation of the system is semiautomatic with automatic valve control and EAA and OPC start after the cycle is initiated by the observer pressing a button. Following the start command, the motorized valves operate in the following sequence. The exhaust valve opens for 18 seconds with  $\overline{\text{Fill}}$  also open and all others closed. This exhausts the inner bag and fills the rigid outer chamber with air from inside the car. Fill and Sample Bag Fill valves then open and  $\overline{\text{Fill}}$  closes for 18 seconds to draw in a sample into the inner bag. At that point the Fill and Sample Bag Fill again close and  $\overline{\text{Fill}}$  opens for the sample period, about three minutes. Immediately after the Fill valves have closed, the controller resets the EAA and OPC and initiates the EAA and OPC acquisition cycles. Following completion of the sample period, the Inside Sample valve opens, allowing the EAA and OPC to continuously sample the atmosphere inside the car.

To record the data, the operator reads the EAA and OPC outputs into a cassette tape recorder, along with a CNC reading. The CNC reading recorded on the tape was that corresponding to the start of the sample period; however, a strip chart recorder was connected so that a continuous record was kept of the CNC count.

Three separate air inlets were used. One provided the sample for the bag; one provided the sample for the filters and also ventilated the trunk compartment; and one provided the sample for the CNC.

#### D. Car Sampling Location:

Samples are taken at various locations on the track; however, the track section nearest the EPA trailer site received the most attention. With the sample bag fill time of 18 seconds, the sample taken was actually an average of conditions over a track length of about 0.5km. Also, a number of measurements of the atmosphere inside the car were also made each day while cruising on the track. Car run data are shown in table 2.

#### E. EPA Mobile Laboratory and Instrumentation

The large EPA mobile laboratory was parked 30m to the east of the test track and about 15m north of the GM instrumented bus. The sampling inlet was 6m above the ground level.

In addition to wind speed, direction, outside temperature, dewpoint, and NO, NO<sub>x</sub>, the following aerosol measurements were made:

- Aitken Nuclei using an Environment One - Rich 100 automatic condensation nuclei counter (CNC) calibrated using the Liu - Pui method (ref. 4).
- Aerosol size distribution in the 0.01 to 1  $\mu\text{m}$  range using a Thermo Systems Model 3030 Electrical Aerosol Analyzer (EAA) using the calibration constants discussed in Appendix I.
- Royco 220 optical counter, measuring aerosols in the 0.56 to 7.5  $\mu\text{m}$  range and calibrated against oil aerosols of 1.49 refractive index, (ref. 5).
- Royco 245 optical particle counter, measuring aerosols in the 5.6 to 40  $\mu\text{m}$  range and calibrated against oil aerosols of 1.4 refractive index. Inlet sampling efficiency corrections for both the Royco 220 and Royco 245 were made (ref. 5).
- Visibility measurements were made using a Meteorology Research Inc. Model 1550 Nephelometer calibrated against Freon.

Table 2 List of test dates, run numbers, fleet arrival and departure times, test period, and U of M car location during the experiment.

<u>Date</u>	<u>Test Day</u>	<u>GMPG</u>	<u>Cars Arrive</u>	<u>Test Begins</u>	<u>Test Ends</u>	<u>Cars Gone</u>	<u>U of M Car Lane</u>	<u>U of M Car Pack</u>	<u>Location No.</u>
10/01	274	1	-	13:35	15:45	16:00	not present		
10/02	275	2	7:10	7:40	9:30	10:00	"		
10/03	276	3	7:10	7:40	9:50	10:10	"		
10/06	279	4	7:15	7:35	9:55	10:15	outside	23	2
10/08	281	5	7:10	7:30	9:50	10:05	"	23	2
10/10	283	6	7:10	7:50	9:50	10:20	"	23	11
10/13	286	7	7:10	7:45	9:45	10:00	"	23	6
10/17	290	8	7:15	7:40	9:40	10:00	"	23	6
10/20	293	9	9:35	10:05	11:05	12:42	"	23	6
10/21	294	10	7:10	7:35	9:35	10:20	"	23	6
10/22	295	11	7:10	7:40	9:40	10:05	"	23	11
10/23	296	12	7:10	7:35	9:35	9:55	inside	8	6
10/24	297	13	7:10	7:35	9:35	10:00	inside	23	11
10/27	300	14	8:10	7:30	9:45	9:55	special tests		
10/29	302	15	7:05	7:35	9:35	10:10	special tests		
10/30	303	16	7:10	7:40	-	10:10	special tests		

- Filter samples for X-ray fluorescence analysis by EPA were taken with an LBL Dichotomous Virtual Impactor located on the roof at the rear of the lab (ref. 6).
  - Some special experiments were performed using a heater borrowed from R. Husar of Washington University, ahead of a TSI 3030 EAA.
- EPA trailer sampling and run information is shown in table 2.

#### F. Data Acquisition

Data from all instruments which provide electrical output is recorded using a computer based Data Acquisition System (DAS). Acquisition of data is based on a 10 minute cycle. During a cycle, continuous analog signals are measured every 20 seconds, averaged for the entire 10 minutes, and reduced on line. The EAA executes one measurement cycle in the first 2.5 minutes of the period and the multichannel analyzers (MCA), used to collect the pulse height data from the Royco 220 and 245 optical particle counters, acquire data for the first 400 seconds of the period. Size distribution data thus generated is recorded by the DAS, reduced and listed together with the analog data averages during the next 10-minute acquisition cycle. Table 3 presents the format of the data listing. Data from each 10-minute cycle is stored on magnetic disc packs during an experimental run and can be later transferred to 9 track industry standard magnetic tape for later analysis. An auxiliary strip chart was also used to record continuous data for the CNC during the experiment. On most days during the GM experiment, data acquisition was started at 0630, about 1 hour before the cars appeared on the track, in order to acquire background data before the test started, then continued for about an hour after the test for the same reason. Due to computer problems, background data were not obtained before the test on some days.

Table 3 This is a sample of the printout format used for all measurements made in both the EPA Mobile Lab and the University of Minnesota car. The specific example chosen is the average of several measurement runs made at the EPA Mobile Lab during the experiment on 10/13/75. Mnemonics and units for the various parameters listed are summarized in Appendix II together with the equipment references used.

SITE: GM PG 7 GM RUN NO. 284 DATE: 10/13/75  
 AVG OF RUNS 5 6 7 8 9 10 11 12 13 14 15 16  
 METEORLOGY  
 WDIR = 1 97E 02 WSPD = 1 28E 01 TOUT = 1 34E 01 PRES = 7 36E 02  
 IRRAD = 3 42E-01 BBRAO = 1 09E 01 DEWPT = 8 00E 00 RELHUM = 6 97E 01  
 GAS CHEMISTRY  
 NO/NOX = 7 04E-01  
 PROCESS DATE: 26-FEB-76  
 PROCESS TIME: 15:47:53

PARTICLE SIZE DISTRIBUTION

DP	DN	DS	DS/DLDP	DV	DV/DLDP
5 42E-03	4 98E 04	8 79E 00	3 51E 01	1 10E-02	4 39E-02
1 00E-02	3 79E 04	2 12E 02	8 47E 02	4 72E-01	1 89E 00
1 78E-02	1 37E 05	2 42E 02	9 71E 02	9 54E-01	3 84E 00
3 14E-02	4 21E-02	3 52E 01	1 41E 02	2 47E-01	9 89E-01
5 42E-02	7 50E-02	5 39E 01	2 14E 02	6 69E-01	2 67E 00
1 00E-01	1 39E-01	1 39E 02	5 54E 02	3 10E 00	1 24E 01
1 78E-01	2 49E 03	9 31E 01	3 73E 02	3 68E 00	1 48E 01
1 14E-01	2 37E-01	1 89E 01	7 95E 01	1 33E 00	5 31E 00
5 42E-01	3 39E 01	3 04E 00	1 21E 01	3 79E-01	1 52E 00
1 00E 00	1 72E 00				
ROYCO 220					
5 42E-01	3 83E 00	6 76E 00	2 70E 01	7 37E-01	2 94E 00
1 00E 00	9 07E-01	5 07E 00	2 02E 01	1 02E 00	4 07E 00
1 79E 00	2 37E-01	4 19E 00	1 68E 01	1 36E 00	5 53E 00
3 16E 00	4 21E 00	4 85E 00	1 94E 01	3 19E 00	1 27E 01
5 42E 00	6 48E 00	3 17E 00	2 55E 01	4 35E 00	3 51E 01
7 48E 00	2 40E-02				
ROYCO 245					
5 42E 00	2 35E-02	3 10E 00	2 50E 01	3 22E 00	2 60E 01
7 48E 00	6 49E-02	1 52E 00	1 20E 01	2 15E 00	1 71E 01
1 00E 01	6 49E-02	6 91E-01	2 76E 00	1 65E 00	6 60E 00
1 78E 01	1 24E-03	9 39E-02	3 77E-01	3 45E-01	1 38E 00
3 16E 01	2 27E 01	5 31E-05	4 98E-01	0 00E-01	0 00E-01
3 50E 01	1 04E-05				

INTEGRAL PARTICLE PARAMETERS  
 CNC = 5 64E 05

SUBRANGE GROUPINGS

NT	N2	N3	N4	N5	N3-	N4+
5 72E 05	5 24E 05	3 05E 03	1 26E 00	1 29E-03	5 37E 05	1 26E 00
S1	S2	S3	S4	S5	S3-	S4+
8 22E 02	5 49E 02	2 58E 02	1 87E 01	7 92E-01	8 02E 02	1 95E 01
VT	V2	V3	V4	V5	V3-	V4+
2 50E 01	2 34E 00	8 95E 00	1 17E 01	1 95E 00	1 13E 01	1 37E 01

MODAL FIT PARAMETERS

NUCLEI			ACCUMULATION			COARSE PARTICLE			NORMALIZED		
MODE	DPG	SG	MODE	DPG	SG	MODE	DPG	SG	MODE	DPG	SG
NUMBER WEIGHT	1 09E-02	1 60	2 68E 05	8 20E-02	1 75	8 75E 03	1 41E 01	1 94	2 17E 00	1 24E-02	2 55E-02
SURFACE WEIGHT	1 70E-02	1 60	5 80E 02	1 54E-01	1 75	3 28E 02	3 43E 00	1 94	2 58E 01	2 55E-02	6 20E-03
VOLUME WEIGHT	2 11E-02	1 60	1 96E 00	2 11E-01	1 75	1 04E 01	5 38E 00	1 94	1 59E 01	6 20E-03	

## DATA ANALYSIS

### A. Method for Characterizing Aerosol Size Distributions

Approximately 900 size distributions were measured by the car and the EPA trailer. Since the prime objective was to determine how much aerosol was added by the cars on the track and in what size range, a method for characterizing the size distributions was needed, which clearly showed in what size range the cars contributed the aerosols, and which would also allow unambiguous calculations of the difference between test data and background data.

In previous work, Whitby (ref. 7,8) has shown that in general, atmospheric aerosols are trimodal, figure 3, with two of the modes occurring below  $1\text{ }\mu\text{m}$  in size. The smallest mode has been named the "Nuclei Mode" and the second mode, the "Accumulation Mode," because all mass added in the submicron size range tends to accumulate in that mode. Figures 4 and 5 show a background and test period size distribution measured by the EPA trailer on a day with a low background. Because of the low background, the trimodal nature of the aerosol is strikingly apparent. Furthermore, by comparing the background with the test distribution, it is apparent that most of the aerosol volume contributed by the cars is to the nuclei mode.

It was therefore decided to characterize all of the aerosol distributions by modeling them with three log normal distributions using the general procedure described by Whitby (ref. 9,10). Since the volume of aerosol in the nuclei mode during background conditions was usually less than  $0.1\text{ }\mu\text{m}^3/\text{cm}^3$ , whereas the volume during a test was in the  $1\text{ to }20\text{ }\mu\text{m}^3/\text{cm}^3$  range, the volume in the nuclei mode during the test period is a clear and unambiguous measure of the aerosol being emitted by the cars, except for a few runs when the wind was almost exactly parallel to the track. Under these conditions, more aerosol volume was observed in the accumulation mode as well as in the nuclei mode.



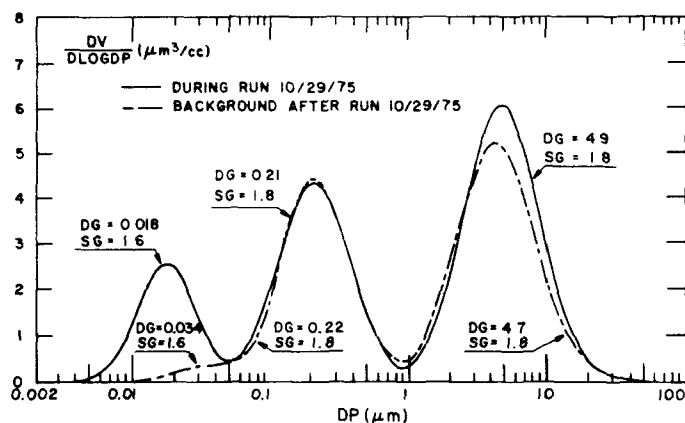


Figure 4 Trimodal model distribution measured by the EPA trailer during GMPG Run No. 15 on 10/29/75. The model distributions were obtained by fitting the data shown in Figure 5. Note that during the test the accumulation and coarse particle modes (center and right modes) have not changed significantly from the background conditions. On the other hand, practically all of the volume of the nuclei mode (left mode) is contributed by the cars on the roadway.

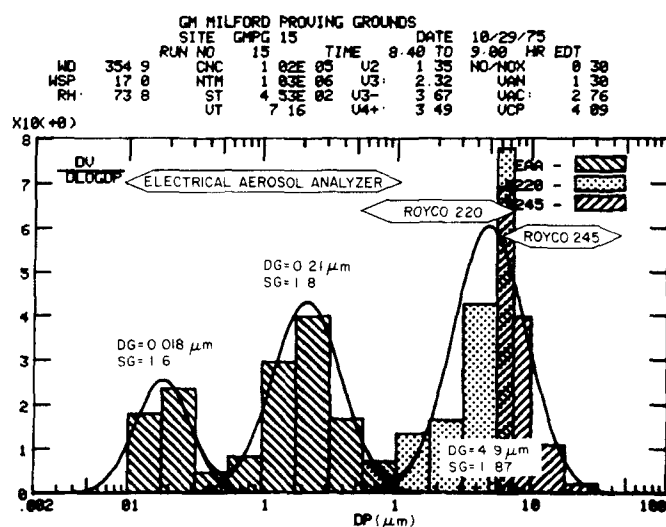


Figure 5 Example of a distinctly trimodal volume size distribution measured by the EPA trailer *in situ* aerosol instruments during GMPG run 15 on 10/29/75. The size ranges measured by each instrument are shown. Note the excellent matching between the instruments where they overlap. The geometric mean sizes and geometric standard deviations are typical of those measured during the test periods.

## B. Model Fitting Procedure and Data Presentation

In order to characterize the trimodal size distributions, each mode of the aerosol size distribution data for both car and trailer is fitted separately, and the resulting log-normal parameters, integral concentration (I) for the mode, geometric mean size (DPG), and geometric standard deviation (SG), are used to describe the mode.

For the trailer size distribution, data which were ordinarily complete from .01 to 40  $\mu\text{m}$ , the following fitting procedure was used.

1. The surface weighting of the aerosol distribution data is first "fitted" to obtain the parameters for the accumulation (AC) mode. To start, an initial estimate for the log-normal parameters is calculated using the data in the range of the accumulation mode. These are then used as a starting point for a non-linear regression employing a Simplex-directed direct search scheme (Nelder and Mead, 1965) (ref. 11) to minimize the function:

$$\text{INDEX} = \sum_i \frac{[D_i - \text{LN}(I, \text{DPG}, \text{SG})]^2}{\text{LN}(I, \text{DPG}, \text{SG})}$$

Here,  $D_i$  is the data in the interval; LN is the evaluation of the integral of the log-normal function with parameters, I, DPG, SG, over the interval i; and INDEX is value of the sum being minimized.  $1/\text{LN}$  is used in the sum as a weight or scaling factor proportional to the square of the error in the data. The values of I, DPG and SG that minimize INDEX are taken as the best estimate of the log-normal parameters. Using these, the AC mode is subtracted from the distribution data, leaving the Aitken nuclei (AN) and coarse particle (CP) modes.

2. The number weighting of the AN mode is next characterized using the same procedure described for the surface weighting of the AC mode. Since the mode was often incomplete due to the inadequacies of the EAA data below .01  $\mu\text{m}$ , the geometric standard deviation was assumed to be equal to 1.6. This is an average value derived from data where the mode was reasonably complete and the surface weighting

of the nuclei mode could be fitted accurately. Therefore, for the nuclei mode, only the amount in the mode and the geometric mean diameter by volume were determined from the fitting procedure. When a best estimate of these parameters is obtained, the AN mode is subtracted from the distribution data leaving only the CP mode.

3. Finally, the log-normal parameters for the volume weighting of the CP mode are determined using the fitting procedure outlined above. Upon completion of this final "fit," modal parameters for all three weightings of the three modes are computed, resulting in a composite parameterization for the entire distribution consisting of 9 parameters for each weighting, 3 per mode. Since the modal parameters for the volume weighting of a given mode are related to the number and surface weightings, we used only the parameters for the volume weighting in this paper. This should be adequate for the present discussion because aerosol volume is more directly related to sulfate aerosol concentration. The symbols used for each parameter and mode are given in table 1. These particular designations were adopted to enable graphs and tables to be prepared as conventional computer outputs. The parameters are tabulated on the printout for each ten-minute size distribution run on the trailer and for each car measurement. The parameters were also plotted by the computer on strip charts as shown in figure 6, and also tabulated in summary form in the DATA MAPS, table 4.

For the car data, the fitting procedure was modified somewhat. Because of the limitations of the Royco 218 optical counter and the sampling inefficiencies of the sampling system, the coarse particle mode was often incomplete. It was therefore decided that fits to the coarse particle mode were probably not meaningful for many runs.

Also, because the electrical aerosol analyzer in the car was often cycled in less than 5 minutes, the current differences in the 0.0056 to 0.01  $\mu\text{m}$  and 0.01 to 0.0178  $\mu\text{m}$  size ranges were lower than they should be. Therefore, only data associated with the size range of 0.0178 to 1.0  $\mu\text{m}$  were used for fitting. As with the trailer data,

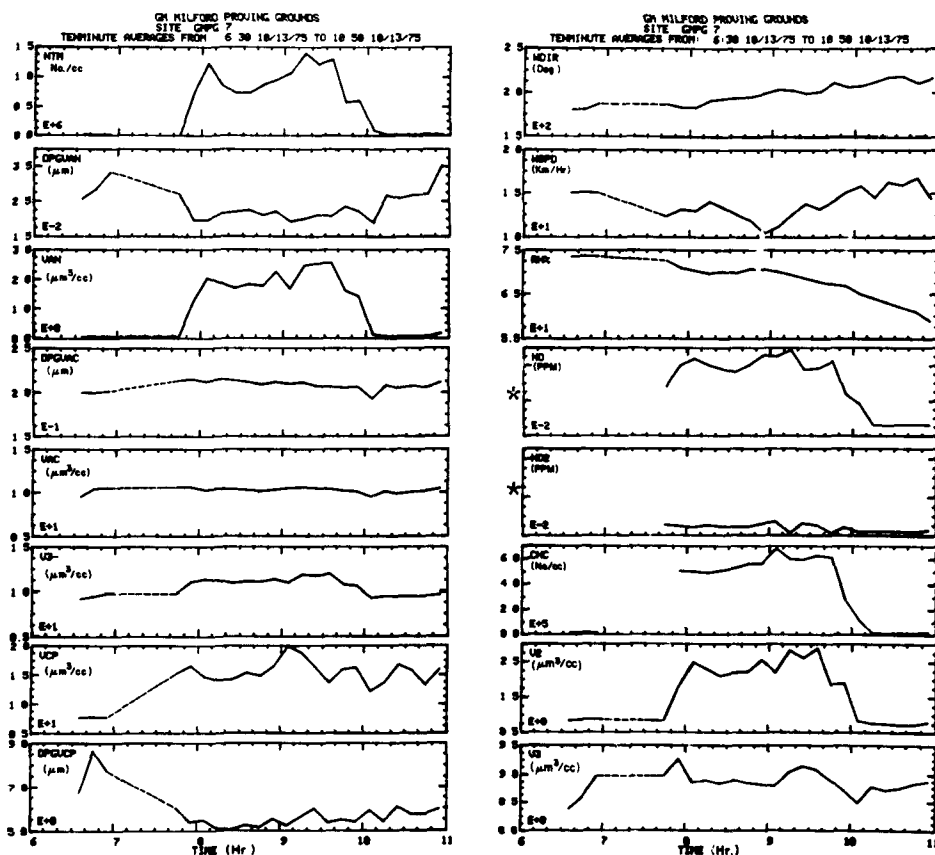


Figure 6 Computer-prepared strip charts of important meteorological and aerosol parameters for GMPG Run 7. The test started at 0740 and ended at 0940. Note the abrupt decrease in NTM, CNC, VAN, NO, and V2 at the end of the run. Note, however, that VAC and VCP did not change significantly. During the test period the geometric mean size of the nuclei mode, DPGVAN, decreased from the background value of  $0.04 \mu\text{m}$  to the test value of about  $0.02 \mu\text{m}$ .

(\* uncalibrated)

Table 4. Data Map of measurements made at the EPA Mobile Lab during the experimental run on 10/13/75, GM Run #286. Mnemonics and units for the various parameters listed are summarized in Appendix II.

DATA MAP			EPA TRAILER			GMPG 7			10/13/75			PROCESS TIME				22-FEB-76		19 59 12	
RUN #	TIME	WDIR	WSPD	RH%	TOUT	DEWPT	GNC	NTM	W2	V3	V3-	V4+	VAN	DPG VAN	VAC	DPG VAC	SG VAC	VCP	
1	06:30	181	15 1	74	11 5	7 0	1 5E 04	2 4E 04	0 85	8 38	9 23	8 37	0 05	0 026	9 58	0 20	1 79	7 75	
2	06:40	181	15 1	74	11 6	7 0	1 9E 04	2 2E 04	0 87	8 52	9 45	6 94	0 06	0 029	10 46	0 20	1 77	7 82	
3	06:50	188	15 1	74	11 6	7 1	1 5E 04	1 8E 04	0 88	8 97	9 84	7 25	0 05	0 022	10 59	0 20	1 78	7 77	
4	07:40	187	12 4	73	12 1	7 3	0 0E-01	2 8E 04	0 85	8 99	9 84	13 85	0 07	0 027	10 69	0 21	1 84	15 28	
5	07:50	184	13 2	71	12 5	7 4	5 1E 05	7 5E 05	1 80	9 26	11 09	14 81	1 22	0 020	10 66	0 22	1 76	16 54	
6	08:00	184	13 0	70	12 8	7 5	5 0E 05	1 2E 06	2 49	8 86	11 35	12 35	2 04	0 020	10 32	0 21	1 77	14 71	
7	08:10	192	14 1	70	12 9	7 5	4 9E 05	8 7E 05	2 30	8 90	11 20	13 11	1 87	0 022	10 50	0 22	1 78	14 13	
8	08:20	194	13 4	70	12 9	7 6	5 1E 05	7 3E 05	2 11	8 84	10 95	13 88	1 69	0 022	10 43	0 21	1 77	14 20	
9	08:30	195	12 6	70	13 0	7 6	5 3E 05	7 4E 05	2 21	8 90	11 11	14 41	1 83	0 023	10 31	0 21	1 76	15 41	
10	08:40	196	11 9	71	13 0	7 8	5 6E 05	8 7E 05	2 23	8 85	11 02	14 33	1 77	0 021	10 16	0 21	1 75	14 84	
11	08:50	200	10 4	71	13 1	7 9	5 7E 05	9 6E 05	2 57	8 81	11 39	13 25	2 26	0 022	10 34	0 21	1 75	14 51	
12	09:00	204	11 2	70	13 4	8 1	6 9E 05	1 1E 06	2 21	8 79	10 99	14 84	1 67	0 019	10 52	0 21	1 75	19 94	
13	09:10	203	12 6	69	13 8	8 3	6 0E 05	1 4E 06	2 84	9 04	11 88	12 92	2 46	0 020	10 62	0 21	1 75	18 84	
14	09:20	200	13 8	69	14 1	8 4	6 0E 05	1 2E 06	2 62	9 14	11 76	13 25	2 54	0 021	10 52	0 21	1 74	16 41	
15	09:30	202	13 2	68	14 6	8 7	6 3E 05	1 3E 06	2 89	9 08	11 98	11 94	2 56	0 021	10 45	0 21	1 73	13 62	
16	09:40	212	14 1	67	15 1	9 1	6 2E 05	5 7E 05	1 87	8 90	10 77	12 96	1 62	0 024	10 25	0 21	1 73	16 01	
17	09:50	207	15 2	67	15 6	9 5	2 9E 05	6 0E 05	1 90	8 70	10 62	14 24	1 42	0 022	10 13	0 21	1 74	16 32	
18	10:00	208	15 9	65	16 0	12 4	1 3E 05	9 4E 04	0 85	8 48	9 34	11 21	0 12	0 019	9 53	0 19	1 71	12 16	
19	10:10	213	14 5	64	16 5	12 8	1 5E 04	2 4E 04	0 77	8 77	9 54	14 20	0 07	0 027	10 20	0 21	1 71	12 75	
20	10:20	218	16 3	63	17 1	13 2	1 4E 04	2 2E 04	0 76	8 70	9 46	13 23	0 06	0 026	9 84	0 21	1 70	16 84	
21	10:30	219	16 0	62	17 7	13 5	1 5E 04	2 3E 04	0 73	8 74	9 47	15 18	0 06	0 027	10 09	0 21	1 71	15 82	
22	10:40	211	16 8	61	18 0	13 9	1 7E 04	2 3E 04	0 73	8 82	9 55	13 23	0 06	0 027	10 17	0 21	1 75	13 26	
23	10:50	217	14 5	59	18 7	13 9	2 3E 04	2 7E 04	0 80	8 87	9 68	14 03	0 18	0 025	10 46	0 21	1 72	15 98	

the SG of the AN mode was fixed at 1.6. Even with this restriction, the number of particles in the distribution agreed within 30-40% with the condensation nuclei count. It is believed that the estimate of the Aitken nuclei volume obtained this way is better than that which would have been obtained by an unrestricted "fit" to the actual EAA data over the complete Aitken nuclei mode size range.

The data weighting used for the fitting of each mode of the distribution was chosen in such a way that the most accurate data from each measuring instrument would determine the fit. This should be a valid procedure if the log-normal characterization provides an adequate description of each mode. That it is adequate can be shown by simultaneously fitting all three modes of the distribution with a composite trimodal log-normal function. This simultaneous fitting of the data, however, requires a prohibitive investment in time for the improvement in fit over that obtained using the procedure outlined above and was not done for this experiment. The procedure used in this study worked quite well for about 90% of the data. For the remaining 10%, there were assorted defects in the data which required the omission of some size ranges, fitting of only part of the mode, or in some cases precluded fitting. The log-normal fitting routine is capable of fitting the mode as long as the mode is visible. This fitting procedure yields the best results for the accumulation mode and reasonably good results for the coarse particle and Aitken nuclei mode.

Log-normal modal parameters have many advantages over the decade size range parameters that have been used previously. Although there is a reasonably good correlation between V2 and VAN, it may be observed from the strip charts of V2 and VAN that a part of the accumulation mode is actually in V2. Therefore, when the volume in the Aitken nuclei mode is close to 0, V2 will have a finite but small value. Therefore, the volume in the Aitken nuclei mode is, for this particular sulfate study, a much more definite description of the contribution of the automobiles on the track.

### C. Nomenclature

A relatively complex nomenclature is required to describe trimodal distributions. Since our computer cannot easily print Greek or lower case letters, only combinations of upper case letters and numerals have been used. Also to simplify data outputs, the units used have been omitted in most cases. Nomenclature and units used are given in Appendix II; a summary of the mnemonics is in table 5.

Table 5 :Summary of mnemonics used for the log-normal parameters associated with the characterization of the volume weighting of the data.

MODE	Parameter:		
	Integral Volume	Geometric Mean Size	Geometric Standard Deviation
Aitken Nuclei (AN)	VAN	DPG VAN	SGAN
Accumulation (AC)	VAC	DPG VAC	SGAC
Coarse Particle (CP)	VCP	DPG VCP	SGCP

### D. Difference Calculations

The amount being contributed by the cars on the track was obtained by subtracting the average volumes in the three modes during background conditions from an average during the test period. There were no problems in doing this for the nuclei mode, since the background was so low. However, the background for the accumulation (AC) and coarse particle (CP) modes were ordinarily about the same as the values observed during the test period. Also, the variations in the volumes in the AC and CP modes with time, due to changes in humidity and air mass changes were sometimes large enough to make the volume differences negative. Therefore, for only a few runs were the AC and CP mode volume changes significant.

## E. Analysis Data Outputs

Each 10-minute data record was reduced using the appropriate calibration data and constants and printed out as shown in table 3. This printout includes the gas and meteorological data at the top, the size distributions in the middle and the various summary parameters calculated from the distribution or from the log normal fitting at the bottom.

Figures 7a-7d show typical surface and volume plots that were prepared by computer for each 10-minute size distribution.

Next, DATA MAPS of the most important meteorological and aerosol parameters were prepared by computer for both the car and trailer data. A typical DATA MAP is illustrated in table 5.

Strip charts of key parameters were next prepared by computer for each run for the trailer and the car. These are illustrated in figure 6.

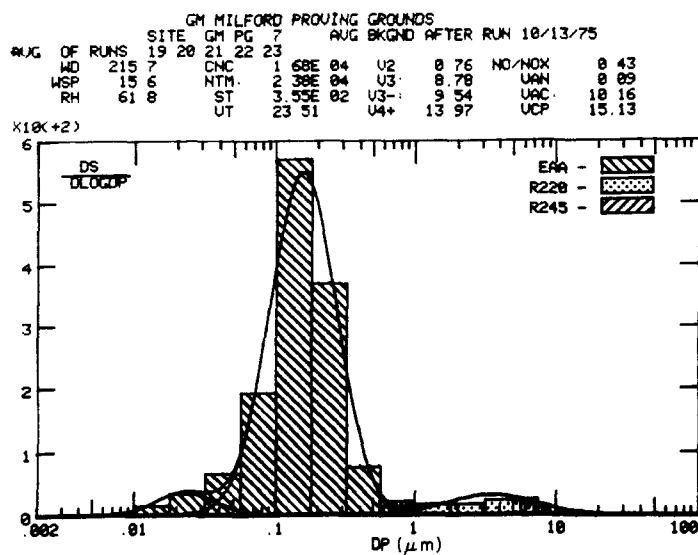
Using the DATA MAPS and the strip charts, runs were selected to be averaged together to obtain the background and test data. Finally, the automobile contribution was calculated by subtracting the background modal volumes from the test values. The background, test and difference volume ( $\Delta V$ ) are tabulated in tables 6 and 7 for the EPA trailer and the car, respectively.

At this time (February 1976), no final decision has been made as to how all of the data outputs described above are going to be distributed to those interested in the complete data and outputs. However, strong consideration is being given to distributing it on microfiche. The total data set is about 2000 pages or about 10 microfiches.

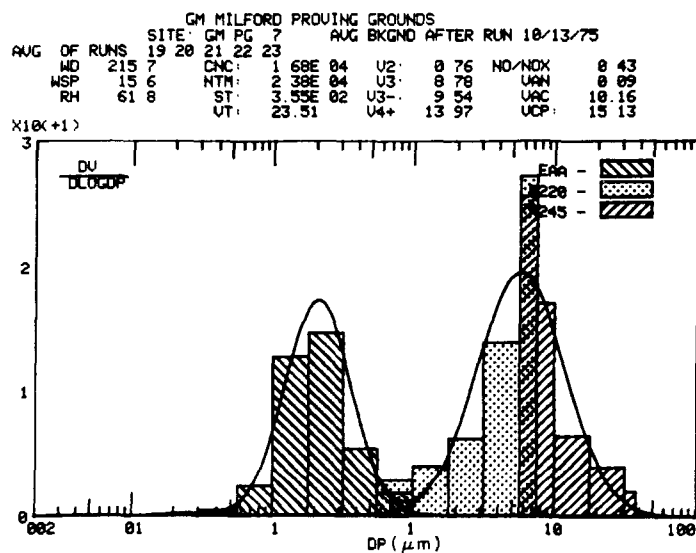
## EPA TRAILER RESULTS

Measurements were taken aboard the trailer every ten minutes from about one hour before the tests began to one hour afterwards. The before and after periods were used to calculate background distributions



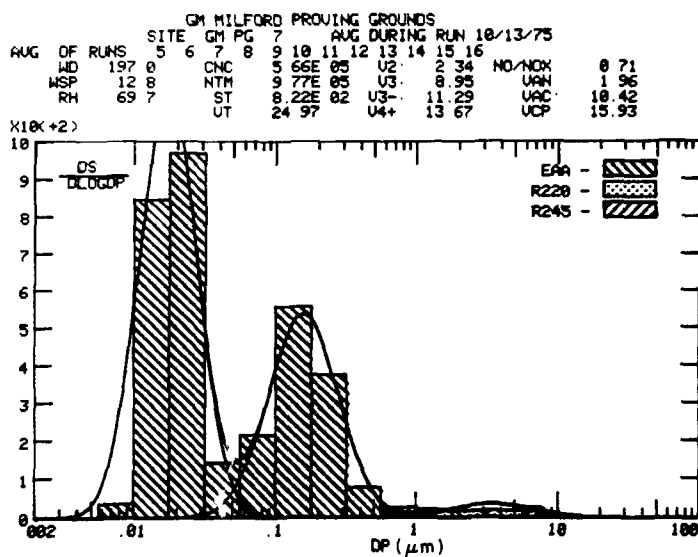


7a Surface  
Distribution

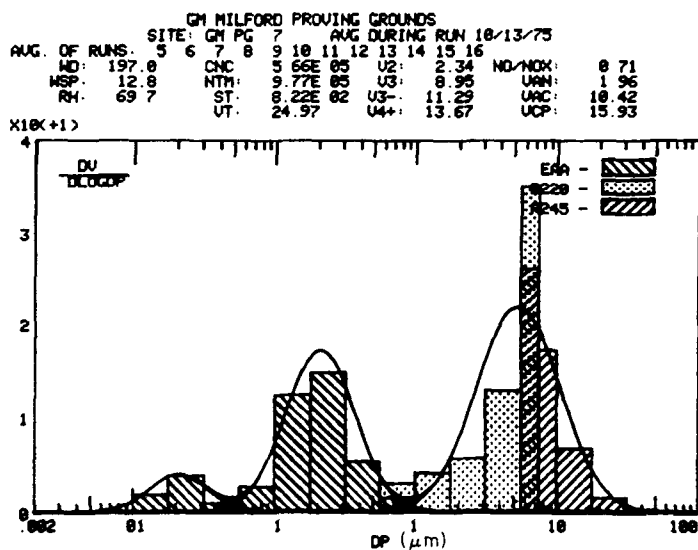


7b Volume  
Distribution

Figure 7a and 7b Average surface and volume distribution for the background period for GMPG run 7. This run is typical of most of the size distribution data. Note the almost complete absence of the nuclei mode for the background aerosol.



7c Surface Distribution



7d Volume Distribution

Figures 7c and 7d Average surface and volume distributions for the test period for GMPG Run 7. This run is typical of most of the size distribution data. Note that during the test period the volume in the nuclei mode, VAN, increased from the background value of  $0.09 \mu\text{m}^3/\text{cm}^3$  to  $1.96 \mu\text{m}^3/\text{cm}^3$ .

Table 6 Summary of EPA trailer data with emphasis on average particle volume for both Aitken nuclei mode (VAN) accumulation mode (VAC), and their associated standard deviations ( $\sigma$ ). Also included are the wind direction (WDIR), wind speed (WSPD), and volume differences for both Aitken nuclei mode ( $\Delta$ VAN) and accumulation mode ( $\Delta$ VAC)

Date: Oct., 75	Average Background Before Test					Average Background After Test					Average Background					Average Data During Test					Difference Test-Avg.Bkg.					
	WDIR <sup>a</sup>		WSPD <sup>b</sup>		$\sigma^c$	VAC <sup>c</sup>		$\sigma$	WDIR		WSPD		$\sigma$	VAN		$\sigma$	VAC		$\sigma$	VAN		$\sigma$	VAC	$\sigma$	$\Delta$ VAN <sup>c</sup>	$\Delta$ VAC <sup>c</sup>
	1	2	3	4		1	2		1	2	1	2		1	2		1	2		1	2					
1	281	15.0	.070	.007	1.93	.145	.071	.020	2.58	.605	.071	2.25	.093	.093	.145	.264	.287	14.7	.535	.145	.271	.264	.264	.464	.46	
2	324	9.3	.093	.003	1.14	.096	-	-	-	-	.093	1.14	332	13.9	.871	.362	1.30	332	13.9	.871	.362	1.30	.348	.778	.16	
6	268	4.4	.156	.032	15.1	.942	.245	.112	6.15	.591	.201	10.6	249	6.2	2.43	.816	13.3	249	6.2	2.43	.816	13.3	1.34	2.23	2.70	
8	50.8	8.2	.056	.004	15.6	1.44	77.6	8.3	2.04	2.26	20.4	.135	1.05	18.0	.75.7	9.2	75.7	9.2	.632	.704	17.5	4.77	4.77	-42	-50	
10	256	6.7	.069	.000	12.4	.000	.075	.010	11.6	.021	.072	12.0	240	5.9	2.06	.763	10.8	240	5.9	2.06	.763	10.8	1.01	1.99	-1.20	
13	184	15.1	.054	.004	10.2	.545	.085	.052	10.2	.215	.070	10.2	197	12.8	1.96	.419	10.4	197	12.8	1.96	.419	10.4	1.52	1.89	.20	
17	66.2	10.8	.112	.009	2.44	.078	.221	.201	3.32	.521	.167	2.88	54.9	11.9	.172	.108	3.28	54.9	11.9	.172	.108	3.28	.659	.005	.40	
20	239	6.3	.063	.007	3.61	.670	.085	.017	4.79	.420	.074	4.20	268	11.5	.865	.155	4.71	268	11.5	.865	.155	4.71	.929	.791	.51	
21	228	10.7	.067	.013	9.44	.874	.114	.012	12.8	.327	.091	11.1	224	7.5	2.16	.716	11.2	224	7.5	2.16	.716	11.2	.644	2.07	.10	
22	183	0.5	1.26	2.00	24.4	1.31	.206	.057	10.1	.544	.733	17.3	55.0	2.9	.395	.876	21.7	55.0	2.9	.395	.876	21.7	1.90	-34	4.40	
23	183	12.6	.067	.025	19.5	3.76	.137	.016	14.8	.288	.102	17.2	181	15.1	2.35	.994	18.3	181	15.1	2.35	.994	18.3	1.01	2.25	1.10	
24	176	12.8	.250	.022	17.1	.339	.253	.053	15.1	.222	.252	16.1	175	14.2	1.61	1.27	16.3	175	14.2	1.61	1.27	16.3	.746	1.36	.20	
27	190	7.7	.079	.029	12.8	.795	.066	.003	9.10	.147	.073	11.0	198	11.0	1.39	.368	13.4	198	11.0	1.39	.368	13.4	.766	1.32	2.40	
29	352	9.1	.026	.005	1.98	.456	.161	.061	3.08	.104	.094	2.53	351	14.0	1.20	.488	2.67	351	14.0	1.20	.488	2.67	.246	1.11	.14	
30	323	6.4	.170	.021	2.54	.228	.066	.047	1.56	.261	.118	2.05	334	5.8	1.76	.525	2.84	334	5.8	1.76	.525	2.84	.074	1.64	.79	

Average<sup>d</sup>: 1.49 0.63  
 $\sigma^d$ : 0.61 1.05

<sup>a</sup>Units for WDIR are degrees clockwise from north.

<sup>b</sup>Units for WSPD are km/hr.

<sup>c</sup>Units for VAN, VAC,  $\sigma$ ,  $\Delta$ VAN,  $\Delta$ VAC are  $\mu\text{m}^3/\text{cm}^3$ .

<sup>d</sup>Omit GMPG 5, 8, & 11.

Table 7 Summary of car data with emphasis on average particle volume for both Aitken nuclei mode (VAN), accumulation mode (VAC), and their associated standard deviations ( $\sigma$ ). Also included are the wind direction (WDIR), wind speed (WSPD), and volume differences for both Aitken nuclei mode ( $\Delta$ VAN) and accumulation mode ( $\Delta$ VAC).

Date: Oct., 75	GMPG	Northbound Average volume <sup>a</sup> and $\sigma$			Southbound Average volume and $\sigma$			Average Inside Car volume and $\sigma$			Outside Average, volume and $\sigma$			Background Average, volume and $\sigma$							
		VAN	$\sigma$	VAC	$\sigma$	VAN	$\sigma$	VAC	$\sigma$	VAN	$\sigma$	VAC	$\sigma$	VAN	$\sigma$	VAC	$\sigma$				
6	4	4.32	2.72	9.23	.759	10.1	3.89	10.8	5.97	7.57	.000	6.89	.000	8.32	4.44	10.4	4.19	.13	.05	7.55	4.02
8	5	10.1	5.17	15.6	1.81	4.56	3.64	15.2	4.16	4.67	.485	11.3	.588	7.34	4.97	15.1	3.11	.20	.01	13.7	2.60
10	6	6.71	.387	13.0	2.01	9.18	1.98	13.5	1.75	8.32	2.07	11.5	.619	8.64	1.93	12.9	1.47	.06	.03	9.55	.28
13	7	4.26	2.41	9.72	.818	5.36	1.30	10.6	1.41	2.31	.155	6.44	.638	4.56	1.72	9.79	0.61	.05	.05	8.43	.22
17	8	6.35	2.82	4.02	2.37	6.43	2.92	5.08	2.72	5.21	1.11	2.65	.792	7.40	3.40	4.10	1.93	.31	.03	2.95	.45
20	9	6.73	6.53	3.72	.428	9.06	.000	3.85	.000	6.01	1.01	3.08	.905	9.11	4.32	5.26	3.17	.11	.00	2.84	.24
21	10	4.73	3.21	8.64	.710	6.67	1.47	8.68	.968	5.95	.720	7.00	.970	4.96	2.65	8.51	0.98	.09	.04	6.95	1.77
22	11	8.46	1.03	18.7	2.26	4.29	1.31	16.6	2.46	5.87	.457	12.8	1.18	6.84	2.14	18.0	2.16	.22	.15	16.1	7.31
23	12	25.5	3.14	23.9	3.45	21.7	2.74	28.0	8.84	17.1	.880	16.1	.20	22.9	3.58	26.6	6.90	.15	.04	12.2	.50
24	13	8.14	2.07	18.9	3.27	7.67	1.25	18.7	2.51	5.20	.353	13.5	.764	7.16	2.37	19.2	2.56	.17	.06	13.4	1.11

Date: Oct., 75	GMPG	Northbound Average			Southbound Average			Average Inside Car			Outside Average <sup>e</sup>			$\frac{\Delta VAC}{\Delta VAN}$				
		WDIR <sup>b</sup>	WSPD <sup>c</sup>	$\Delta VAN^a$	WDIR	WSPD	$\Delta VAN$	WDIR	WSPD	$\Delta VAN$	WDIR	WSPD	$\Delta VAN$		$\Delta VAC$			
6	4	252	6.5	4.19	1.68	251	6.0	9.98	3.25	244	4.7	7.47	1.61	249	6.4	8.19	2.85	.348
8	5	72.3	8.8	9.90	1.90	74.9	9.3	4.36	1.50	36.0	7.8	4.51	1.71	71.3	9.1	7.14	1.40	.196
10	6	246	6.5	6.65	3.45	250	6.0	9.12	3.95	226	7.3	8.27	4.82	242	6.1	8.58	3.35	.390
13	7	194	12.9	4.21	1.29	196	12.9	5.31	2.17	206	13.6	2.27	.54	191	13.2	4.51	1.36	.302
17	8	57.4	11.8	6.04	1.10	55.8	11.3	6.12	2.13	56.5	12.1	4.97	.59	55.2	11.6	7.09	1.15	.162
20	9	265	12.2	6.62	.88	258	12.0	8.95	1.01	270	11.7	5.92	1.09	262	11.9	9.00	2.42	.269
21	10	222	6.8	4.64	1.69	224	7.1	6.58	1.73	218	5.5	5.89	2.13	224	7.5	4.87	1.56	.320
22	11	63.9	2.7	8.24	2.60	67.0	2.9	4.07	.50	35.1	2.1	5.70	1.53	62.5	2.8	6.62	1.90	.287
23	12	180	14.7	25.4	11.7	181	14.0	21.5	15.8	180	14.1	17.0	7.56	180	14.5	22.7	14.4	.634
24	13	175	13.6	7.97	5.50	176	14.3	7.50	5.30	176	14.1	5.08	4.12	176	13.7	6.99	5.8	.830

<sup>a</sup> Units for VAN, VAC,  $\sigma$ ,  $\Delta$ VAN,  $\Delta$ VAC are  $\mu\text{m}^3/\text{cm}^3$ .

<sup>b</sup> Units for WDIR are degrees clockwise from north.

<sup>c</sup> Units for WSPD are km/hr.

<sup>d</sup> Omit GMPG 12 and 13 since wind was parallel to the track for these tests.

<sup>e</sup> Includes northbound, southbound, north loop and south loop data.

Average:  $\sigma$ : 5.63 1.75  
Average:  $\sigma$ : 7.00 2.00

Average:  $\sigma$ : 6.71 2.57  
Average:  $\sigma$ : 8.57 3.62

for comparison to the values during the test period. Data from each ten-minute run were calculated as shown in table 3, then the most important aerosol and meteorological parameters were tabulated by computer as shown in the DATA MAPS for GM run #7, shown in table 4.

Next, the background periods were averaged together and the test periods were averaged together, using care to exclude system start-up transients and the transient periods at the beginning and the end of the test period. During runs #5, 8, and 11, the wind was from the east, so that aerosol from the roadway did not consistently reach the trailer. These are included for comparison to the car data, which are valid for those runs. These runs were not included in the averages calculated in table 6.

The last two columns in table 6 show the differences between the test and background volume in the Aitken nuclei mode, and the accumulation mode. The grand average increase in volume in the Aitken nuclei mode was  $1.49 \pm .61 \mu\text{m}^3/\text{cm}^3$ . The average increase in volume in the accumulation mode was  $0.63 \pm 1.05 \mu\text{m}^3/\text{cm}^3$ . However, it will be noted that the standard deviation of the grand average is larger than the average for the accumulation mode, and it is therefore doubtful that the increase in the accumulation mode is significant.

Figures 7a-7d show typical surface and volume distributions for the background and the test period measured at the trailer. These are the averages during the test period for GM Run #7. By comparing the surface distributions for the background and the test periods, it is obvious that the nuclei mode is mostly due to the cars on the track. The small nuclei mode during background conditions is undoubtedly contributed by cars upwind of the proving grounds roadways, probably at distances of several miles.

Figure 6 shows strip charts of the major variables measured. An examination of this figure shows that condensation nuclei (CNC) increased abruptly at the beginning of the test at 0740 and declined sharply at the end of the test. This is also true of the volume in the Aitken nuclei mode, VAN, V2, and N0. On the other hand, the volume in the accumulation mode (VAC) stayed practically constant during the run,

indicating that little volume was being added to the accumulation mode by the cars on the roadway. It can also be noted that the mean size of the Aitken nuclei mode decreased from  $0.034\ \mu\text{m}$  during the background periods to  $0.018\ \mu\text{m}$  during the test period. This indicates that the emitted size of the fresh aerosol from the cars on the roadway is about a factor of 2 smaller than the aged nuclei mode aerosols contributed by combustion sources at a much greater distance in the background. It will also be noted that there was little addition of aerosol to the coarse particles or little change in the coarse particle size.

Figure 8 shows strip charts for GM Run #16. During this run, there was an abrupt change in the wind from the NW of the roadway around to the NE at 0840. Figure 9 shows the response of various parameters to this step function change in the wind direction and hence in the roadway as a source of aerosol. From the figure, note that there were abrupt decreases in NO, CNC, and the volume of the Aitken nuclei mode, VAN, with this wind shift. There was a small change in the volume of the coarse particles and a nonsignificant change in the volume of the accumulation mode. This is further evidence that the roadway aerosols are essentially all in the nuclei mode.

Figure 9 shows a difference distribution for GM Run #7. This provides further evidence that all the aerosol is added in the nuclei mode. If figure 9 is contrasted with figure 10 for the car, it is seen that at the trailer, there is not significant addition of aerosol to the accumulation mode. However, the car distributions for GM 12 shown in figure 10, show significant additions of aerosol to the accumulation mode. The conclusions that can be drawn from this is that the aerosol additions to the accumulation mode shown in figure 10 are occurring after the aerosol has left the exhaust system of the automobile. When the wind is across the roadway at reasonably high velocities, it is diluted so rapidly that little aerosol is added to the accumulation mode by the time it reaches the trailer. This is the situation shown in figure 9. However, when the wind was traveling parallel to the roadway as during Run 12, illustrated in figure 10, coagulation transferred almost half the volume to the accumulation

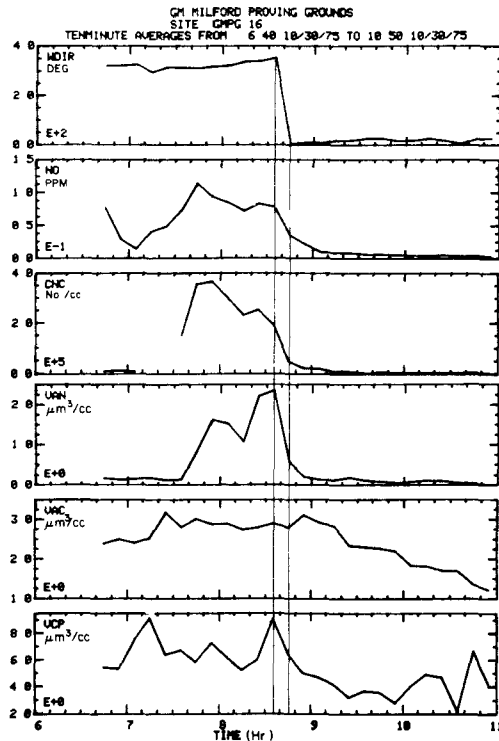


Figure 8 Strip charts of principal aerosol parameters measured by the EPA trailer during GMPG Run 16. During this run, the wind abruptly shifted between 0840 and 0850 from blowing the emissions from the cars on the roadway toward the trailer to blowing away from it. This step function in the aerosol source caused abrupt decreases in NO, CNC, and VAN, but not in VAC. It is not clear whether there was a significant change in the coarse particle volume, VCP.

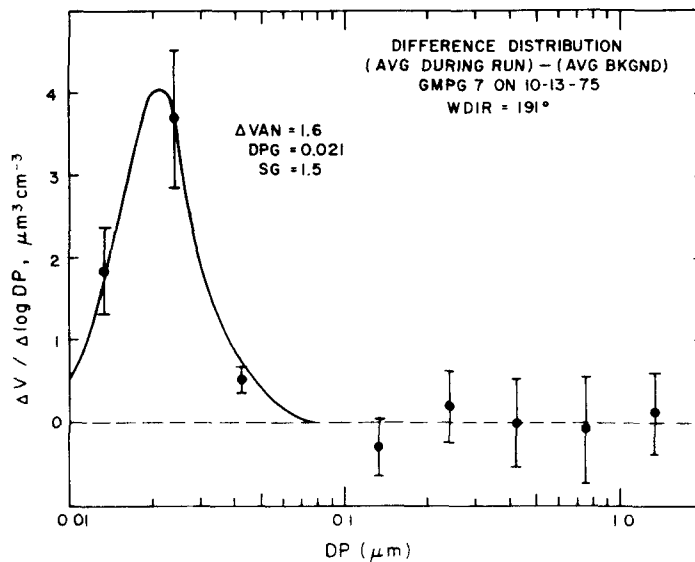


Figure 9 Difference distribution calculated from the background and test period averages for GMPG Run 7 measured by the EPA trailer. Note that there is a significant addition of volume in only the nuclei mode.

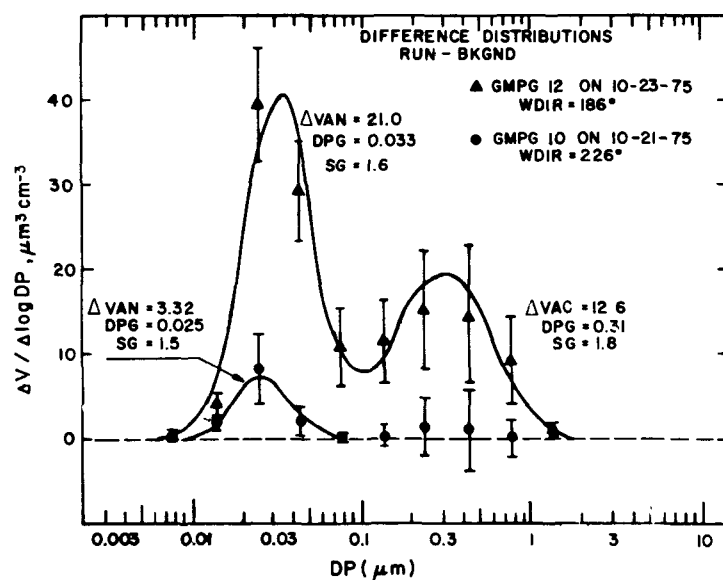


Figure 10 Shown are difference distributions calculated from averages of the size distributions measured by the car on the roadway during the indicated runs and measurements of background aerosol made before and after the test period. Included in the figure are the volume (V), mean geometric size (DPG), and geometric standard deviation for the resulting modes. These are based on a fit of the difference data using the log-normal fitting procedures.



mode. It is interesting to observe that in spite of this mass transfer, the nuclei mode and accumulation mode geometric standard deviations remain essentially constant. There is, however, about a 30% increase in the accumulation mode geometric mean diameter and a 100% increase in the nuclei mode geometric mean diameter as measured by the car during Run 12 as compared to the background value.

## RESULTS FROM THE UNIVERSITY OF MINNESOTA CAR

The University of Minnesota (UM) car was used to obtain aerosol data and sulfate samples. Most of the discussion here concerns the UM aerosol data, although some comparisons with the available sulfate data have been made.

The car arrived in Detroit in time to start participating in the test program on October 6, 1975, GMPG Run #4. In Runs 4-13, aerosol samples were obtained both inside and outside the car as the car traveled around the track with the test fleet. For Runs 14-16, the car was used to measure aerosol at different positions around the track and did not travel with the test fleet. The off-the-track data obtained by the car were used to compare the response of the car aerosol sampling system with the trailer aerosol sampling system. These data were used to calculate the background aerosol size distributions that would have been measured by the car had the car been used to obtain background data.

### A. Data Format

The test conditions for all runs are summarized in table 2. Presentation and interpretation of the aerosol data obtained with the car is complicated by the fact that the car was a moving sampling platform, so that both space and time variations of aerosol characteristics were encountered. Hence, the data are presented in several different ways. Tables 8 and 9 are DATA MAPS for the car obtained during Runs 7 and 12, respectively. These tables give run number, time, track position, meteorological and aerosol data. The position on the track is indicated by distance from the northern end when the car is traveling

south and distance from the southern end when the car is traveling north. The northern and southern ends of the track are designated as the north and south loops, respectively. The cars circled the track in a clockwise direction. Thus, when the car was traveling in a southerly direction, it emerged from the north loop (at a location designated 0 miles south), traveled down the east side of the track passing the position labeled 0.5 mi. (S), 1.0 mil. (S), etc. The trailer was located at a position 30m east and approximately 1.3 miles south (midway between the north and south loops).

When the aerosol data were obtained from inside the car, it was impossible to identify the aerosol with a specific location on the track because the car acted as a large volume which integrated the sample over the spatial distances on the order of the track length.

Aerosol data listed for each run include: condensation nuclei counts (CNC), total number concentration calculated during aerosol modeling (NTM), V2, V3, V3<sup>-</sup>, Aitken nuclei volume concentration (VAN), volume mean diameter for the Aitken nuclei mode (DPG VAN), accumulation mode volume concentration (VAC), and volume mean diameter for the accumulation mode (DPG VAC).

The variation of VAN and VAC with track position and time are presented in a more graphic form in figure 11. In its center, a map of the track is illustrated. A set of time coordinates have been superimposed on the map. These axes read away from the center of the sheet with earliest times near the center and later times further away. Aerosol data for outside samples (samples taken from outside the car through the bag sampling system) have been plotted on the figure with the numerical values of VAC and VAN placed on the figure in the position corresponding to the space and time at which the data were obtained. The format is (VAN, VAC).

#### B. Discussion of Aerosol Data Size Distributions

It is apparent from tables 8 and 9 and figure 11 that both aerosol nuclei and accumulation mode volumes, VAN and VAC, vary as the car moves around the track. Although the ratio of VAN to VAC

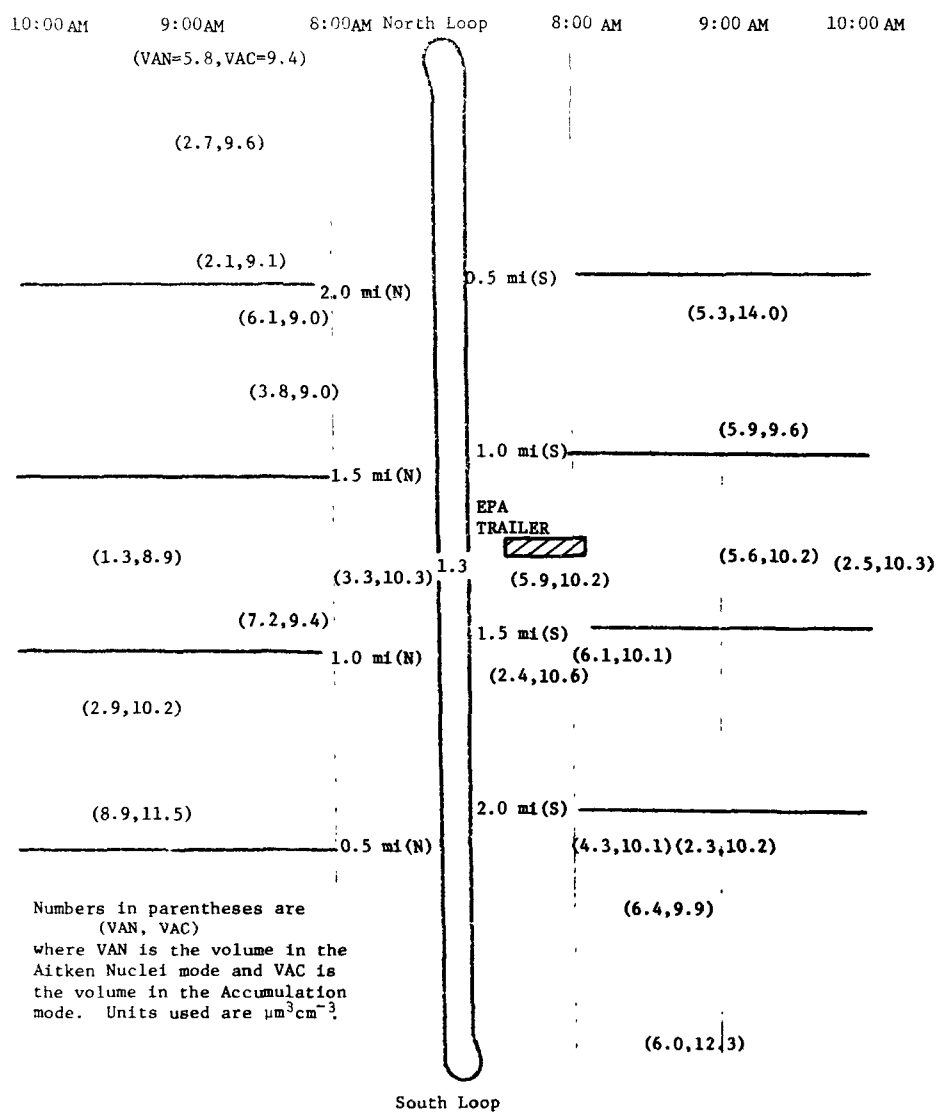


Figure 11 Distribution of the nuclei and accumulation mode aerosol volumes around the roadway for GMPG Run 7.

Table 8 Data Map of measurements made with the U of M car during the experimental run on 10/13/75, GM Run #286.  
Mnemonics and units for the various parameters listed are summarized in Appendix II.

DATA MAP U OF M CAR										10/13/75						PROCESS TIME		14-FEB-76		16 32 33	
GM PG 7																DPG		VAC		TRACK SITE	
RUN #	TIME	WDIR	WSFD	RHY	TOUT	DEMT	CNC	NTM	V2	V3	V3-	VAN	VAN	VAC	DPG	VAC					
1	7 15	187	12 4	73	12 1	7 3	2 3E 04	5 0E 04	1 10	10 72	11 83	0 32	0 035	13 14	0 22		PARKING LOT				
2	7 19	187	12 4	73	12 1	7 3	2 3E 04	1 9E 04	0 71	8 83	9 56	0 39	0 052	10 03	0 24		PARKING LOT				
3	7 20	187	12 4	73	12 1	7 3	1 9E 04	1 7E 05	1 40	9 70	11 10	0 91	0 037	11 04	0 25		ENTERING TRACK				
4	7 35	187	12 4	73	12 1	7 3	0 0E-01	1 1E 05	5 15	64 75	69 91	2 90	0 040	75 85	0 25		PARKED ON TRACK				
5	7 42	187	12 4	73	12 1	7 3	0 0E-01	1 2E 04	2 95	9 63	12 67	2 41	0 021	10 64	0 21		1 5 MILES SOUTH				
6	7 48	184	13 2	71	12 5	7 4	2 4E 04	3 5E 04	3 31	8 61	12 03	4 25	0 018	10 20	0 24		1 5 MILES NORTH				
7	7 54	184	13 2	71	12 5	7 4	3 3E 04	2 7E 04	2 60	8 23	10 89	3 34	0 018	10 32	0 25		1 3 MILES NORTH				
8	7 58	184	13 0	70	12 8	7 5	1 9E 04	1 2E 04	4 37	8 82	13 24	5 94	0 038	10 15	0 24		1 4 MILES SOUTH				
9	8 03	184	13 0	70	12 8	7 5	3 3E 04	5 4E 04	5 29	8 32	13 66	7 22	0 018	9 44	0 22		1 1 MILES NORTH				
10	8 06	192	14 1	70	12 9	7 5	9 3E 05	1 2E 04	4 38	8 76	13 16	6 14	0 028	10 08	0 23		1 5 MILES SOUTH				
11	8 10	192	14 1	70	12 9	7 5	1 9E 04	1 0E 04	2 47	7 98	10 47	3 78	0 026	9 00	0 23		1 7 MILES NORTH				
12	8 15	194	13 4	70	12 9	7 6	1 4E 04	3 8E 04	4 16	9 15	13 35	5 28	0 019	10 84	0 24		2 MILES SOUTH				
13	8 18	194	13 4	70	12 9	7 6	2 3E 04	4 1E 04	3 81	7 93	11 82	6 14	0 017	9 03	0 22		1 8 MILES NORTH				
14	8 23	194	13 4	70	12 9	7 6	1 9E 04	2 9E 04	3 45	8 80	12 27	4 29	0 019	10 14	0 23		2 MILES SOUTH				
15	8 26	195	12 6	70	13 0	7 6	2 1E 04	1 0E 04	2 01	8 05	10 08	2 12	0 021	9 05	0 23		2 1 MILES NORTH				
16	8 30	195	12 6	70	13 0	7 6	3 5E 04	1 2E 04	2 21	8 91	11 12	2 34	0 021	10 17	0 24		2 2 MILES SOUTH				
17	8 35	196	11 9	71	13 0	7 8	7 0E 05	1 7E 04	2 35	8 02	10 37	2 71	0 020	9 64	0 24		2 4 MILES NORTH				
18	8 38	196	11 9	71	13 0	7 8	2 3E 04	4 6E 04	4 74	8 58	13 33	6 38	0 018	9 93	0 23		2 5 MILES SOUTH				
19	8 50	200	10 4	71	13 1	7 9	3 5E 04	3 6E 04	4 54	8 21	12 84	5 81	0 019	9 45	0 22		NORTH LOOP				
20	8 55	204	11 2	70	13 4	8 1	4 2E 04	4 4E 04	4 51	10 87	15 39	6 03	0 019	12 30	0 23		SOUTH LOOP				
21	8 58	204	11 2	70	13 4	8 1	4 7E 04	3 9E 04	5 21	12 20	17 42	6 36	0 020	14 28	0 24		0 6 MILES SOUTH				
22	8 03	204	11 2	70	13 4	8 1	4 2E 04	5 3E 04	7 32	9 34	16 66	8 88	0 020	11 47	0 23		0 6 MILES NORTH				
23	8 07	203	12 6	69	13 6	8 3	5 1E 04	4 9E 04	4 33	8 25	12 62	5 90	0 018	9 58	0 23		0 9 MILES SOUTH				
24	9 12	203	12 6	69	13 8	8 3	1 9E 04	1 4E 04	2 53	8 60	11 15	2 86	0 020	10 17	0 25		0 9 MILES NORTH				
25	9 16	200	13 8	69	14 1	8 4	4 4E 04	4 5E 04	3 96	8 88	12 88	5 56	0 018	10 48	0 24		1 2 MILES SOUTH				
26	9 20	200	13 8	69	14 1	8 4	1 9E 04	4 4E 05	1 48	7 94	9 44	1 31	0 024	8 93	0 23		1 3 MILES NORTH				
27	9 25	202	13 2	68	14 6	8 7	4 7E 05	1 1E 04	1 87	6 30	8 17	2 09	0 021	7 48	0 25		INSIDE				
28	9 28	202	13 2	68	14 6	8 7	9 3E 05	1 4E 04	2 01	5 70	7 71	2 31	0 020	6 40	0 22		INSIDE				
29	9 32	202	13 2	68	14 6	8 7	7 0E 05	9 1E 05	2 28	5 49	7 79	2 33	0 023	6 50	0 23		INSIDE				
30	9 37	212	14 1	67	15 1	9 1	5 8E 05	7 1E 05	2 20	5 48	7 70	2 53	0 025	5 84	0 23		INSIDE				
31	9 40	212	14 1	67	15 1	9 1	9 3E 05	1 3E 04	2 11	5 14	7 25	2 30	0 020	6 00	0 22		INSIDE				
32	9 48	207	15 2	67	15 6	9 5	0 0E-01	5 0E 05	2 86	9 20	12 05	2 54	0 029	10 27	0 23		1 3 MILES SOUTH				
33	9 50	207	15 2	67	15 6	9 5	0 0E-01	5 3E 03	2 82	7 52	10 34	0 00	0 000	8 40	0 22		1 3 MILES NORTH				

Table 9 Data Map of measurements made with the University of Minnesota car during the experimental run on 10/23/75, GM Run #296. Mnemonics and units for the various parameters listed are summarized in Appendix II.

DATA MAP U OF M CAR										10/23/75			PROCESS TIME 24-FEB-76				10 08 50	
RUN #	TIME	WDIR	WSPD	RHY	TOUT	DEUPT	CNC	NTM	V2	V3	V3-	VAN	DPG VAN	VAC	DPG VAC	TRACK SITE		
1	7 30	179	14 6	83	12 8	9 9	2 8E 06	2 9E 06	5 44	13 78	19 36	5 62	0 021	16 71	0 26	INSIDE WHILE PARKED 0		
2	7 47	175	13 5	83	12 4	9 7	4 7E 06	1 0E 07	22 92	18 16	42 07	28 29	0 023	22 68	0 26	2 4 MILES NORTH		
3	7 52	175	12 5	83	12 4	9 7	7 0E 06	6 9E 06	20 38	20 14	40 76	21 85	0 024	24 41	0 29	2 5 MILES SOUTH		
4	7 55	177	15 5	85	12 2	9 7	6 1E 06	3 8E 06	17 93	19 18	37 33	18 01	0 028	23 20	0 30	NORTH LOOP		
5	8 00	177	15 5	85	12 2	9 7	7 0E 06	3 6E 06	20 91	31 06	52 18	20 42	0 030	36 96	0 30	SOUTH LOOP		
6	8 05	178	13 2	85	12 1	9 7	6 5E 06	8 2E 06	19 49	35 09	53 58	22 94	0 023	26 15	0 30	1 5 MILES SOUTH		
7	8 08	178	13 2	85	12 1	9 7	1 0E 07	6 1E 06	25 48	19 41	44 89	26 61	0 027	23 57	0 28	1 3 MILES NORTH		
8	8 12	178	13 2	85	12 1	9 7	6 5E 06	6 7E 06	24 06	20 39	44 44	25 50	0 026	25 12	0 29	1 3 MILES SOUTH		
9	8 16	173	16 5	86	12 0	9 8	8 9E 06	6 0E 06	27 11	18 22	45 33	28 43	0 028	21 83	0 29	1 3 MILES NORTH		
10	8 20	173	16 5	86	12 0	9 8	7 0E 06	2 4E 06	23 97	15 50	39 51	24 10	0 036	17 89	0 25	INSIDE		
11	8 28	180	14 1	86	12 2	9 8	7 0E 06	1 8E 06	18 15	13 91	32 20	17 75	0 035	16 00	0 24	INSIDE		
12	8 31	180	14 1	86	12 2	9 8	7 5E 06	1 7E 06	17 48	14 00	31 48	16 50	0 035	16 28	0 24	INSIDE		
13	8 25	188	15 1	82	13 1	10 1	7 0E 06	4 7E 06	21 48	17 68	39 19	21 99	0 028	21 66	0 30	0 7 MILES NORTH		
14	8 28	188	15 1	82	13 1	10 1	5 1E 06	5 5E 06	18 77	35 85	54 83	20 18	0 026	43 37	0 35	1 3 MILES SOUTH		
15	8 34	188	15 1	82	13 1	10 1	9 3E 06	4 9E 06	21 76	25 19	47 19	22 39	0 028	29 95	0 30	1 6 MILES NORTH		
16	8 38	188	15 0	81	13 5	10 4	7 0E 06	6 7E 06	16 11	17 35	33 69	18 26	0 023	20 81	0 31	2 0 MILES SOUTH		
17	10 38	192	15 5	72	15 9	10 9	1 9E 04	1 8E 04	0 47	10 93	11 31	0 20	0 041	12 90	0 29	BACKGROUND		
18	10 42	192	15 5	72	15 9	10 9	1 9E 04	3 0E 04	0 45	10 18	10 63	0 15	0 030	11 95	0 30	BACKGROUND		
19	10 46	193	17 8	71	16 1	10 8	1 9E 04	2 1E 04	0 31	10 39	10 70	0 11	0 031	12 04	0 29	BACKGROUND		
20	10 48	193	17 8	71	16 1	10 8	1 9E 04	1 9E 04	0 39	10 38	10 77	0 15	0 036	11 76	0 29	BACKGROUND		

varied somewhat with track position and time, the basic submicron bimodal character of the aerosol, which was apparent in the trailer data, was always present. Figures 12 and 13, which show the outside average volumetric size distributions obtained for Runs 7 and 12, respectively, clearly illustrate this bimodality. Run 7 was quite typical for both car and trailer. The average Aitken nuclei mode volume, VAN, and accumulation mode volume, VAC, are  $4.56 \pm 1.72$  and  $9.79 \pm 0.61 \mu\text{m}^3/\text{cm}^3$ , respectively. The uncertainties given are one standard deviation. This compares with background values of  $0.05 \pm .05$  and  $8.43 \pm .22 \mu\text{m}^3$  for VAN and VAC, respectively. Thus most of the aerosol produced by the cars is added to VAN. The main difference between the average car size distribution and the average trailer size distribution for Run 7 is that VAN outside average for the car is significantly larger than VAN average for the trailer:  $4.56 \pm 1.72 \mu\text{m}^3/\text{cm}^3$ , compared to  $1.96 \pm 0.42 \mu\text{m}^3/\text{cm}^3$ . The average values of VAC for the car and trailer are about the same,  $9.79 \pm 0.61$  and  $10.4 \pm 0.15 \mu\text{m}^3/\text{cm}^3$ , respectively. This behavior is consistent with the view that the direct aerosol contribution from the car exhaust is to VAN.

Run 12 is of particular interest because extremely high values of both VAN and VAC were measured by the car. The average wind direction during this run was  $180^\circ$ ; in other words, the wind was blowing directly down the track. This apparently allowed significant buildup in concentration along the track. The average values of VAN and VAC are  $22.9 \pm 3.6$  and  $26.6 \pm 6.9 \mu\text{m}^3/\text{cm}^3$ , respectively. Background values of VAN and VAC were  $0.15 \pm 0.04$  and  $12.2 \pm 0.5 \mu\text{m}^3/\text{cm}^3$ . It is apparent that under these conditions, there is significant volume addition to both VAN and VAC by the cars. The wind direction along the track allows the aerosol to build up with little dilution so that there is time for significant mass transfer by heterodisperse coagulation from VAN to VAC; thus a large contribution to VAC as well. The phenomena will be examined further in the section entitled "Discussion of Car Data."

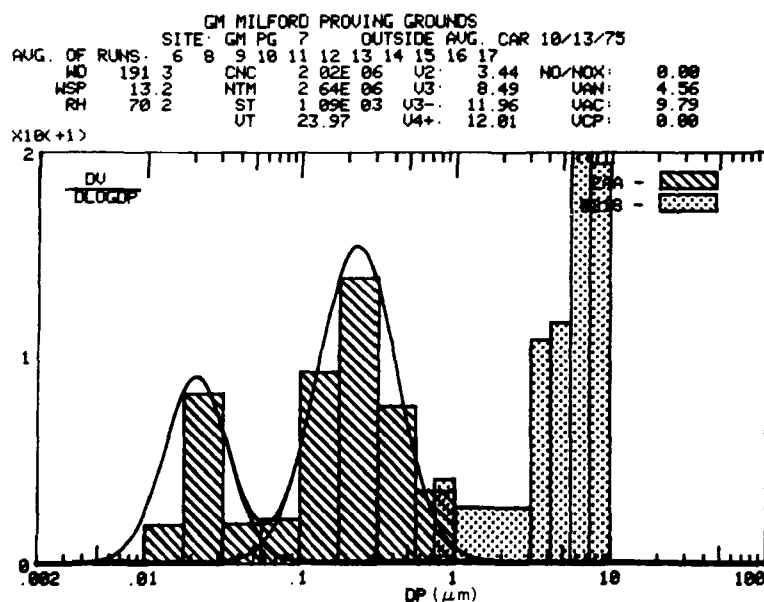


Figure 12 Car average aerosol volume distribution for GMPG Run 7. The average is for the samples taken in the center portion of the track, nearest the EPA trailer.

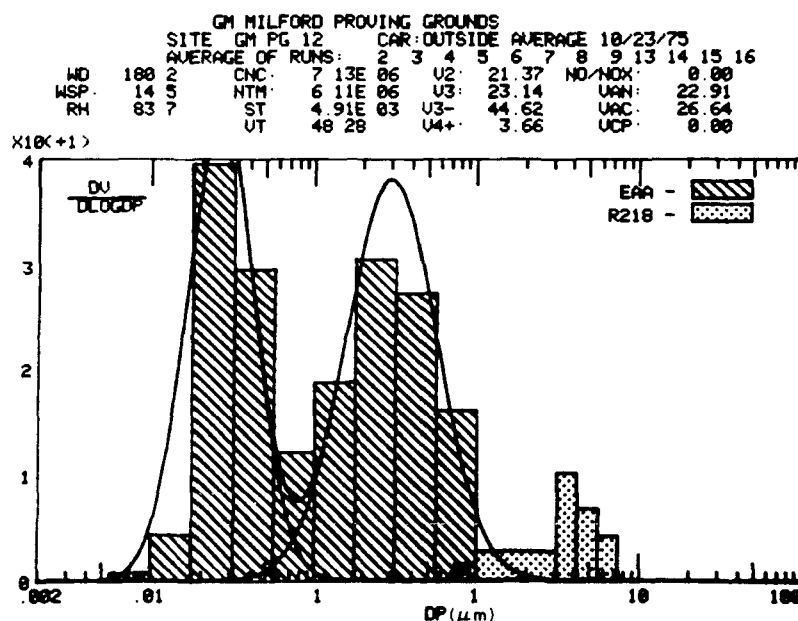


Figure 13 Car average aerosol volume distributions for GMPG Run 12. The average is for the samples taken in the center portion of the track. For this run, the wind was almost exactly parallel to the roadway. Note that  $\text{VAN} = 22.91 \mu\text{m}^3/\text{cm}^3$  for this run as compared to  $\text{VAN} = 4.56 \mu\text{m}^3/\text{cm}^3$  when the wind was across the roadway (GMPG Run 7, Figure 12)

Figures 12 and 13 also shown an aerosol volume mode above 1.0  $\mu\text{m}$ , the coarse particle mode. The average size distribution for Run 7 (figure 7d) shows that coarse particle volume is comparable to the volume below 1  $\mu\text{m}$ , the fine particle volume. On the other hand, the average size distribution for Run 12 (figure 12) shows that the coarse particle volume is small compared to the fine particle volume. This provides evidence that little coarse particle volume is being added by the cars. Otherwise, a buildup in concentration similar to that observed in the submicron range would be expected to occur in the supermicron range.

C. Variation of Aerosol Concentrations and Size Distributions with Car Position and Time

Examination of the data map in table 9 and the around-the-track aerosol map in figure 11 for this run shows that there is a significant variation in VAC and VAN during the run, and that the total nuclei plus accumulation mode volume sometimes exceeds 60  $\mu\text{m}^3/\text{cm}^3$ . The relatively large variation observed during the run probably resulted from the fact that the wind was shifting slightly during the run, and the slight shift away from the down-the-track wind direction would significantly change the aerosol volumes observed.

This behavior is also apparent in the plots shown in figure 14. Here the variation of CNC, VAN and VAC are plotted against time. The values of CNC and VAN vary with time in essentially the same manner. Since most of the nuclei count should be contributed by the nuclei mode, this is to be expected. However, VAN and CNC were measured by two independent, completely different instruments (the EAA and the CNC), so that it is pleasing to the high level of agreement between them. Note that all through the run, the nuclei count was very high. Its average was  $7.1 \times 10^6 \pm 1.6 \times 10^6$  number/ $\text{cm}^3$ . CNC, VAN and VAC all show significant variation with time. The standard deviations were 22, 16, and 26% of the mean for CNC, VAN and VAC, respectively. These variations probably result from changes in the vehicle operating



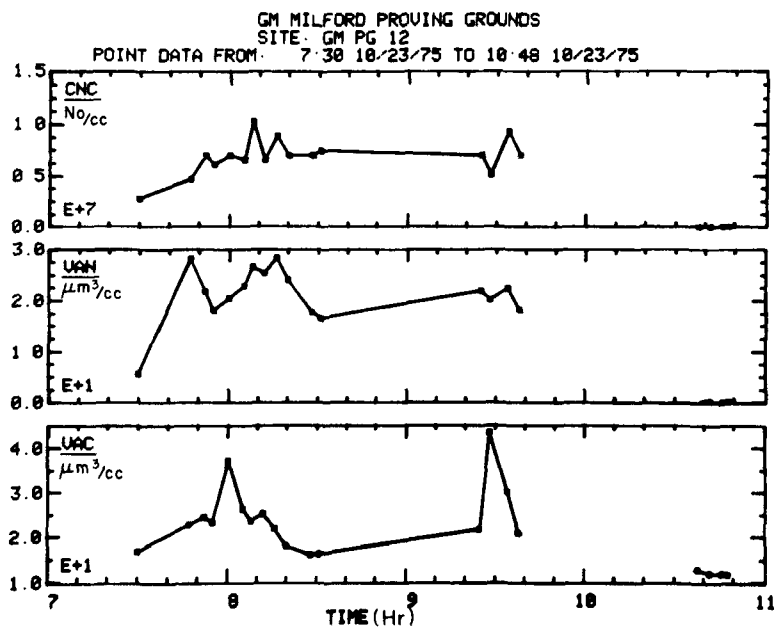


Figure 14 Strip charts of CNC, VAN and VAC for GMPG Run 12. Note the increase VAC at the beginning and end of the test period. This suggests that when the cars are idling or moving at low speeds there is an increased output of aerosol in the accumulation mode or a decrease in the effective dilution of aerosol emissions.

conditions as they circle the track as well as changes in wind direction and velocity which alter the aerosol dilution and residence time over the track.

Average values of VAN, VAC, wind direction and wind speed for all test days are summarized in table 7. For each day, averages of all northbound runs, all southbound runs, overall average of all outside-the-car data, and overall average of all inside-the-car data are presented. In addition, the difference volumes,  $\Delta$ VAN and  $\Delta$ VAC, are presented. These difference volumes are obtained by subtracting the best available average background values of VAN and VAC from those measured using the car system during the test. Unfortunately, in most cases, the background data was only available from the aerosol analyzing system in the trailer.

When the background aerosol sampled through the trailer inlet system and measured with the trailer EAA was compared with the same background aerosol sampled through the car inlet system and measured with the car EAA, a systematic difference was observed. The values of VAN determined by the car system were about 70% of those obtained by the trailer system, and the values of VAC obtained by the car system were about 85% of those obtained by the trailer system. Whenever it was necessary to use background data obtained with the trailer to obtain difference distributions for the car, the trailer values were corrected by multiplication by .7 for the nuclei mode volumes and .85 for the accumulation mode volumes. In addition, since the background aerosol concentration changed with time during the run, an average based on the data obtained both before and after the run was used for the background correction.

The background values of VAN were small compared to run values; hence, any errors in them will not significantly alter the  $\Delta$ VAN. However, the background value of VAC was always a large fraction of the run VAC. An examination of the data listed in table 7 shows that typically  $\Delta$ VAC determined by this method was only slightly larger than the standard deviation in the average run VAC. These measurements

are thus not believed to be highly significant. On the other hand, the values obtained under all conditions were positive and it is believed that there was a contribution by the cars to VAC in most cases. Under certain conditions, for example at 7:35 (Run #4) of GMPG 7 when the cars were parked on the track idling (see table 8), and for most cases in GMPG 12 and GMPG 13 where the wind direction was parallel to the track, the contributions to VAC by the test fleet are indisputable.

D. Comparison of Aerosol Measurements Made Inside and Outside of the Car

Aerosol concentrations measured inside the car in both the nuclei and accumulation modes are significantly lower than comparable measurements made outside the car. Average values of VAN and VAC both inside and outside are listed in table 7.

The ratio of VAN inside to VAN outside averaged over all the runs is 0.79 and the corresponding ratio for VAC is 0.70. This loss of aerosol evidently results from impaction and diffusion to the walls in the fresh air ducts, the heater core and fan, and the air conditioner. It is rather surprising to note that the loss of volume from the accumulation mode is greater than that from the nuclei mode. Losses through duct systems of this type would be expected to be lower in the size range of the accumulation mode rather than that of the nuclei mode. It is difficult to deduce a plausible explanation for this behavior without further detailed analyses of particle losses along the aerosol path to the passenger compartment. Since the difference between these ratios is probably not significant, such a detailed analysis is not warranted at this time.

As a consequence of aerosol losses in the car ventilation ducts, determination of the difference volumes for the aerosols measured inside the car was complicated slightly. These difference volumes would be strictly valid only if background aerosols were obtained with the car moving through the background aerosol under exactly the

same sampling conditions as during a run. It was impossible to obtain such background data, so the following corrections were made. As described above, the average inside-to-outside volume ratios were 0.79 and 0.70 for VAN and VAC, respectively. It was assumed that the same ratios would apply to background measurements, and they were corrected accordingly. Difference volumes were calculated using these corrected background levels.

These difference volumes indicate a substantial aerosol contribution by the test fleet to both VAN and VAC. The overall average contribution to the nuclei mode measured inside the car is  $6.7 \pm 3.95 \mu\text{m}^3/\text{cm}^3$ , and the contribution to the accumulation mode is  $2.57 \pm 2.25 \mu\text{m}^3/\text{cm}^3$ . This compares with average outside contributions of  $8.57 \pm 5.17$  and  $3.62 \pm 4.03 \mu\text{m}^3/\text{cm}^3$  for  $\Delta\text{VAN}$  and  $\Delta\text{VAC}$ , respectively.

#### E. Influence of Wind Direction and Track Position on Measured Aerosol Volumes

Whenever there was a significant across-the-track wind component, car data obtained on the upwind side showed lower aerosol concentrations than on the downwind side. For example, during Run 7, the average wind direction was  $198^\circ$ ; thus, there was a significant crosswind component with the southbound lanes in the downwind direction and the northbound lanes in the upwind direction. As a result of this crosswind, the car measured higher aerosol concentrations in the southbound lane than in the northbound lane. The average value of VAN measured in the southbound lane was  $5.4 \mu\text{m}^3/\text{cm}^3$ , and in the northbound lane,  $4.3 \mu\text{m}^3/\text{cm}^3$ . The same type of upwind-downwind dependence was observed in most runs, which is of course to be expected. Figure 15 shows a plot of the ratio of  $\Delta\text{VAN}$  measured in the southbound lane to  $\Delta\text{VAN}$  measured in the northbound lane, plotted against wind direction. For wind directions between  $0$  and  $180^\circ$ , the northbound lane is downwind and should be higher, whereas for wind directions between  $180$  and  $360^\circ$ , the southbound lane is downwind and should be higher. Figure 15 shows this to be the case, and as can be seen, a simple sine wave describes the data fairly well.

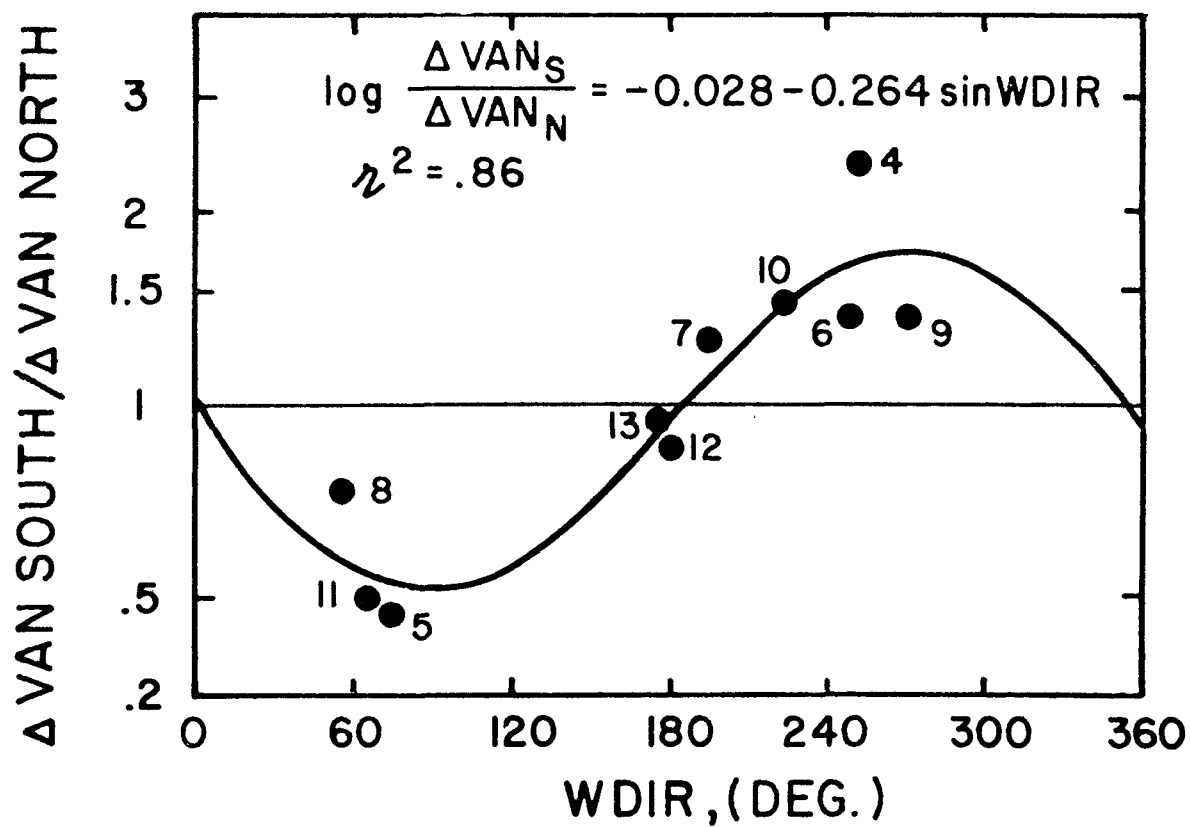


Figure 15 Shown is the ratio of the aerosol volume added to the nuclei mode on the southbound side of the roadway to the volume on the northbound side plotted against the wind direction. It is seen that the data is fitted well by a sine function.

## F. Discussion of Car Data

The data described above show that aerosols produced by catalyst equipped cars appear in the atmosphere mainly in two size ranges: (1) nuclei mode at about  $0.02\text{ }\mu\text{m}$  volume mean diameter, and (2) accumulation mode at about  $0.25\text{ }\mu\text{m}$  volume mean diameter. The ratio of average  $\Delta\text{VAC}$  to  $\Delta\text{VAN}$  for each day is given in table 7. It varies from about 0.83 to 0.16 with an average value of 0.37. Thus on the average, about 3/4 of the aerosol added by the cars appears in the nuclei mode. The large run-to-run variation is mainly due to uncertainties in  $\Delta\text{VAC}$ , which is small in magnitude compared with the two VAC values (both subject to errors) used to calculate  $\Delta\text{VAC}$ .

It appears that the primary emissions from the car add to VAN and the observed addition to VAC results from heterodisperse coagulation. Thus aerosols which have had more opportunity to age before sampling should exhibit a higher ratio of  $\Delta\text{VAC}$  to  $\Delta\text{VAN}$ . This effect is clearly illustrated in figure 10, which shows volumetric difference size distributions for Runs 10 and 12. For Run 10 with a crosswind ( $\text{WDIR} = 224^\circ$ ), and therefore a short aging time before sampling, nearly all of the volume appears in the nuclei mode. For Run 12, on the other hand, for which the wind was blowing nearly straight down the track ( $\text{WDIR} = 180^\circ$ ), the aerosols could build up and age over the track. Hence time was available for mass transfer to the accumulation mode by heterodisperse coagulation. The difference distribution for Run 12 shows that under these conditions a significant volume, about 1/3 the total submicron volume, was added to the accumulation mode. Also note the size shift in the nuclei mode between Run 10 and 12 from  $\text{DPG} = 0.025$  to  $0.033\text{ }\mu\text{m}$ . This suggests that under the conditions existing during Run 12, the nuclei mode also grew by monodisperse coagulation.

Further evidence of transfer from the nuclei mode to the accumulation mode -- when wind directions are nearly parallel to the track, is provided in table 7. For Runs 12 and 13, both with down-the-track wind directions, the ratios of  $\Delta\text{VAC}$  to  $\Delta\text{VAN}$  are 0.63 and 0.83, respectively, compared with an average ratio for the other eight runs of 0.28. Run

13 ( $\text{WDIR} = 176^\circ$ ) however, does not show the very high values of both  $\Delta\text{VAC}$  and  $\Delta\text{VAN}$  observed in Run 12 ( $\text{WDIR} \approx 180^\circ$ ). Apparently the slight departure from exactly down-the-track wind conditions in Run 13 significantly increases aerosol dilution, thus reducing aerosol concentrations; while at the same time, still allowing enough residence time over the track for heterodisperse coagulation to take place.

## APPENDIX I

### ELECTRICAL AEROSOL ANALYZER CONSTANTS

To obtain aerosol particle size distributions from the currents measured with the TSI Model 3030 Electrical Aerosol Analyzer it is necessary to multiply the  $\Delta I$ 's calculated from the  $I$ 's by a constant. When the EAA is operated at an  $nt = 10^7$  as it was in the GM study, it has been found that the sensitivities as published by Liu and Pui<sup>a</sup> are not applicable as they are given in the paper. The published calibration was done with monodisperse aerosols, and the response on heterodisperse aerosols will not be the same. Although various more complex calculation schemes are being developed at Minnesota and by other investigators using the EAA, it was decided to develop a single set of constants that would improve the calculated distributions but would not require complex calculations.

Constants "B" were used for the on-line data reduction performed in Milford. Constants HC were used for all of the results presented in this report.

To develop these new constants, a new matrix applicable to a distributed aerosol was first derived from the Liu-Pui matrix<sup>a</sup>. Then currents for a model distribution having both a nuclei and accumulation mode were calculated. Next, using the  $\Delta N$ 's from the model distribution and the  $I$ 's calculated from the matrix, new sensitivities were calculated so that when the new sensitivities were multiplied by the  $\Delta I$ 's, the model  $\Delta N$ 's are obtained.

These new constants were evaluated against a variety of model distributions before use, and it was concluded that the maximum errors in integral parameters such as VT, ST, and NT were less than 15% for the extreme cases observed in the sulfate study. A complete report on the derivation and calculation of these constants is being written for distribution in early April.

<sup>a</sup>PTL Publication #237



Table I-1. Electrical Aerosol Analyzer Constants for  $nt = 10^7 \text{ cm}^{-3} \text{ sec}^{-1}$

$$\Delta N_i = (\Delta N / \Delta I)_i \quad \Delta I_i = (\Delta N / \Delta I_i)_i (I_{i+1} - I_i)$$

<u>Channel No.</u>	<u>Dpi - <math>\mu\text{m}</math></u>	<u><math>(\Delta N / \Delta I)_i</math> particle/pa</u>	
		(B) <u>Liu - Pui</u>	(HC) <u>Whitby - Cantrell</u>
1	.0042	---	---
2	.0075	$9.52 \times 10^6$	$1.36 \times 10^6$
3	.0133	$4.17 \times 10^5$	$3.16 \times 10^5$
4	.0237	$1.67 \times 10^5$	$1.53 \times 10^5$
5	.0422	$8.70 \times 10^4$	$1.57 \times 10^5$
6	.075	$4.44 \times 10^4$	$3.09 \times 10^4$
7	.133	$2.41 \times 10^4$	$2.43 \times 10^4$
8	.237	$1.23 \times 10^4$	$1.52 \times 10^4$
9	.422	$6.67 \times 10^4$	$5.68 \times 10^3$
10	.750	$3.51 \times 10^3$	$1.33 \times 10^3$

Note: Constants HC developed for DPGVAN = .04  $\mu\text{m}$ ,  
 SGN = 1.7, VAN = 1  $\mu\text{m}^3 \text{cm}^{-3}$ , DPGVAC = 0.35  $\mu\text{m}$ ,  
 SGAC = 2 and VAC = 30  $\mu\text{m}^3 \text{cm}^{-3}$

## Appendix II

### Nomenclature, a Description of Terms and Units

Below are listed the mnemonics, definitions and units for the various parameters referred to in the text.

#### General

TIME                      hours, eastern daylight time

#### Meteorology

WDIR, WD                  wind direction, clockwise degrees from north  
WSPD, WSP                wind speed, kilometers/hr.  
TOUT                      outside temperature, °C  
DEWPT                    dew point, °C  
RH, RELHUM              relative humidity, percent  
PRESS                    barometric pressure, mm-Hg  
BBRAD                    broad band radiation, mW/cm<sup>2</sup>  
UVRAD                    ultraviolet radiation, mW/cm<sup>2</sup>

#### Gas Chemistry

NO                        Nitric Oxide, PPM  
NO<sub>2</sub>                      Nitrogen Dioxide, PPM  
NO<sub>x</sub>                      total Oxides of Nitrogen, PPM  
NO/NO<sub>x</sub>                ratio of Nitric Oxide to total Oxides of Nitrogen

#### Equipment References

EAA                      electrical aerosol analyzer; Thermo-Systems, 3030  
CNC                      condensation nuclei counter, Environment One, RICH 100  
ROYCO 220, R220        Royco model 220 optical particle counter  
ROYCO 225, R225        Royco model 225 optical particle counter  
ROYCO 218, R218        Royco model 218 optical particle counter  
TWO MASS                Impactor - filter sampler with cut point at 2.0 μm

### Aerosol Mass Fraction

SC	calculated sulfur concentration $\mu\text{g}/\text{m}^3$
SM	measured sulfur concentration, $\mu\text{g}/\text{m}^3$
$\rho$	Aerosol particle density, g/cc

### Particle Size Distribution

DP	particle diameter-interval boundary, $\mu\text{m}$
DPI	particle diameter-geometric midpoint, $\mu\text{m}$
DN	particle number concentration, in a size interval number/cc
DN/DLDP	particle number concentration per log-size interval, $\text{No}/\text{cc} \cdot \log D_p$
DS	surface area concentration, in a size interval, $\text{mm}^2/\text{cc}$
DS/DLDP	surface area concentration per log-size interval, $\mu\text{m}^2/\text{cc} \cdot \log D_p$
DV	volume concentration, in a size interval, $\mu\text{m}^3/\text{cc}$
DV/DLDP	volume concentration per log-size interval, $\mu\text{m}^3/\text{cc} \cdot \log D_p$

### Integral Particle Parameters

BSCAT	light scattering coefficient, $\text{m}^{-1}$ (nephelometer data)
ANC, CNC	Aitken Nuclei concentration, number/cc
1,2,3,4,5	particle size subranges, see diagram above.
NT,ST,VT	total number, surface area, and volume concentrations
N2,S2,V2	number, surface area, and volume concentrations in subrange -2
N3,S3,V3	number, surface area, and volume concentrations in subrange-3
N4,S4,V4	number, surface area, and volume concentrations in subrange-4
N5,S5,V5	number, surface area, and volume concentrations in subrange-5

### Integral Particle Parameters (cont.)

N3-,S3-,V3-	number, surface area, and volume concentrations in subranges 2 & 3
N4+,S4+,V4+	number, surface area, and volume concentrations in subranges 4 & 5

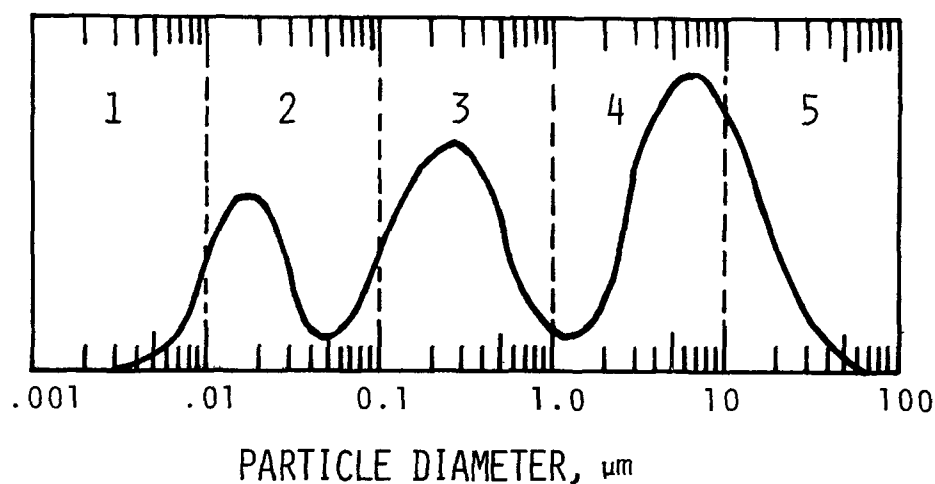


Figure II-1. Particle Size Subranges

### Modal Fit Parameters

VAN	volume in the Aitken Nuclei mode, $\mu\text{m}^3/\text{cc}$
VAC	volume in the accumulation mode, $\mu\text{m}^3/\text{cc}$
VCP	volume in the coarse particle mode, $\mu\text{m}^3/\text{cc}$
VFP = VAN + VAC	volume of fine particles, $\mu\text{m}^3/\text{cc}$
SGAN, SGAC, and SGCP	Geometric Standard Deviations of the AN, AC and CP modes respectively
DPGVAN, DPGVAC, and DPCVCP	Geometric Mean Diameter of the AN, AC and CP modes respectively $\mu\text{m}$ .
NTM	total number concentration derived from the log-normal distributions fitted to the data, No./cc.

#### ACKNOWLEDGMENTS

The work was performed under the financial support of Environmental Protection Agency Research Grant No. R 803851, Aerosol Research Branch, Environmental Sciences Research Laboratory. Since we were not requested to participate until July 1975, our participation was only made possible by the efforts of W. E. Wilson of the EPA, the program officer, who arranged funding in a short time.

The authors would like to thank Ping Auw and Kui-Chiu Kwok for their help during the assembly of the car; Dr. V. Marple for his help in locating and arranging the lease of the car; Mr. Ruben Falldin, Mechanical Engineering Department shop superintendent, for his help in getting things done on very short notice; and Dr. R. Jordan, Head of the Mechanical Engineering Department, for his help in making the many arrangements that such a project entails. We would also like to thank Tom Ellestad, Lester Spiller, and Ron Speer of EPA for their help during operations in Milford.

#### REFERENCES

1. GMR - 1967 "Plans for General Motors Sulfate Dispersion Experiment," General Motors Environmental Science Department Research Laboratories, Warren, Mich., (Sept. 1975).
2. E. S. Macias and R. B. Husar, "A Review of Atmospheric Particulate Mass Measurement Via the Beta Attenuation Technique," *Fine Particles: Aerosol Generation, Measurement, Sampling, and Analysis*, pp. 535 Academic Press New York (1976).
3. J. D. Husar, R. B. Husar and D. K. Stibits, *Analy. Chem.* 47:2062 (1975).
4. B. Y. H. Liu and D. Y. H. Pui, "A Sub-Micron Aerosol Standard, and the Primary Absolute Calibration of the Condensation Nuclei Counter," *J. Colloid Interface Sci.* 47:155-171 (1974).
5. B. Y. H. Liu, R. N. Berglund and J. K. Agarwal, "Experimental Studies of Optical Particle Counters," *Atmos. Environ.* 8:717-732 (1974).

6. B. W. Loo, J. M. Jaklevic and F. S. Goulding, "Dichotomous Virtual Impactors for Large Scale Monitoring of Airborne Particulate Matter," *Fine Particles: Aerosol Generation, Measurement, Sampling, and Analysis*, Academic Press, pp. 311 New York (1976).
7. K. T. Whitby and B. K. Cantrell, "Atmospheric Aerosols - Characteristics and Measurements," Presented at ICESA Conference, Las Vegas, Nev. (Sept. 1975).
8. K. T. Whitby "On the Multimodal Nature of Atmospheric Aerosol Size Distributions," presented at the VIII International Conference on Nucleation, Leningrad, U.S.S.R. (Sept. 1973).
9. K. T. Whitby, "Modeling of Multimodal Aerosol Distribution," presented at GAF, Bad Soden, Germany (1974).
10. K. T. Whitby "Modeling of Atmospheric Aerosol Size Distributions," Report on Grant #R 800971, "Sampling and Analysis of Atmospheric Aerosols," submitted to Atmospheric Aerosol Res. Sec., Div. of Chem. and Phys., Air Pollution Control Office, Environmental Protection Agency (May 1975).
11. J. A. Nelder and R. Mead, *The Computer J.* 7:308 (1965).
12. D. F. Miller, D. A. Trayser and D. W. Joseph, "Size Characterization of Sulfuric Acid Aerosol Emissions," Presented at the 1976 Automotive Engineering Congress and Exposition, Feb. 23-27, Detroit, Mich. (1976).

PARTICULATE SULFUR EMISSION RATE FROM A SIMULATED FREEWAY  
E. S. Macias, R. A. Fletcher, J. D. Husar, and R. B. Husar\*

ABSTRACT

*The particulate sulfur emission rates from a roadway traversed by catalytic converter equipped cars was determined by measuring the particulate sulfur concentration profile and vertical wind velocity profile 15m from the edge of the road. Filter samples were collected in half-hour intervals with two stage samplers and were subsequently analyzed for sulfur, using the flash vaporization-flame photometric detection method. Particulate mass was also monitored with a beta attenuation mass monitor. The sulfur flow rate for this experiment was found to be  $5.3 \pm 1.2$   $\mu\text{g}/\text{m}/\text{sec}$  and the sulfur emission rate per car was  $3.5 \pm 0.8$   $\mu\text{g}/\text{m}$ . This corresponds to a  $12. \pm 3.0\%$  conversion of the fuel sulfur emitted as particulate sulfur. It was also found that sulfur accounted for approximately 20% of the fine particulate mass. Measurements in an automobile indicated that the sulfur concentrations on the roadway and inside a passenger vehicle were comparable and were similar to the concentrations measured 15m downwind.*

INTRODUCTION

Gasoline contains trace quantities of sulfur, on the order of 0.03 weight percent. From non-catalyst equipped cars, the sulfur is emitted largely as  $\text{SO}_2$ . In catalyst equipped cars, however, a substantial portion of the fuel sulfur may be emitted in oxidized form. The current available data (ref. 1) suggest that most of the sulfate emissions have the chemical form of sulfuric acid. At present,

---

\*The authors are with Washington University, St. Louis, Missouri, where Drs. Macias and Fletcher are in the Department of Chemistry and the Drs. Husar are in the Department of Mechanical Engineering.

# GM PROVING GROUND SULFATE DISPERSION STUDY

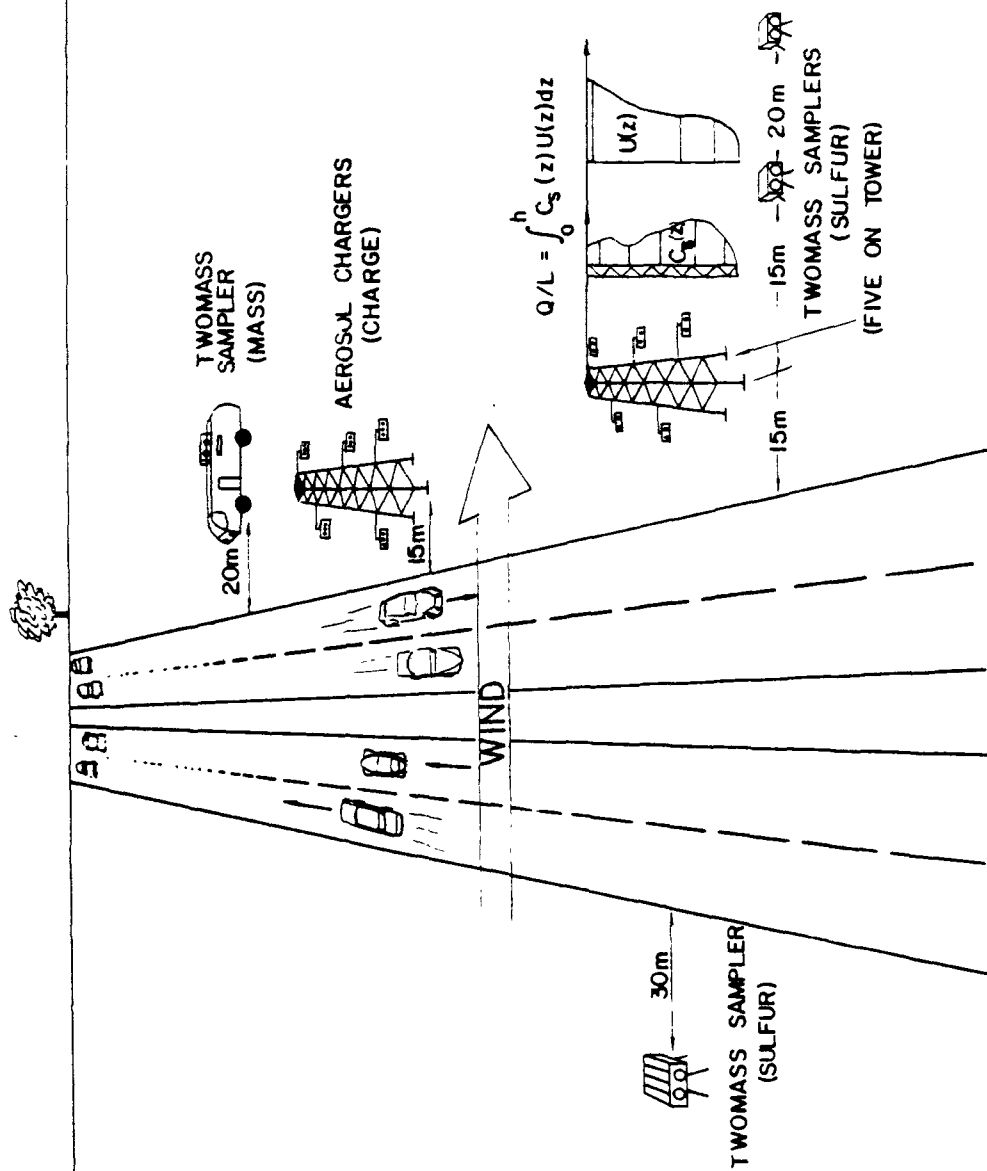


Figure 1 Schematic diagram of the experimental arrangement at the GM Proving Grounds.



however, the only information available is from dynamometer tests. In this paper we present results of measurements of roadway aerosol emission rates obtained as participants in the GM Sulfate Dispersion Study during October 1975.

The primary objective of this work is the determination of the particular sulfur emission rate from the roadway. The method employed was the determination of the roadway particulate sulfur flow rate across a plane 15m from the edge of the road. The fine particulate sulfur concentration was determined at five heights above the ground at 15m from the road as shown in figure 1. The wind velocity profile perpendicular to the roadway was measured at three heights above the ground and at 15m from the road. The automobile generated particulate sulfur level was distinguishable from a background level of comparable magnitude by employing high time resolution sampling (30 min) using a two stage on-line mass monitor with aerosol size separator (TWOMASS) sampler (refs. 2-4) and high sensitivity sulfur analysis using the flash vaporization-flame photometric detection methods (refs. 5, 6). The total mass concentration of both fine and coarse particles was determined in 10-minute intervals using a TWOMASS automated mass monitor located in a van.

A TWOMASS sampler was also operated by the University of Minnesota in a car traveling with the test fleet. These filter samples were also analyzed for sulfur.

Four aerosol charge detectors and three high response anemometer bivanes were operated at several heights above the ground to illustrate the aerosol concentration and flux fluctuation with subsecond time resolution. This work will be reported in a later paper.

The daily configuration of the Washington University experiment is given in table 1.

Table 1. Experiment Summary

Date	Run	Equipment in Operation			Aerosol Chargers	Prevailing Wind Direction
		TWOMASS Sulfur Samplers		TWOMASS Mass Analyser		
		On Towers	In Car			
9/29/75	272	5				E
10/1/75	274	7			5	NW
10/2/75	275	7			5	NW-N
10/3/75	276	7		1	5	SW
10/6/75	279	7	1	1	5	W
10/8/75	281	7	1	1	5	E
10/10/75	283	9	1	1		W
10/13/75	286	9	1	1		SW
10/17/75	290	10	1		4	NE
10/20/75	293	9			4	W
10/21/75	294	9	1		4	SW
10/22/75	295	10	1		4	NE
10/23/75	296		1			S
10/24/75	297	9	1		4	S
10/27/75	300	9			4	SW
10/29/75	302	9				N

NOTE: West wind component required for useful data.

## EXPERIMENTAL PROCEDURES

### A. Test Conditions

The experiment was conducted on the 10km North-South Straightaway at the GM Proving Ground in Milford, Michigan during October 1975. The Proving Ground is located about 50km northwest of Detroit and 30km north of Ann Arbor in a very flat, lightly wooded area. The test track is 30m (6 lanes) wide; however, the experiment was conducted with two lanes of traffic in each direction simulating a four-lane freeway.

The test fleet consisted of 350 catalyst-equipped vehicles from model years 1975 and 1976 (equipped with air pumps) with relatively low mileage (1000-5000 miles). The vehicles were driven in packs of 22, synchronized so that two packs (one in each direction) arrived at the experiment site simultaneously every 29 seconds; therefore, the automobiles arrive in pulses of 44 vehicles every 29 seconds or 5462 vehicles per hour. The fuel used was Amoco unleaded, with a sulfur content of  $0.33 \pm 0.0005$  weight percent. The fleet had a weighted average fuel consumption calculated from EPA dynamometer tests on similar models of 7.74 kilometers per liter (18.2 miles per gallon). Actual fuel consumption figures for the GM test fleet were not available; therefore, we have assumed a realistic fleet average value of 6.97 kilometer per liter (16.4 miles per gallon), which is 90% of the EPA test value. A typical run was conducted as follows: at 0715 (E.S.T.) vehicles began to arrive on test track, and the test run was conducted from 0745-0945. By 1000, all vehicles were off test track.

### B. Aerosol Sampling

Aerosol sampling was performed with the TWOMASS sampler which separates particles into two size fractions. Coarse particles are impacted on a glass fiber filter; the remaining particles are collected on an identical high-efficiency glass fiber filter. This system is

shown schematically in figure 2. The single stage impactor head has a 4.5mm diameter inlet aperture with a 4.5mm jet-to-plate distance. The impactor was designed to have 50% efficiency for 3.5  $\mu\text{m}$  particles. This cutoff size was chosen as a compromise between the proper separation of the two modes of the atmospheric aerosol size distribution and the simulation of the aerosol removal characteristics of the human upper respiratory system.

One sampler was located at 30m west of the roadway at a height of 1m and five samplers were located 15m east of the roadway at heights of 1.0, 1.9, 3.9, 5.6, 8.2m. One to four additional samplers were operated at various heights and distances from the roadway. Results from these extra samplers were used for cross-comparison and determination of internal consistency. These samplers were used to collect aerosol for sulfur analysis. One additional TWOMASS sampler located in a van 20m from the roadway at a height of 3m was fully instrumented for particulate mass analysis as described below.

The samplers were synchronized to advance the filter tape and begin a new sample every 30 minutes on the half hour. The filter tape on the TWOMASS mass monitor in the van advanced at 0700 and 1100. Samples taken between 0800-0930 were used to determine the roadway aerosol contribution. Samples taken between 0630-1730 and 1000-1100 were used to determine background concentrations.

The horizontal and vertical wind conditions were determined by GM at 15m east of the roadway at heights of 1.5, 4.5, and 10.5m above the ground.

### C. Atmospheric Particulate Mass Measurement

A TWOMASS sampler employing the beta attenuation technique was used for high resolution monitoring of atmospheric aerosols as shown in figure 2. This instrument independently analyzed the mass concentrations of two particle size fractions in 10 minute intervals. Both the impaction and filtration heads of the TWOMASS had independent source detector systems. Carbon-14 was used as a source of beta

# TWOMASS

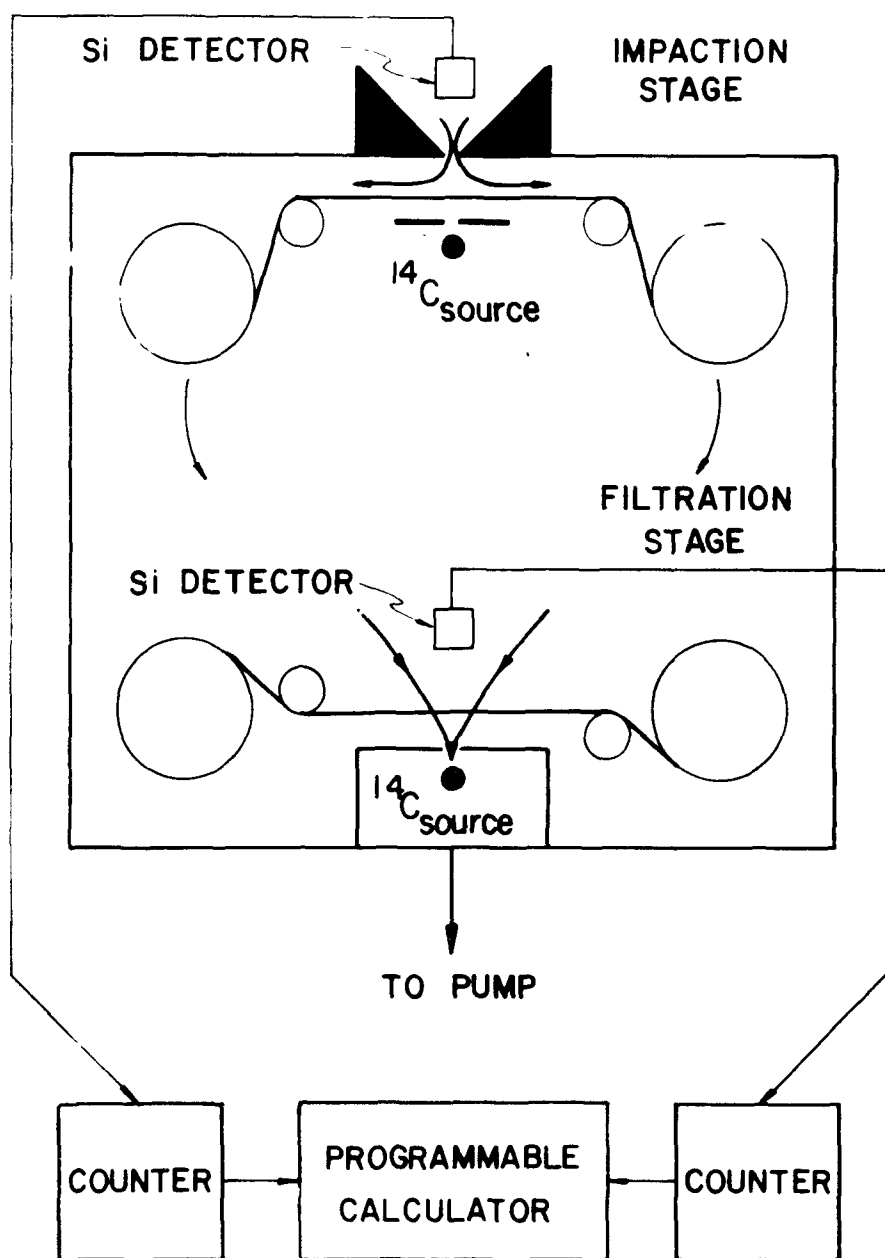


Figure 2 Schematic diagram of the TWOMASS sampler and mass monitor.

particles which were detected by a solid state surface-barrier detector. The accuracy of the aerosol mass concentration with this instrument is 11%, with a precision of  $4 \mu\text{g}/\text{m}^3$ .

#### D. Particulate Sulfur Analysis

Analysis of water soluble fine particulate sulfur was performed using a flash vaporization-flame photometric detection method (refs. 5,6). The analyzing system shown in figure 3 consists of a flash vaporization vessel, flame-photometric detector, integrator and strip chart recorder. The sample vaporization is accomplished by capacitor discharge across a tungsten boat, resulting in resistance heating to  $1100^\circ\text{C}$ . Vaporized gaseous decomposed products of sulfur compounds are carried to the flame-photometric detector by a stream of clean, charcoal filtered air at a flow rate of  $2 \text{ cm}^3/\text{sec}$ . The detector used in the Meloy SA-160 flame-photometric total sulfur sensor.

Samples were collected with TWOMASS samplers on a portion ( $0.3 \text{ cm}^2$ ) of a light weight ( $1.9 \text{ mg}/\text{cm}^2$ ) low pressure drop glass-fiber filter (Pallflex E 70/2075 W) with a consistent and low sulfur blank of  $0.36\text{--}0.5 \mu\text{g}/\text{cm}^2$ . A water extract of each fine particulate sample was prepared by punching out a circular filter segment ( $0.6 \text{ cm}^2$ ) containing the aerosol deposit ( $0.3 \text{ cm}^2$ ). The segments were extracted in double distilled-deionized water. The sulfur samples were collected over one-half hour intervals. Under the conditions of this experiment, for an uncertainty of 11%, the minimum detectable ambient sulfur concentration was  $0.44 \mu\text{g}/\text{m}^3$  (ref. 6). This includes inaccuracies in sample air volume determination, sulfur determination and variations in sulfur blank on the filter. The fine particle sulfur concentration determinations from this work are given in table 2.

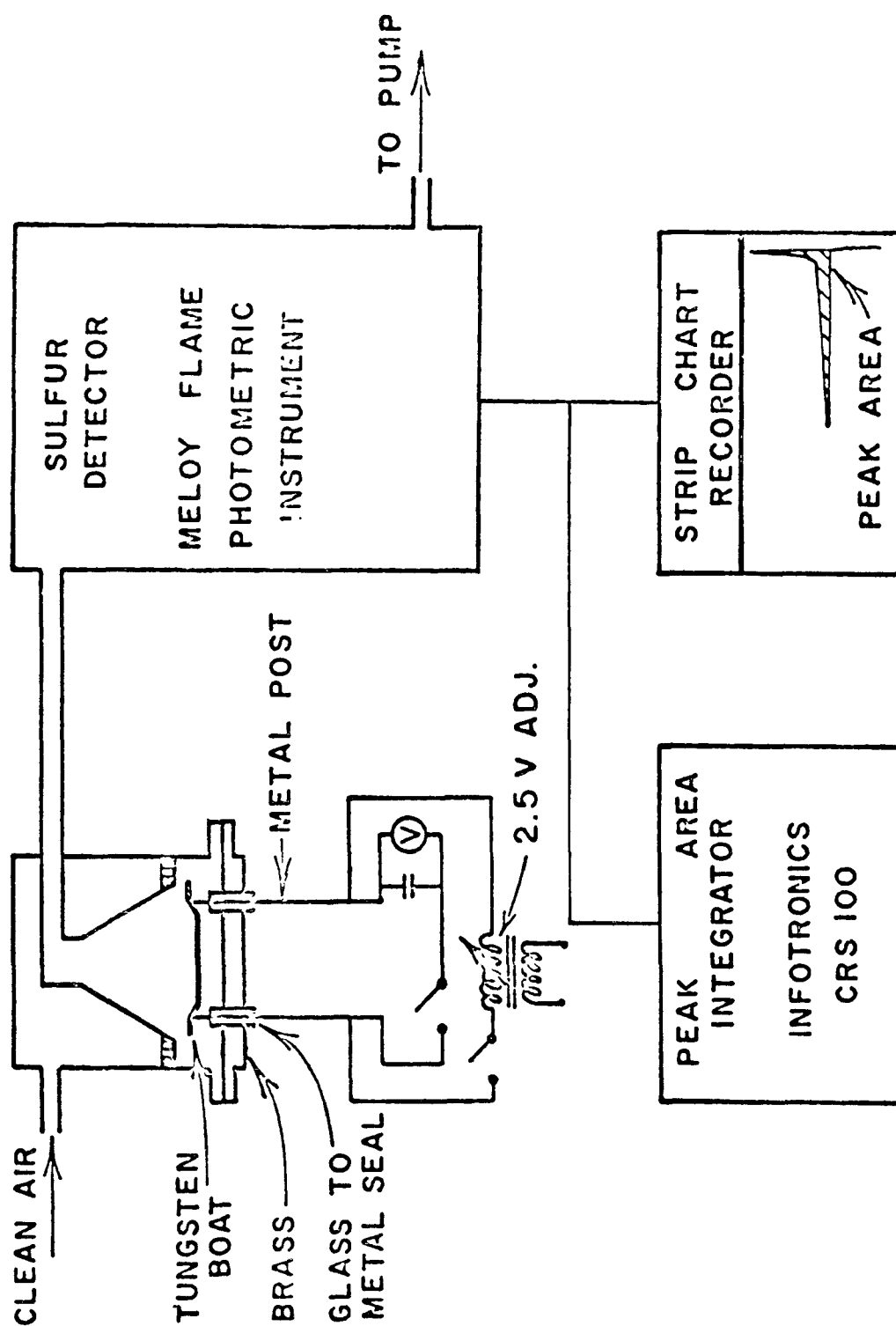


Figure 3 Schematic diagram of the sulfur detection system.

Table 2. Fine Particle Sulfur Concentration.  
30 min Average Values Ending at Time Indicated  
(in  $\mu\text{g}/\text{m}^3$ )

Date	Run	Tower	Height (m)	Time (EDT)		0800	0830	0900	0930	1000	1030	1100	
				0700	0730								
9/29/75	272	GM 5 (15m East)	1.0				1.18	1.89	2.81	8.63			
			1.9				1.74	4.21	12.67	12.15			
			3.6				0.15	3.13	3.30	9.53			
			5.6				0.65	1.16	3.32	8.23			
			8.2				4.03	4.03	4.03	4.03			
10/1/75	274	GM 1 (30m West)	1.0	Time (EDT)		1400	1430	1500	1530	1600	1630		
				1300	1330								
			1.0	0.38	2.46	1.23	0.26	0.39		0.58	0.75		
		GM 5 (15m East)	1.0	0.42	1.20	2.23	1.71	0.81	1.45	2.77	0.51		
			1.9	0.02	0.165	0.0	0.44	0.56	0.165	1.09	0.07		
			8.2	0.46	0.03	0.08	0.07	0.11	0.71	0.38	0.35		
10/10/75	283	GM 1 (30m West)	1.0	Time (EDT)		0800	0830	0900	0930	1000	1030	1100	
				0700	0730								
			1.0	2.80			2.04	2.45	2.76	2.77	3.01		
		GM 5 (15m East)	1.0			3.39	3.84	3.62	3.84	3.48	2.99		
			1.9		2.97	3.26	3.48	3.48	3.60	3.15	2.57	2.23	
			3.6		3.12	3.13	2.72	3.93	3.73	3.43	2.61	3.22	
			5.6		2.46	2.79	2.66	3.01	2.66	2.42	2.14	2.35	
			8.2		2.77		2.91	3.19	3.48	3.89	3.45		
		GM 6 (30m East)	1.0			7.30	4.71	4.23	4.17	3.37	3.21	3.49	
		GM 7 (50m East)	1		3.31	3.16	3.00	2.80	2.95	2.74	2.38	2.54	
10/13/75	286	GM 1 (30m West)	1.0	Time (EDT)		0800	0830	0900	0930	1000	1030	1100	
				0700	0730								
			1.0	1.48	1.39	1.51	1.50	2.12	1.79	1.91	2.14	2.16	
		GM 5 (15m East)	1.0	1.52	1.64	2.02	2.73	3.03	3.50	3.00	3.37	2.63	
			1.9	1.44	1.88	2.63	3.29	3.51	3.59	1.44	2.72	3.50	
			3.6	1.20	1.49	2.43	2.96	2.17	2.09	2.49	1.64	2.30	
			5.6	1.12	1.66	2.09	2.17	2.26	1.85	2.88	2.65	2.70	
			8.2	1.48	3.38	1.45	2.20	2.25	3.10	2.44	2.46	2.45	
		GM 6 (30m East)	1.0		1.02	1.17	1.78	1.60	1.94	1.84	1.28	1.40	
		GM 7 (50m East)	1.0		1.68	2.42	2.15	2.69	2.65	3.04	2.99	2.70	
10/20/75	293	EQR (15m East)	1.0	Time (EDT)		1130	1200	1245	1300				
				1030	1100								
			1.0	1.00	1.34	1.75	1.92	1.17	1.17				
			1.0	0.31	1.14	0.82	1.45	0.95	1.12				
10/21/75	294	EQR (15 m East)	1.0	Time (EDT)		0800	0910	0940	1022	1132	1200	1215	1250
				0735									
			1.0	2.02	2.40	3.52	4.36	5.32	2.37	1.43	2.73	3.19	
			1.0	1.40	1.70	8.24	2.10	1.69	1.72	0.55	1.71	1.15	
10/24/75	297	EQR (15 m East)	1.0	Time (EDT)		0800	0830	0900	0930	1000	1030	1100	
				0700	0730								
					4.47	3.34	3.64	3.27	4.03	5.34	4.53	2.52	
10/27/75	300	GM 1 (30 m West)	1.0	Time (EST)		0800	0830	0900	0930	1000	1030	1100	
				0700	0730								
					1.49	1.39	1.69	1.65	1.33	1.29	1.51	1.53	
10/29/75	302	GM 5 (15m East)	1.0	Time (EST)		0800	0830	0900	0930	1000	1030	1100	
				0700	0730								
			1.0		1.60	2.20	2.80	1.72	3.08	2.24	1.20	1.20	
			1.9		2.07	2.99	3.04	2.94	3.11	2.60	1.60	1.95	
			3.6		1.23	1.62	2.11	1.69	2.94	2.02	1.51	1.36	
			5.6		1.87	1.97	2.00	2.48	2.30	1.69	1.42	1.33	
			8.2		1.39	1.77	1.91	2.17	1.97	1.46	1.22	1.48	
		EQR (15 m East)	1	1.46	2.31	2.90	3.07	3.20	3.21	1.47	2.20	1.92	
10/29/75	302	EQR (15 m East)	1	0.26	0.48	0.93	0.75	0.75	0.43	0.33	0.11		
		GM 1 (30 m West)	1		0.72	0.21	0.095	0.42	1.14	0.40	0.55	0.44	
		GM 1 (15 m East)	1		0.36	0.25	0.66	0.78	0.92	1.21	1.97	0.29	
			1.9		0.50	1.11	1.07	2.10	1.07	0.34	0.48	0.20	
			3.6		0.07	0.43	0.93	0.78	0.48	0.17	0.63	0.11	
			5.6		0.49	0.44	1.07	1.12	0.85	0.20	0.0	0.20	
			8.2		0.04	0.76	0.41	0.71	0.69	0.17	0.0	0.01	



## RESULTS

### A. Particulate Sulfur Emission Rate from the Simulated Freeway

The particulate sulfur flow rate across a plane was determined by simultaneous measurement of the particulate sulfur concentration profile and wind velocity profile 15m downwind from the edge of the roadway. The flow rate per unit length of the roadway ( $Q/L$ ) is determined by the separate measurement of the fine particulate sulfur concentration as a function of height [ $C_s(z)$ ], and the component of the velocity profile perpendicular to the roadway [ $U(z)$ ]. This flow rate is calculated from the following integral:

$$Q/L = \int_0^h C_s(z)U(z) dz .$$

It is assumed that this flow rate corresponds to the actual emission rate, which is valid for fine particulates, but is not correct for settling coarse particles. The average emission rate per car per unit length of roadway can be calculated by dividing this flow rate by the traffic density.

The particulate sulfur concentration from each sampler was determined in half-hour averages. A linear interpolation of sulfur concentration from samples collected prior to and after each run was used to determine the background concentrations. A sampler located 30m upwind was used to monitor the temporal variation of the background during each run and was used as a check on the linear background used. The sulfur contribution from the roadway was obtained by subtracting the background concentration from each half-hour sulfur measurement. It should be noted that the background concentration was at least as large as the roadway contribution and it should be mentioned that as in figure 4, on some days the background varied as a function of time.

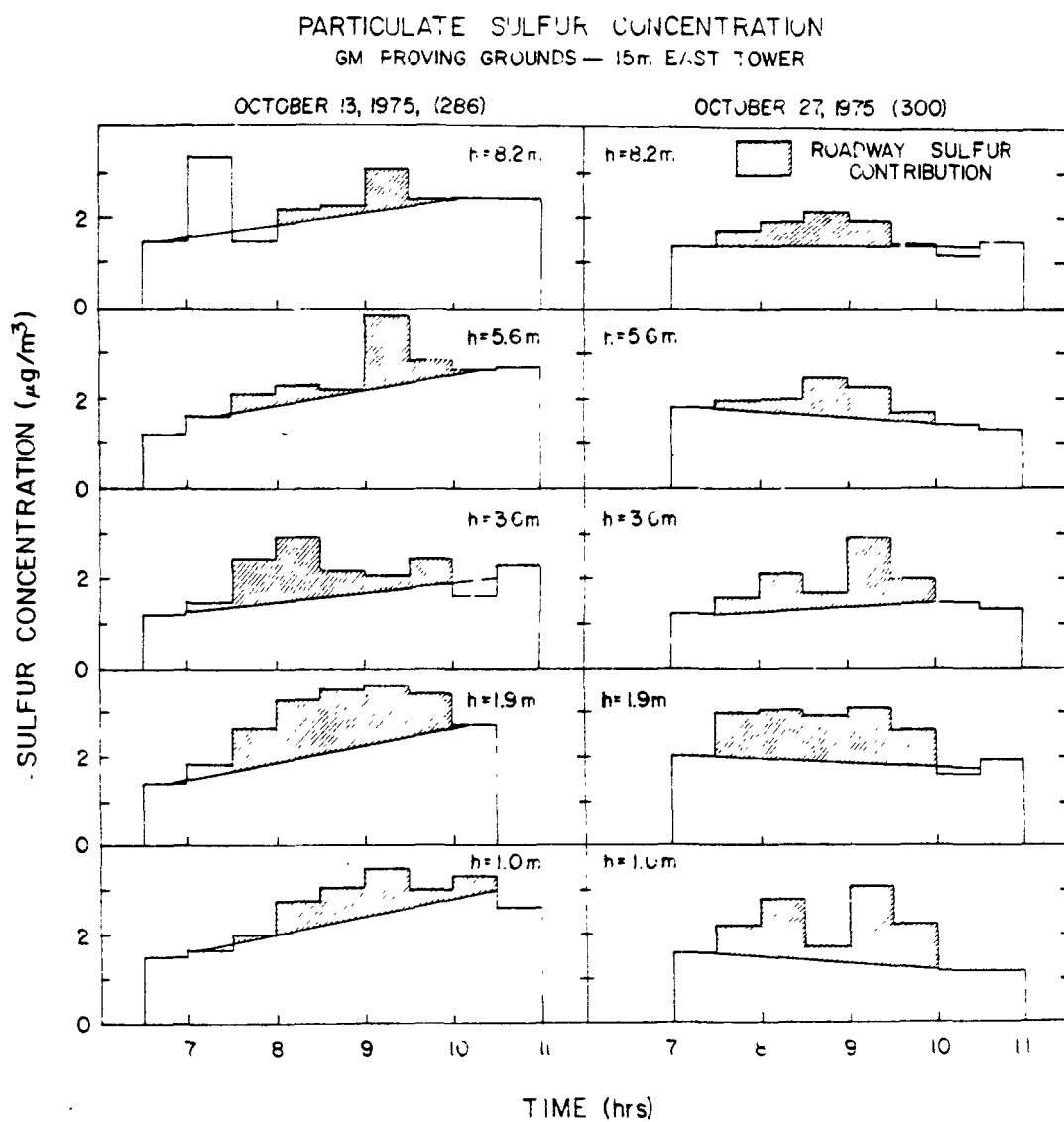


Figure 4 Half-hour average sulfur concentration data from runs 286 and 300. The shaded area is the excess sulfur concentration due to the roadway.

The excess sulfur concentrations due to the roadway for run 286 (10/13) and 300 (10/27) at the five heights (1.0, 1.9, 3.6, 5.6, and 8.2m) are shown as the shaded area in figure 4. The excess sulfur values generally vary between 0-1.5  $\mu\text{g}/\text{m}^3$ . At a height of 2m (approximately the height of an adult), for run 286 (10/13), the average roadway particulate sulfur concentration was 1  $\mu\text{g}(\text{S})/\text{m}^3$ .

The vertical variation of roadway particulate sulfur concentration and the wind profile perpendicular to the roadway was determined for each half-hour interval and then averaged for the entire run as shown in figure 5. The third frame of this figure shows the vertical profile of the horizontal roadway particulate sulfur flux,  $C_s(z)U(z)$ , in units of  $\mu\text{g m}^{-2}\text{sec}^{-1}$ . Numerical integration of the flux with respect to height yields the flow rate per unit length of roadway Q/L. It is evident from figure 5 that the roadway plume height exceeded 9m. This phenomenon has also been observed in the aerosol charge profile measurements. The concentration profile above 8.2m was estimated as indicated by the dashed portion of the curve. The half-hour average flow rates for the four runs analyzed in detail are given in table 3. Half-hour average sulfur concentration data from runs 286 and 300 (October 13 and 27) are shown in figure 4. The wind direction on run 302 (10/29) was within 15% of being parallel with the roadway. Under these wind conditions, measurement of the sulfur flow rate by this technique gives results with large uncertainties. Therefore, the data from this run will not be included in the determination of the particulate sulfur emission rate.

The particulate sulfur flow rate from the roadway averaged over the entire experiment was  $5.3 \pm 1.2 \mu\text{g}/\text{m}/\text{sec}$ . For the traffic density of this experiment, 1.52 cars/sec, the particulate sulfur emission rate per car was  $3.5 \pm 0.8 \mu\text{g}/\text{m}$  ( $5.6 \pm 1.3 \text{ mg}/\text{mile}$ ). This emission rate corresponds to a  $12 \pm 3.0\%$  conversion of the fuel sulfur emitted as particulate sulfur using the fuel sulfur content and fuel consumption rate given above.

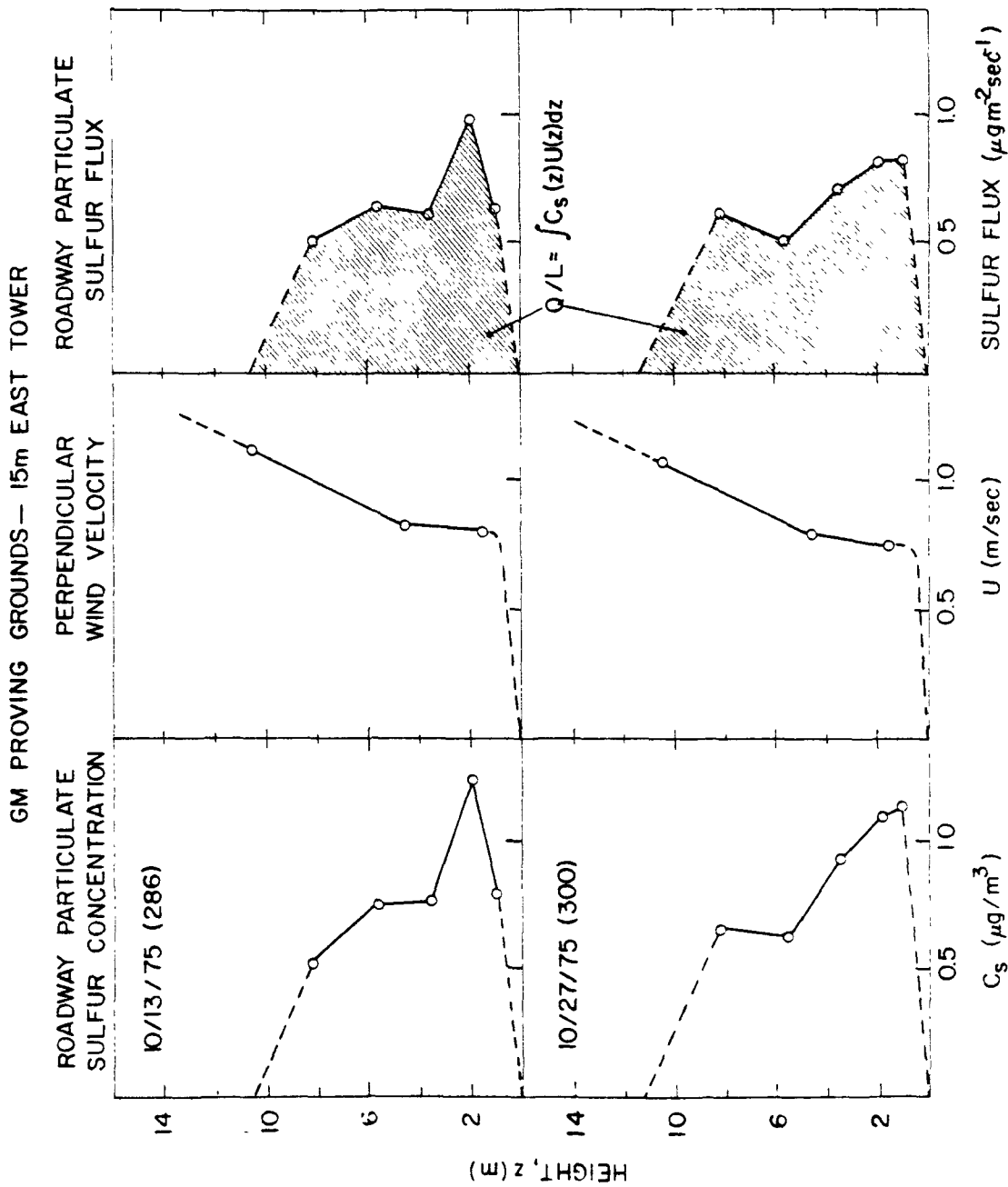


Figure 5 The vertical profile of roadway particulate sulfur concentration, wind velocity perpendicular to the roadway, and roadway particulate sulfur flux determined from runs 286 and 300.

Table 3. Sulfur Flow Rates, Q, ( $\mu\text{g}/(\text{m}\cdot\text{sec})$ )

Half-hour Ending Time	Run			
	283	286	300	302
0830	2.4	4.2	5.2	2.7
0900	4.6	3.7	5.1	1.2
0930	4.6	10.5	7.6	---
Daily Average	3.9	6.1	5.9	2.0

#### B. Roadway Aerosol Mass

The TWOMASS mass monitor gave no indication of an increase in coarse particle mass during the experiment due to the roadway. The fine particle mass did show a definite roadway component as indicated by the shaded portion in figure 6. The mass monitor indicated an average fine particle mass increase due to the roadway of  $4.4 \pm 0.8 \mu\text{g}/\text{m}^3$  for four days of the experiment. These measurements and the sulfur measurements were made at a different distance from roadway and, therefore, can not be directly compared. However these data indicate that sulfur accounts for approximately 20% of the fine particle mass.

#### C. Temporal Variability of the Roadway Aerosol

The driving pattern of the GM test runs was such that packs of automobiles arrived at the sampling site in 29-second intervals; thus, the source intensity was pulsed with the period of half a minute. The use of rapid response aerosol detection devices, such as the aerosol charger, permits the temporal resolution of the emission strength as shown in figure 7. This typical chart recording of the charger output clearly indicates the periodicity of the concentration with a period of 29 seconds. The data suggest the utility of the charger for diffusion experiments and other cases where time resolution is important.

It may also be noted that the charger signal downwind of the simulated freeways was about  $3 \times 10^{-12}$  amps which is about a factor of 20 to 50 higher than the charge values for background aerosol - that is, upwind of the roadway.

#### D. Particulate Sulfur Concentration on the Roadway

Fine particulates sampled inside and external to the passenger compartment of the University of Minnesota vehicle driving in the test fleet were analyzed for sulfur in order to assess the particulate sulfur concentrations on the roadway. These data, summarized in

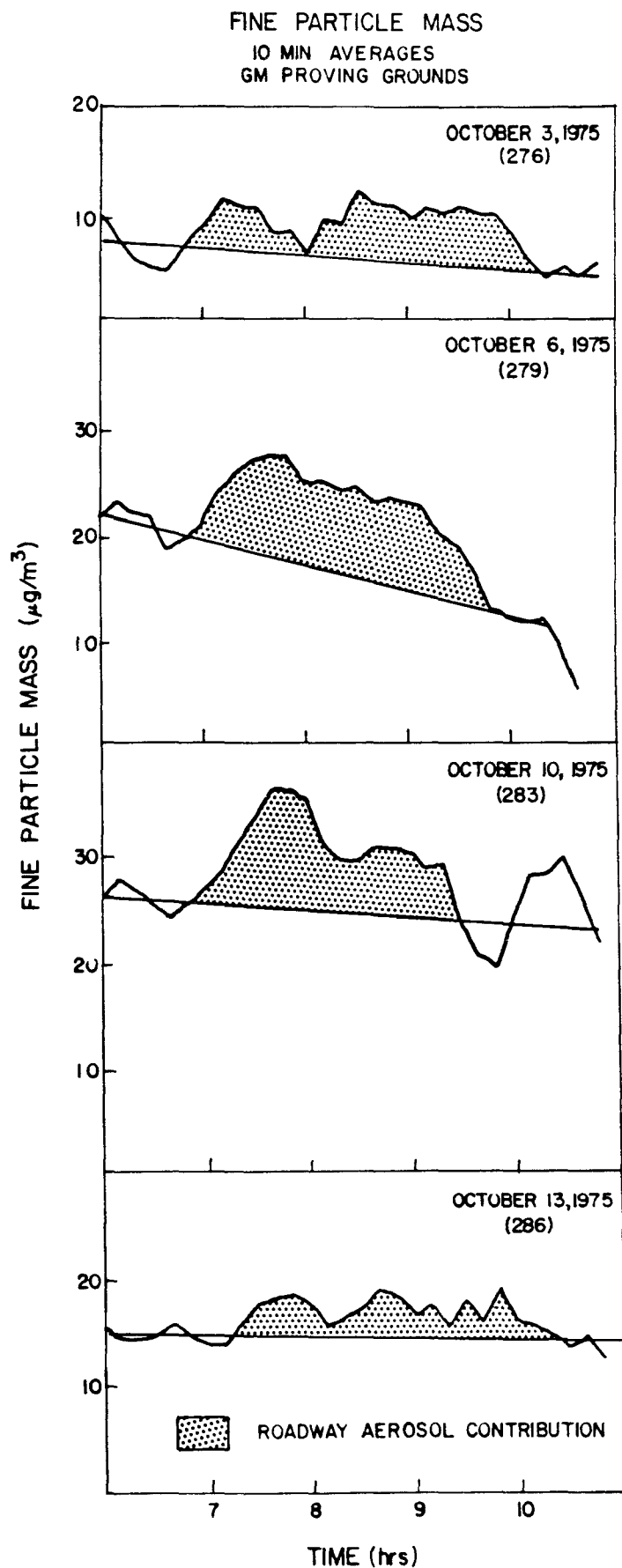


Figure 6 10 min average fine particle mass concentration data. The shaded area is the excess fine particle mass due to the roadway.

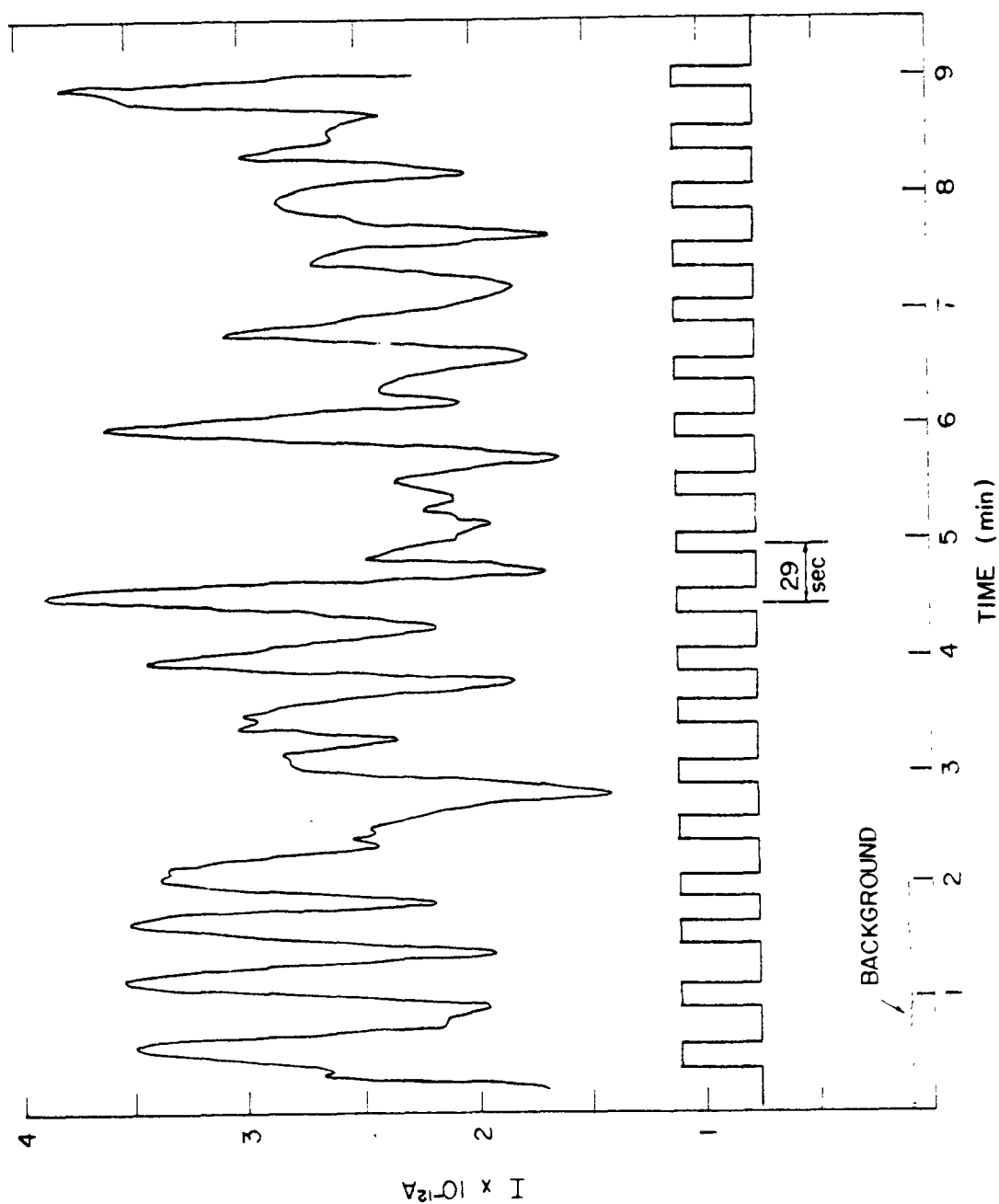


Figure 7 Typical chart recording of the aerosol charge detector output as a function of time. The periodicity of the vehicle pack passage with a period of 29 sec is also shown in the figure..



Table 4. Roadway Particulate Sulfur Concentration,  $\mu\text{g}/\text{m}^3$

Particulate Sulfur Concentration During Run

Date	Run	Samplers Mounted on Automobile in Test Fleet			Sampled Air in Passenger Compartment	Sampler Mounted 15 m E of Roadway h = 1 m	Background	Wind Direction
		Sampled External Air	TM <sup>a</sup>	LV <sup>b</sup>	Ave <sup>c</sup>			
10/10/75	283	3.1	5.8	4.4	5.1	3.8	2.4	W
10/13/75	286	3.4	2.9	3.2	3.2	3.1	2.3	SW
10/17/75	290	2.3	2.1	2.2	2.6	---	---	NE
10/21/75	294	3.2	2.7	3.0	---	2.8	1.6	SW
10/23/75	296	5.4	5.5	5.4	4.7	---	---	S
10/24/75	297	4.4	3.7	4.1	3.0	3.6	3.5	S

<sup>a</sup>Results from TWOMASS Sampler

<sup>b</sup>Results from Low Volume Sampler

<sup>c</sup>Average of TWOMASS and Low Volume Sampler results

table 4, indicate that under a variety of wind conditions, the particulate sulfur concentrations were comparable within experimental error inside and outside the vehicle. Furthermore, these concentrations were about the same as the concentrations measured at 15m from the roadway.

### CONCLUSIONS

In this study, we have measured the sulfur emission rate from automobiles traveling on a simulated freeway in order to assess the impact of automobiles, specifically those equipped with catalytic converters, on the ambient particulate sulfur levels. The particulate sulfur emission rate per car was determined to be  $3.5 \pm 0.8 \mu\text{g/m}$ . This corresponds to a  $12 \pm 3.0\%$  conversion of the fuel sulfur into emitted particulate sulfur. It was also found that sulfur accounted for approximately 20% of the fine particulate mass. Measurements in an automobile indicated that the sulfur concentrations on the roadway and inside a passenger vehicle were comparable and were similar to the concentrations measured 15m downwind.

### ACKNOWLEDGMENT

The authors are deeply grateful to the General Motors Corporation for their hospitality during this experiment. Thanks go to Dr. Steven Cadle of the GM Technical Research Center for his help in providing wind data and information on the test fleet. The authors are also grateful to Dr. William Pierson for his comments on this work.

This work was supported in part by the U. S. Environmental Protection Agency under grant OZR80389601.

### REFERENCES

1. W. R. Pierson, "Sulfuric Acid Generation by automotive Catalysts," paper #42, Symposium on Auto Emission Catalysis, Div. of Colloid and Surface Chem., ACS 170th National Meeting, Chicago, August 27, 1975; *Chem. Technol.* (to be published)

2. E. S. Macias and R. B. Husar, "A Review of Atmospheric Particulate Mass Measurement via the Beta Attenuation Technique," In: *Proc. of the Symposium on Fine Particles*, Minneapolis, Minn. (1975).
3. E. S. Macias and R. B. Husar "High Resolution On-Line Aerosol Mass Measurement by the Beta Attenuation Technique," In: *Proc. of the Second International Conference on Nuclear Methods in Environmental Research*, Vogt, J. R. (ed.) USAEC, Oak Ridge, Tenn., 1975.
4. E. S. Macias and R. B. Husar "Atmospheric Particulate Mass Measurement with the "TWOMASS" Beta Attenuation Mass Monitor," Submitted for publication, 1975.
5. J. D. Husar, R. B. Husar and P. K. Stubits, "Determination of Submicrogram Amounts of Atmospheric Particulate Sulfur," *Anal. Chem.* 47, 26062, 1975.
6. J. D. Husar, R. B. Husar, E. S. Macias, W. E. Wilson, J. L. Durham, W. K. Shepherd and J. A. Anderson "Particulate Sulfur Analysis: Application to High Time Resolution on Aircraft Sampling in Plumes," *Atmospheric Environment* (in press).

# COMPARISONS OF DISPERSION MODEL ESTIMATES WITH MEASURED SULFATE CONCENTRATIONS

William B. Petersen\*

## ABSTRACT

A fleet of about 400 catalyst equipped vehicles were operated on the 20-km test track at GM's Milford Proving Ground. This type of controlled experiment provides an excellent opportunity to compare estimates from the EPA HIWAY Model with measured  $\text{SO}_4$  concentrations. Concentration estimates from HIWAY are compared with sampling measurements observed for several weeks during morning hours. Performance of the model at the receptor heights and at several distances downwind from the test track is also investigated.

HIWAY gives concentration estimates best in cases when the winds were near perpendicular to the track. It overestimates concentrations when the winds were near parallel. During unstable atmospheric conditions, HIWAY models concentrations well. For stable conditions, HIWAY overestimates concentrations.

## INTRODUCTION

Recent interest in sulfate emissions from catalyst equipped vehicles caused an experiment to be initiated in which roadside sulfate exposures from a fleet of catalyst equipped vehicles were measured. A major purpose of this experiment was to gather data to determine the physical and chemical properties of aerosols emitted by automobiles equipped with catalytic converters under simulated freeway conditions. The purpose of this paper is to compare the

---

\*The author is a physical scientist with the U. S. Environmental Protection Agency's Research Triangle Park, North Carolina Environmental Sciences Research Laboratory.

measured sulfate concentrations with estimated concentrations for each sampling period and receptor location from the EPA HIWAY Model (Zimmerman and Thompson, 1975). It should be *emphasized* that the results contained here are *preliminary* and do not represent an exhaustive analysis of the data. Although further analysis may indicate how the model may be improved, that is not our main purpose here.

In the past there have been a number of studies in which estimates from HIWAY were compared with measured concentrations. For the State of Tennessee, Noll (1975) used CO data from several highways to evaluate the performance of three highway models, one of which was the EPA HIWAY Model. Badgley (1975) conducted air quality studies at several different sites for the Washington State Highway Commission, Department of Highways, and made comparisons between estimates and measured concentrations for several models including HIWAY. Kenneth Noll et al. found that HIWAY tends to overestimate concentrations when the winds are parallel to the roadway and underestimate concentrations when the winds are perpendicular to the roadway. Regarding atmospheric stability categories, Noll found that HIWAY tends to overestimate for stable conditions and underestimate during unstable conditions. The study prepared for the Washington State Highway Commission shows similar results for the wind direction categories.

While the above study sites were on public highways, the General Motors Sulfate Dispersion experiment was at Milford Proving Ground. A fleet of about 400 vehicles was driven on a 10-km test track during the morning hours on 16 different days. Air quality measurements were made over half-hour periods and meteorological parameters measured and averaged over half-hour periods.

A test track provides several advantages in a dispersion study. Traffic volumes and vehicle speeds can be determined accurately. The automobiles in this study were all catalyst equipped. Also, this experiment included the use of a tracer, sulfur hexafluoride, which was measured at the same receptors as was sulfate. This enabled checks of dispersion independent on the vehicle emissions and without high background interferences.

## SITE DESCRIPTION

The test track used for the experiment was a 5-km north-south straightway at the Milford Proving Ground. Milford Proving Ground is located in the gently rolling hills and lightly wooded area of southeastern Michigan about 50 km northwest of Detroit and 30 km north of Ann Arbor. There are only two major highways near the test track--I-96, 7 km to the south, and M-23, 6 km to the west. The test track is essentially level, with elevations varying less than 1 m over the length of the track except at the ends where the track is banked. For a more detailed description of the surrounding terrain and the facilities located at the site, see GMC (1975).

Meteorological instrumentation and sequential samplers for measuring  $\text{SO}_4$  and  $\text{SF}_6$  concentrations were mounted on eight towers. Figure 1 shows the perpendicular distances of the eight towers from the center of the test track. The width of the four-lane track is 25.4 m, with a median width of 11.8 m. Although the roadway would facilitate three lanes of traffic in each direction, the lane closest to the median on either side was not used and therefore was included in the median width. Temperature sensors and uvw anemometers were located at 1.5, 4.5, and 10.5 m on Towers 1 through 6. The temperature and wind sensors were located at 1.5 m on Towers 7 and 8. The sequential samplers were at 0.5, 3.5, and 9.5 m on Towers 1 through 6 and at 0.5 m on Towers 7 and 8.

## MODEL

The EPA HIWAY Model (Zimmerman and Thompson, 1975) is a short-term Gaussian model providing estimates for averaging times of about 1 hour. Traffic emissions are simulated by a straight-line source of finite length for each lane of the highway. A uniform emission rate is assumed for each line source. Air pollution concentrations downwind from each line source are formed by a numerical integration along the line source of a simple Gaussian point-source plume. Initial spreading of the pollutant in the turbulent wake of a vehicle is modeled by specifying appropriate values for the standard deviations

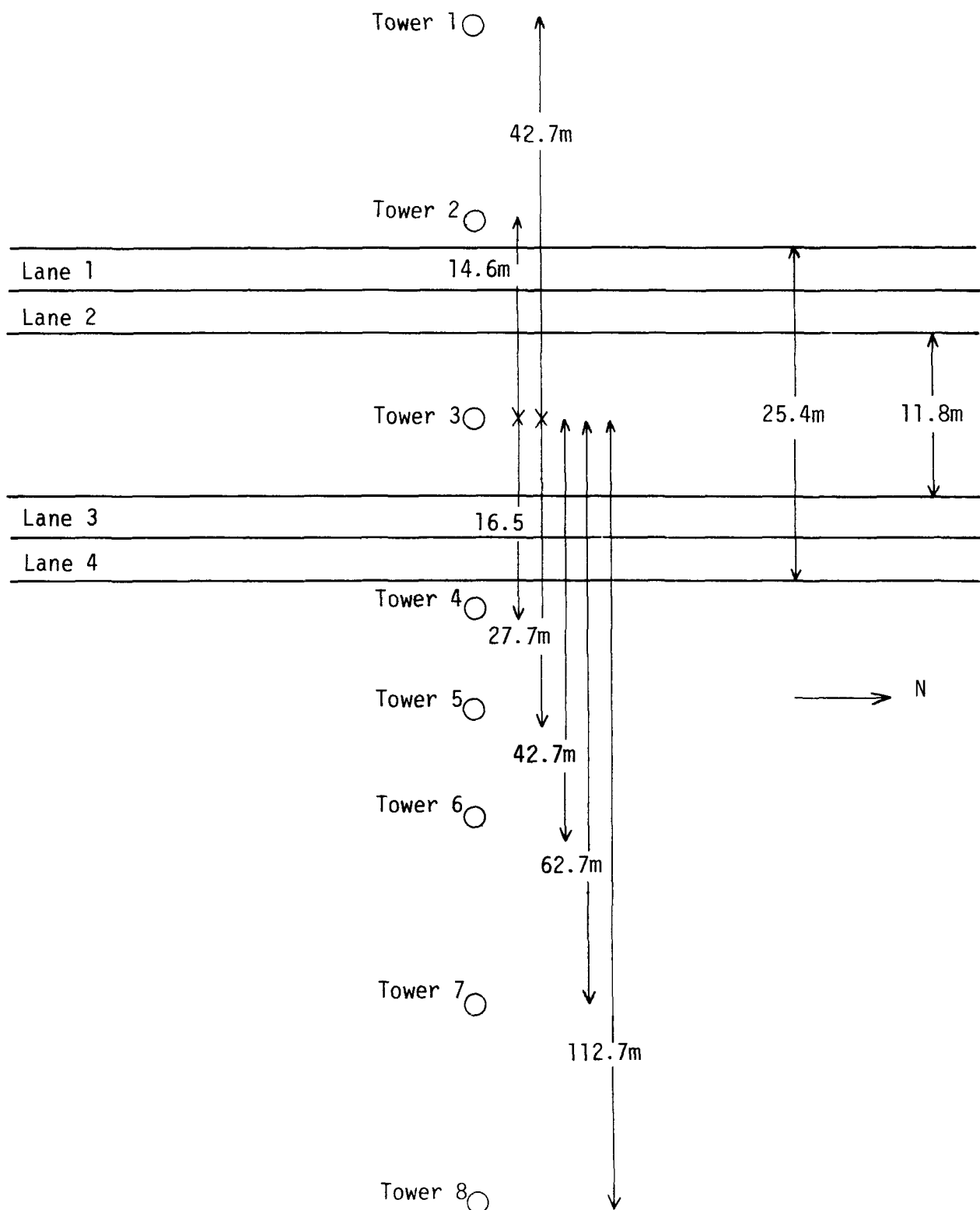


Figure 1. Orientation of test track and perpendicular distances of the meteorological towers from the center of the test track.

of pollutant distributions (i.e., dispersion coefficients). Based on a limited amount of data, a conservative estimate of the initial vertical standard deviation of the plume was determined to be 1.5 m. The initial horizontal standard deviation of the plume was selected as 3 m. The HIWAY Model requires information about highway geometry, automotive emissions, and meteorological conditions.

#### EMISSION FACTORS

Probably nothing more dramatically emphasizes the importance of a good estimate of the emission factor than to simply state that the concentration estimates are directly proportional to the emission factor. Personal communication with Dr. David Chock at General Motors concluded in an estimate of the sulfate emission of 0.037 g/vehicle-mile. Dr. Chock indicated that 0.037 was a mean value of the sulfate emission applicable for the cars driving at a steady speed of 50 mph. However, he also pointed out that there was considerable scatter about the mean. The traffic volume was held constant during the experiment at about 1,365 vehicles per hour per lane. Since the traffic volume and the vehicle speed remained constant during the experiment, it was assumed that the emission rate also remained constant.

Emission rates for sulfur hexafluoride ( $\text{SF}_6$ ) are given in table 1. The tracer ( $\text{SF}_6$ ) was released continuously from eight specially equipped vehicles. In order to simulate the dispersion of  $\text{SO}_4$ , the  $\text{SF}_6$  gas was released directly into the exhaust streams. The eight vehicles were evenly spaced in the traffic, with four in each lane. At an average speed of about 50 mph, a total of 64 passes by the sampling point was made by tracer-releasing vehicles during each 30-minute sampling interval.



Table 1. SF<sub>6</sub> Emission Rate per Unit Length  
(in  $\mu\text{L}/\text{m}/\text{s}$ )\*

<u>Day</u>	<u>Outer Lanes (1&amp;4)</u>	<u>Inner Lanes (2&amp;3)</u>
274	3.166	2.941
275	3.085	2.362
276	3.053	3.085
279	2.282	3.150
281	3.150	3.166
283	3.150	2.394
286	3.182	2.378
290	3.214	2.411
293	3.214	3.182
294	3.198	3.166
295	3.166	2.394
296	3.166	3.166
297	2.378	3.166
300	3.166	3.150
302	3.053	3.037
303	3.134	3.134

---

\*This table was provided by Dr. David Chock of General Motors Corporation in a personal communication.

## BACKGROUND CONCENTRATIONS

Background concentrations of  $\text{SO}_4$  for each half-hour period were determined from the measurements and were added to the modeled concentrations before comparisons were made. Measurements of  $\text{SF}_6$  at the sampling sites upwind of the roadway were so low that the  $\text{SF}_6$  background was assumed zero.

In order to make the estimate of background concentrations as objective as possible, the following scheme was used. The test track is oriented north-south with the meteorological towers oriented basically east-west, Tower 1 being on the west side of the track and Tower 8 being the farthest tower on the east side. When the wind direction was between  $0^\circ$  and  $180^\circ$ , the concentrations at Towers 7 and 8 were averaged and that value was used for the background concentration. If, however, the wind direction was between  $180^\circ$  and  $360^\circ$ , the three measured concentrations on Tower 1 were averaged and used as background.

Table 2 shows the extreme half-hour estimates of background concentrations for  $\text{SO}_4$  for different azimuth ranges. The number of half-hour periods in each azimuth range is also recorded. There appears to be only a slight relationship between background concentration and wind direction. However, when the wind was from the north there was a consistently low background. Figure 2 gives daily fluctuations of  $\text{SO}_4$  background concentrations. The daily background concentration is the average of half-hour background concentrations during that day (the experiment was conducted mostly during the morning hours). The lowest average daily background concentration was  $0.57 \mu\text{g}/\text{m}^3$  and the highest average concentration was  $16.33 \mu\text{g}/\text{m}^3$ . The range of the background concentration for individual periods is shown for each day in figure 2.

## ATMOSPHERIC STABILITY

The dispersion parameters  $\sigma_y$  and  $\sigma_z$  used in the EPA HIWAY Model are basically extrapolations to shorter travel distances of the dispersion parameter values of the Pasquill stability type used in

Table 2. Range of Sulfate Background Concentrations ( $\mu\text{g}/\text{m}^3$ )  
for Different Wind Direction Azimuths

<u>Azimuth Range</u>	<u>High</u>	<u>Low</u>	<u>Number of Observations</u>
1-15	7.30	3.69	2
16-30	11.52	2.97	3
31-45	10.74	10.26	2
46-60	8.87	2.85	4
61-75	7.09	2.55	5
76-90	16.96	6.68	3
91-105	13.47	13.47	1
106-120	-	-	0
121-135	-	-	0
136-150	-	-	0
151-165	-	-	0
166-180	12.64	11.13	2
181-195	15.07	5.96	13
196-210	13.00	1.60	8
211-225	14.51	3.57	4
226-240	7.22	2.34	5
241-255	17.69	8.23	6
256-270	18.72	17.86	2
271-285	4.79	4.05	2
286-300	9.35	2.46	5
301-315	-	-	0
316-330	2.44	0.92	3
331-360	3.63	0.37	10

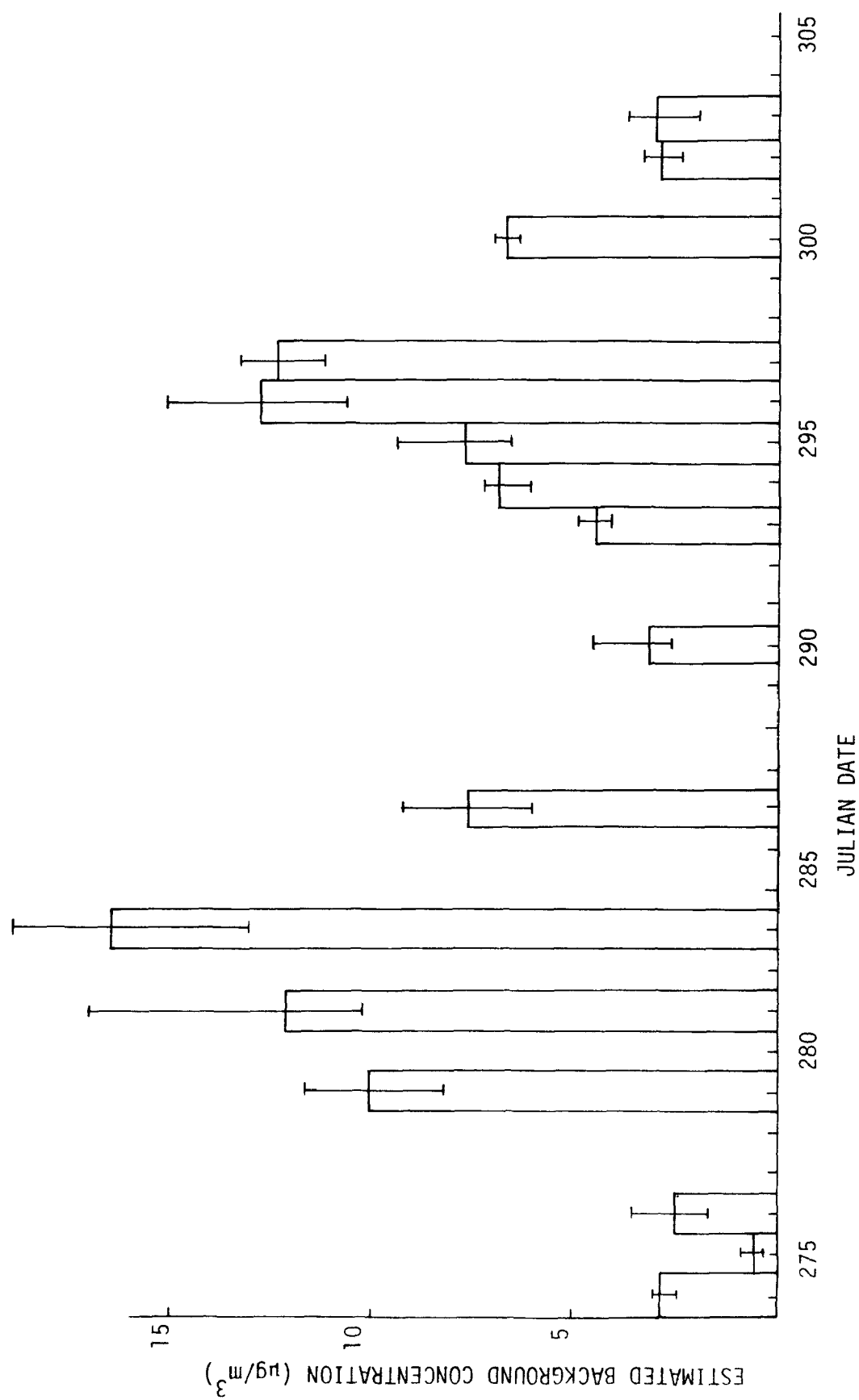


Figure 2. Average sulfate background concentration for each day. Lines indicate range in the data.

Turner (1970). Table 3 is a summary of the meteorological data gathered during the experiment (GMC, 1975). The atmospheric stability was given in terms of the Richardson Number, which HIWAY cannot use directly. Golder (1972) showed a technique to convert the Richardson Numbers to the Pasquill stability classes. However, the method was not applicable for Richardson Numbers greater than 0.14. Since Golder's method was not applicable for all the data, the original Pasquill method (1961) was used to specify stability class from cloud cover, ceiling height, and wind speed. The stability class was determined using the wind speed at the experimental site and the observations of cloud cover and ceiling at 3-hour intervals for Flint, Michigan (about 44 km north of the site). The stabilities determined from the Richardson Number were used subjectively in determining how fast the atmospheric stability was changing from half-hour to half-hour. The stability class never changed more than one class from one half-hour period to the next.

#### METHOD OF ANALYSIS ANALYSIS AND RESULTS

Estimates from the EPA HIWAY Model, using meteorological and emission input for each half-hour period, were compared with measured concentrations at each receptor location for every half-hour period. In order to compare model estimates with measured concentrations, factors influencing model performance were isolated. The important factors are wind speed, wind direction, stability, and receptor location.. The available time for analysis of the data did not permit an exhaustive investigation of these factors; for example, the simultaneous influence of two or more factors on model performance was not investigated.

Individual factors were considered as follows. All the data were separated into three wind direction categories and analyzed for each category. Next, the data were separated into stability classes and analyzed. No interactions between stability and wind direction were considered. All data were analyzed by receptor height and were

Table 3. Meteorological Summary

Date	Time	W.Speed (cm/sec.)	W.Dir. (deg)	Ri	T (°K)	R.H. (%)	Pressure (mmHg)	Duration of Sampling (min)	Vehicles Running
272 09/29/75	082033	27	59.2	7.119	277.65	95.7	738.6	30	Yes
	085033	84	77.8	1.548	280.87	93.3	738.8	30	Yes
	092032	67	75.0	-2.087	283.25	91.6	738.9	30	Yes
	095032	60	116.3	-3.334	285.62	80.3	738.7	30	Yes
274 10/01/75	140958	287	291.1	-.147	284.15	70.2	734.0	30	Yes
	143957	256	292.1	-.531	284.77	68.9	734.0	30	Yes
	150957	281	290.9	-.331	285.10	64.9	734.0	30	Yes
	153956	298	291.7	-.250	284.41	67.1	734.0	30	Yes
275 10/02/75	080959	107	321.3	-.178	273.99	92.8	740.3	30	Yes
	083959	156	335.4	-.404	275.17	91.6	740.7	30	Yes
	090959	218	341.0	-.259	275.96	87.1	740.9	30	Yes
	093958	244	345.3	-.381	276.86	81.2	741.2	30	Yes
276 10/03/75	081459	231	209.3	-.045	275.22	76.9	743.8	30	Yes
	084459	215	213.6	-.213	276.21	70.9	743.9	30	Yes
	091459	265	227.4	-.387	278.23	65.8	743.9	30	Yes
	094459	307	236.5	-.419	279.94	59.9	743.9	30	Yes
279 10/06/75	080959	100	251.1	0.409	282.52	87.7	734.2	30	Yes
	084000	97	246.7	0.327	282.81	86.8	734.2	30	Yes
	090959	145	253.2	-.312	284.54	79.7	734.2	30	Yes
	093959	182	250.1	-.349	286.17	70.2	734.9	30	Yes

Table 3. (cont.)

Date	Time	W.Speed (cm/sec.)	W.Dir. (deg)	Ri	T (°K)	R.H. (%)	Pressure (mmHg)	Duration of Sampling (min)	Vehicles Running
281 10/08/75	071000	136	35.7	0.271	281.51	94.8	737.7	30	No
	080504	182	35.7	0.138	281.91	94.7	737.8	30	Yes
	083504	121	29.4	0.257	282.41	97.0	737.8	30	Yes
	090504	94	77.7	0.338	284.38	98.6	737.8	30	Yes
	093504	205	94.2	0.015	285.15	90.5	737.8	30	Yes
	104054	168	76.0	-.500	286.93	88.6	737.8	30	No
283 10/10/75	071621	148	259.5	0.0357	284.95	96.4	735.5	15	No
	081959	124	254.4	0.0237	284.19	95.9	735.5	30	Yes
	085000	95	263.2	-.176	283.95	96.4	735.8	30	Yes
	092000	112	241.6	-.432	283.90	94.8	735.9	30	Yes
	095000	129	220.3	-.584	283.85	91.0	735.9	30	Yes
	104900	180	206.0	-.410	285.24	83.1	735.9	30	No
286 10/13/75	071212	286	188.8	0.060	284.36	69.5	735.0	25	No
	081501	229	187.1	0.106	284.83	70.0	734.9	30	Yes
	084501	244	195.4	0.039	285.36	66.4	734.9	30	Yes
	091501	265	201.8	0.010	285.64	66.6	734.9	30	Yes
	094501	286	202.3	-.110	286.98	62.9	734.9	30	Yes
	103857	288	217.0	-	-	-	-	30	No
290 10/17/75	070200	219	65.9	0.112	278.74	84.7	737.3	30	No
	080958	217	68.0	0.133	278.83	82.6	737.4	30	Yes
	083958	213	58.5	0.120	278.81	81.3	737.4	30	Yes
	090958	217	61.7	0.068	279.05	80.0	737.4	30	Yes
	093957	246	56.0	0.015	279.48	78.6	737.4	30	Yes
	103843	386	68.7	0.003	280.42	76.4	737.4	30	No

Table 3. (cont.)

Date	Time	W.Speed (cm/sec.)	W.Dir. (deg)	Ri	T (° K)	(%)	Pressure (mmHg)	Duration of Sampling (min)	Vehicles Running
293 10/20/75	103458	200	272.3	-0.072	281.69	94.9	729.9	30	Yes
	110458	210	271.3	-0.114	282.17	92.7	730.0	30	Yes
294 10.21/75	070901	191	226.7	0.172	283.72	72.1	727.5	22	No
	080502	159	229.7	0.198	282.94	76.3	727.1	30	Yes
	083502	152	234.7	0.220	283.09	76.6	727.1	30	Yes
	090501	113	209.8	-0.140	283.28	74.4	727.2	30	Yes
	093501	138	219.2	-0.584	284.43	70.2	727.5	30	Yes
295 10/22/75	070901	8	300.0	68.27	277.41	101.5	729.5	20	No
	080958	45	51.4	3.962	277.68	95.8	730.2	30	Yes
	083958	62	75.1	1.058	278.04	93.8	730.2	30	Yes
	090958	62	48.9	0.339	279.18	97.3	730.2	30	Yes
	093958	35	7.8	7.534	281.11	98.5	730.2	30	Yes
	103500	141	76.9	-0.106	284.34	88.8	730.2	30	No
296 10/23/75	071106	223	185.2	0.212	285.22	82.4	731.2	30	No
	080500	292	181.4	0.095	285.00	81.6	731.4	30	Yes
	083459	299	182.8	0.077	284.54	82.1	731.4	30	Yes
	090459	301	184.3	0.017	284.87	79.2	731.6	30	Yes
	093458	250	186.8	-0.026	285.60	76.0	731.8	30	Yes
	103500	288	192.6	-0.132	288.03	70.1	732.4	30	No



Table 3. (cont.)

Date	Time	W.Speed (cm/sec.)	W.Dir. (deg)	Ri	T (°K)	R.H. (%)	Pressure (mmHg)	Duration of Sampling (min)	Vehicles Running
297 10/24/75	070800	252	181.4	0.133	284.96	72.3	735.0	30	No
	080458	249	182.2	0.136	285.47	69.5	735.1	30	Yes
	083458	224	183.3	0.134	285.46	69.5	735.2	30	Yes
	090458	304	177.1	0.051	285.92	67.8	735.3	30	Yes
	093458*	355	179.2	0.021	285.51	65.7	735.3	30	Yes
*Filter samples were taken between 909458 and 903458. The wind speed and direction are for the period from 090458 to 091358.									
300 10/27/75	080000	177	194.4	0.172	276.98	75.3	735.9	30	Yes
	083000	233	203.3	-0.063	278.11	71.1	735.9	30	Yes
	090000	238	199.5	-0.177	279.19	67.8	735.9	30	Yes
	093000	223	201.4	-0.393	280.65	66.6	735.9	30	Yes
302 10/29/75	070830	155	348.8	0.202	277.00	73.8	741.9	20	No
	080456	183	345.7	0.070	277.09	76.5	742.0	30	Yes
	083456	257	351.7	-0.016	277.68	75.7	742.0	30	Yes
	090457	289	351.8	-0.053	278.68	73.0	742.3	30	Yes
	093457	312	354.3	-0.068	279.58	70.6	742.5	30	Yes
	104357	349	356.3	-0.048	280.02	68.1	742.6	30	No
303 10/30/75	071000	101	326.8	0.255	269.69	82.2	746.5	23	No
	080957	91	320.6	0.137	270.59	83.6	746.6	30	Yes
	083957	99	351.3	-1.190	271.56	81.4	745.8	30	Yes
	090957	147	10.5	-0.563	272.66	79.2	747.1	30	Yes
	093956	176	17.3	-0.570	274.15	75.7	747.2	30	Yes
	104754	247	24.4	-0.410	276.48	60.1	746.9	30	No

separated and analyzed by tower location. Finally, performance of the model at different wind speeds was investigated.

#### A. Comparison of Concentrations With Wind Angle

Figure 3 shows plots of measured versus estimated sulfate concentrations for three broad categories of angle of wind with the roadway. The perpendicular category includes angles of wind with the roadway from  $60^\circ$  to  $120^\circ$  (also  $240^\circ$  to  $300^\circ$ ); that is, within  $\pm 30^\circ$  of normal to the test track. The oblique category includes angles of wind with the roadway from  $30^\circ$  to  $60^\circ$ . The parallel category includes angles of wind with the roadway from  $0^\circ$  (actual parallel) to  $\pm 30^\circ$  (within  $30^\circ$  of parallel).

For the perpendicular wind case, eight points were not plotted because the estimated concentrations were outside the range of the ordinate. These eight points all occurred during the same half-hour period (on October 22) when the wind speed was extremely light, 0.08 m/sec, the lowest average wind speed recorded during the experiment. The estimated concentrations during this half-hour period ranged from 57 to 217  $\mu\text{g}/\text{m}^3$ , with the corresponding measured concentrations ranging from 6 to 10  $\mu\text{g}/\text{m}^3$ .

For the oblique wind case, all the data points were plotted. For the parallel wind case, five data points were plotted. For the parallel wind case, five data points were not plotted because the estimated concentrations were outside the range of the ordinate on the plot. These five data points also occurred during the same day (October 22) when the half-hour average wind speed was 0.35 m/sec; concentration estimates during this period were as high as 122  $\mu\text{g}/\text{m}^3$ .

In all, there were 13 data points that were not plotted from the data set. The high estimated concentrations all occurred during very low wind speed conditions, less 1 m/sec, when the HIWAY model would not be expected to perform well, since steady-state conditions are not a good assumption in low wind speeds. During such low wind

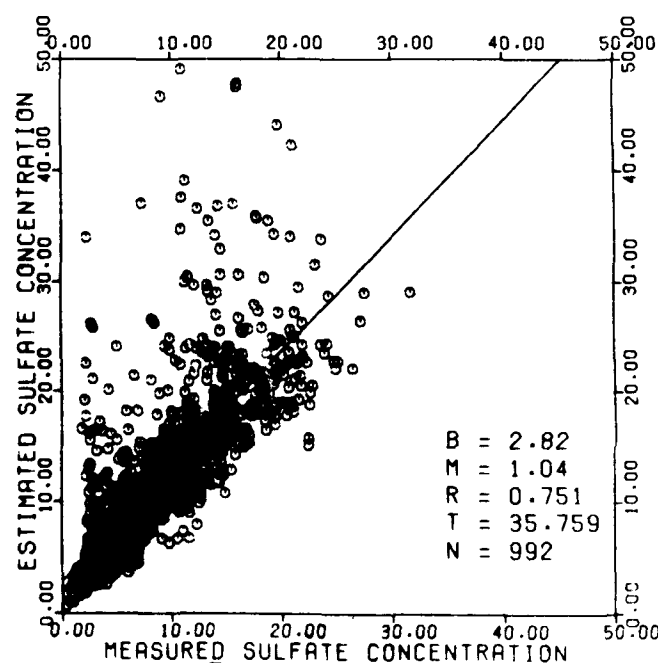
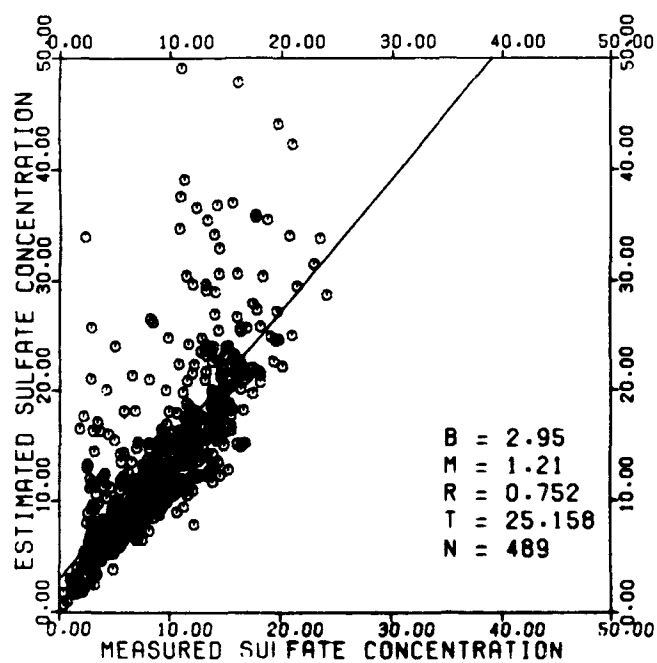
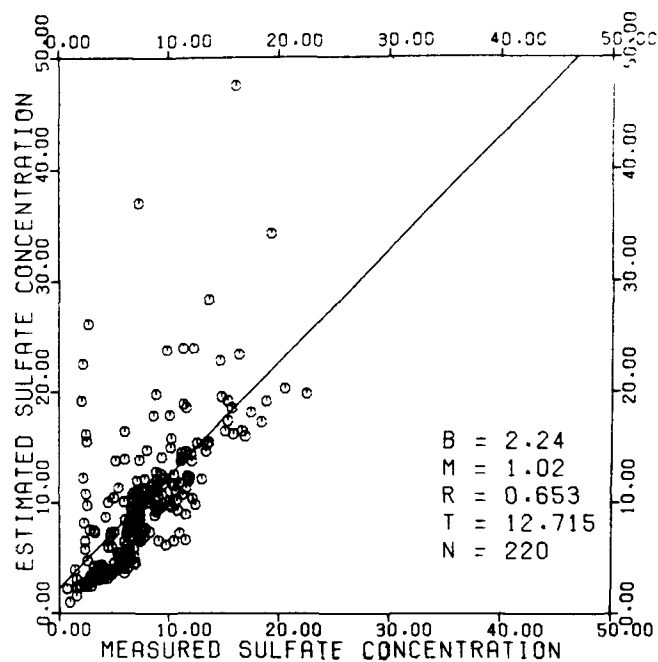
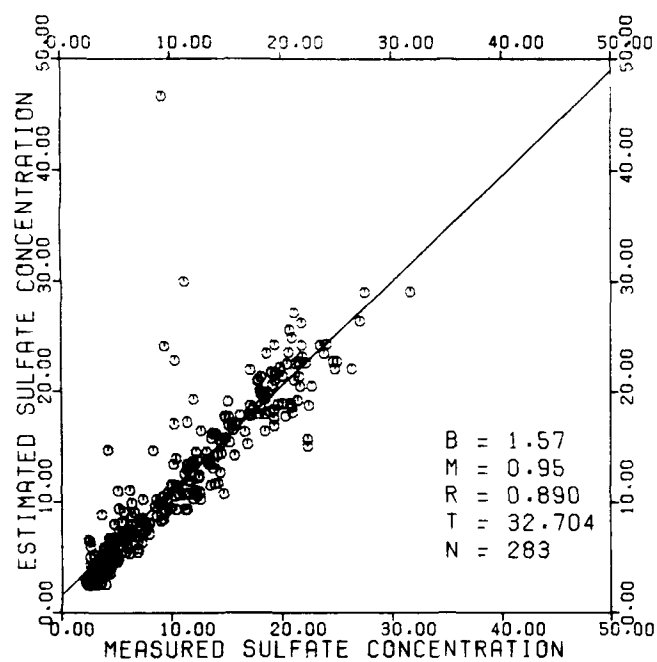


Figure 3. Sulfate concentrations ( $\mu\text{g}/\text{m}^3$ ). B, M, R, T, N in the plots are the intercept, slope, correlation coefficient, T test, and number of data points respectively.

speeds, wind directions frequently meander over wide ranges. The regression analyses shown in the figures were performed on only the plotted points.

Estimating background concentrations during conditions when the wind is nearly parallel to the test track is a rather formidable task, since the roadway emissions may be affecting samplers on both sides of the roadway. However, in this case the background concentrations were calculated as stated in a previous section. The bottom part of figure 4 shows the parallel wind comparisons with no background concentration added to the estimated concentration from the model. It is evident from a comparison of this figure with the lower left portion of figure 3 that the background concentrations are significant. Perhaps other techniques for estimating background concentrations would yield even better agreement between the model and measured concentrations.

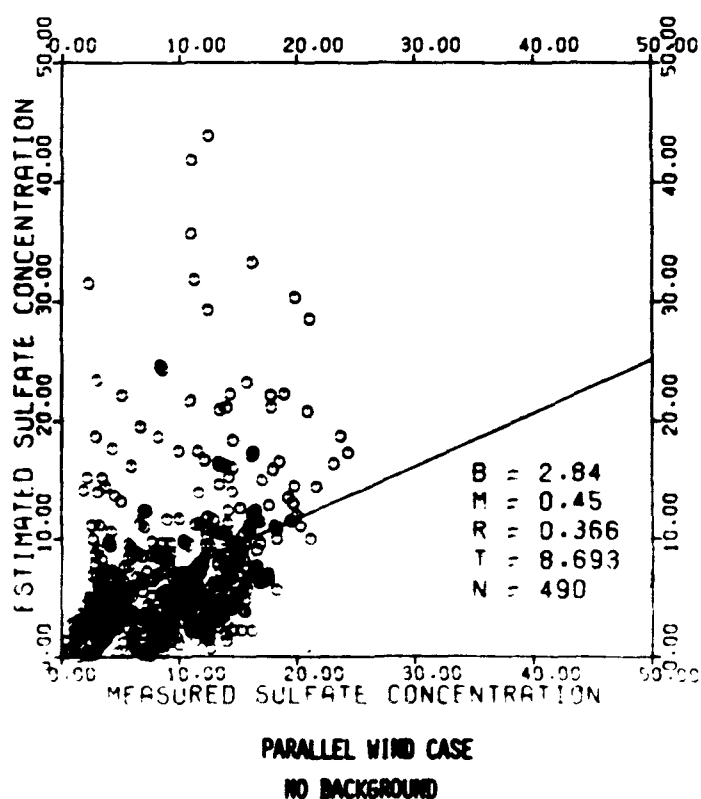


Figure 4. Sulfate concentrations in ( $\mu\text{g}/\text{m}^3$ ). B, M, R, T, N in the plot are the intercept, slope, correlation coefficient, T test, and number of data points respectively.

HIWAY performs best for the perpendicular wind case for both  $\text{SO}_4$  and  $\text{SF}_6$  as shown by the upper left portion of figures 3 and 5. At measured sulfate concentration near  $20 \mu\text{g}/\text{m}^3$  for the perpendicular wind case, the range about the regression line is nearly  $\pm 5 \mu\text{g}/\text{m}^3$ . For the oblique wind case at the same measured concentration, 20, the model yields  $23 \mu\text{g}/\text{m}^3$ . Scatter is much larger than in the perpendicular wind case, ranging from about 17 to  $35 \mu\text{g}/\text{m}^3$ . At measured concentrations of  $20 \mu\text{g}/\text{m}^3$ , during parallel wind conditions, the model estimates concentrations at  $27 \mu\text{g}/\text{m}^3$ , with a range in the data from 20 to  $48 \mu\text{g}/\text{m}^3$ . The  $\text{SF}_6$  data show basically the same trend as that of  $\text{SO}_4$ . However, from the regression line the model overestimates concentrations by about a factor of 2 for the parallel wind case.

Whenever the model estimated very high concentrations, the wind speeds were generally less than 1 m/sec. The low wind speed conditions occurred mostly when the winds were nearly perpendicular to the test track. Figure 3 for the perpendicular wind case was replotted, but not shown, for wind speeds greater than 1 m/sec. The slope remained nearly the same, with an intercept shifting from 1.57 to 1.07 and the correlation coefficient improving from 0.89 to 0.96. Removing low wind speed conditions thus removed some scatter about the regression line.

#### B. Comparison of Concentrations with Stability Class

Figure 6 shows the measured concentration versus the estimated concentration for the stabilities B through F. In general, the more unstable the conditions, the better the model performed. During B and C stability conditions, the model slightly overestimates at the  $20\text{-}\mu\text{g}/\text{m}^3$  level. The results for stability B and C are very similar, with intercepts of 2.86 and 2.42 respectively. The slope of the regression line for B stability is .89, as is that of stability C. The correlation coefficients were 0.94 and 0.92 respectively. Stability D occurred more often than any other stability, having a total of 413 data points. During this condition, the model had a tendency to overpredict by  $5 \mu\text{g}/\text{m}^3$  at the  $20\text{-}\mu\text{g}/\text{m}^3$

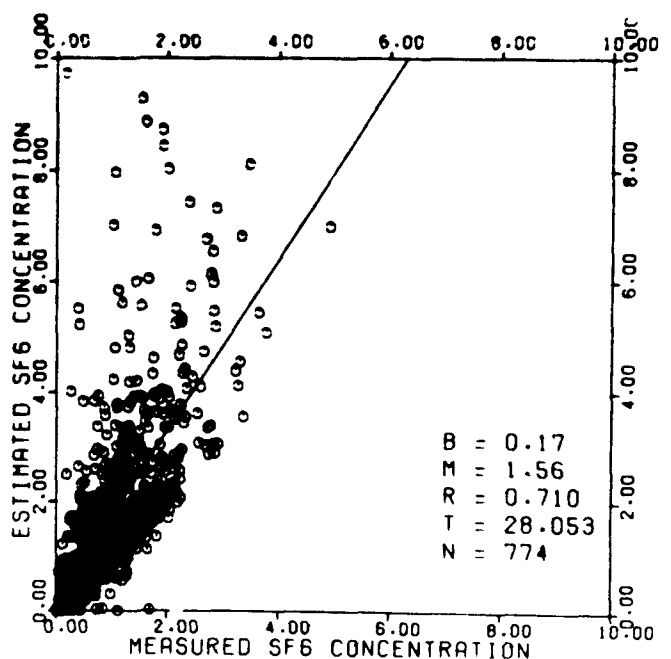
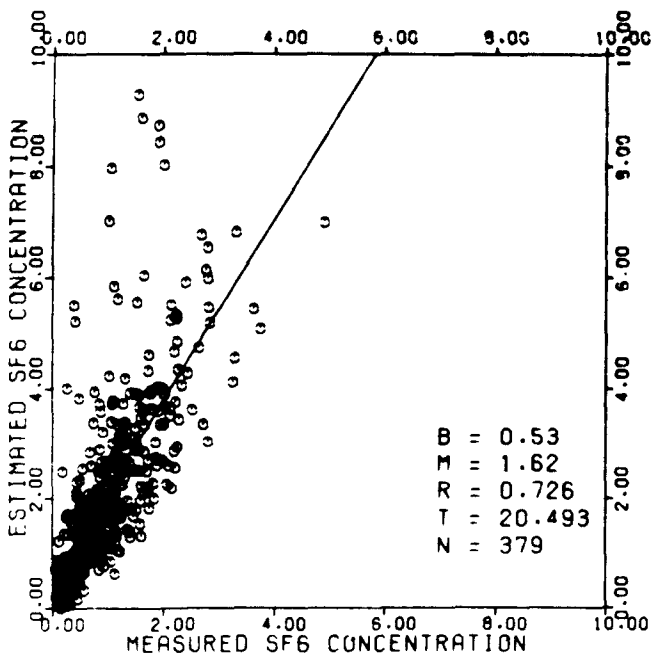
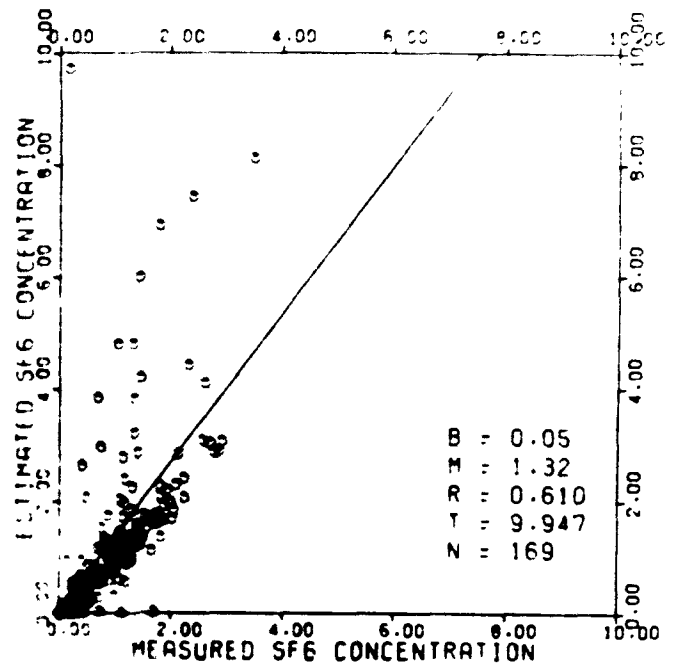
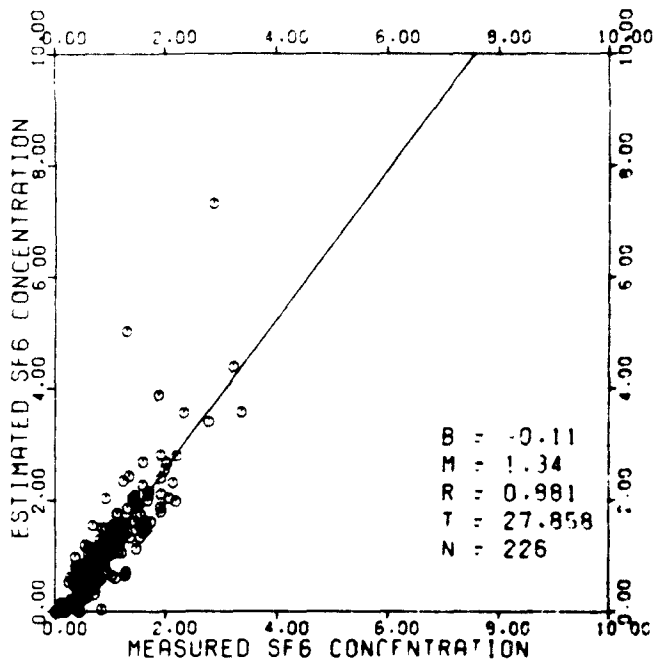


Figure 5. SF<sub>6</sub> concentrations in (PPb). B, M, R, T, N in the plots are the intercept, slope, correlation coefficient, T test, and number of data points respectively.

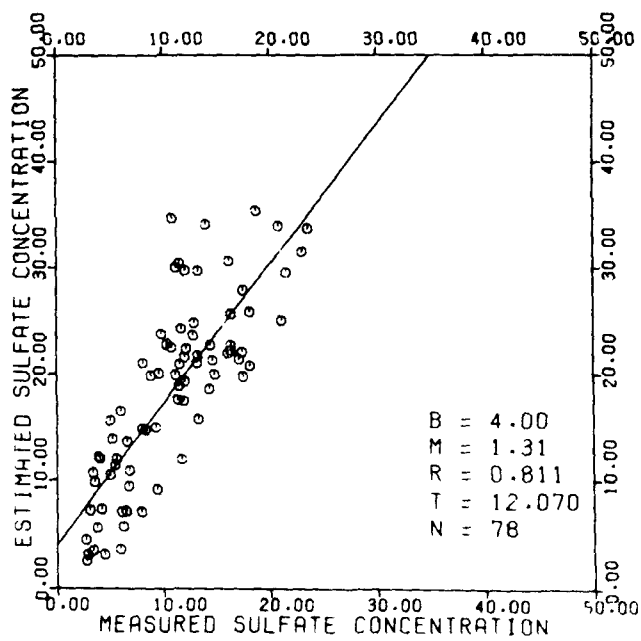
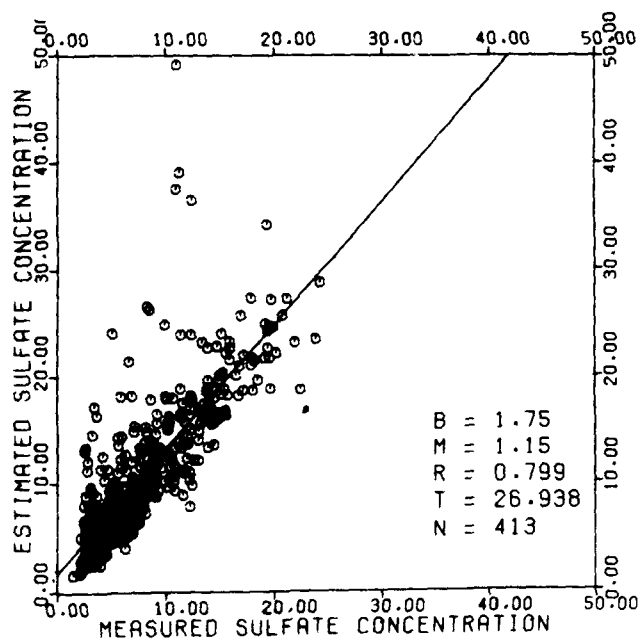
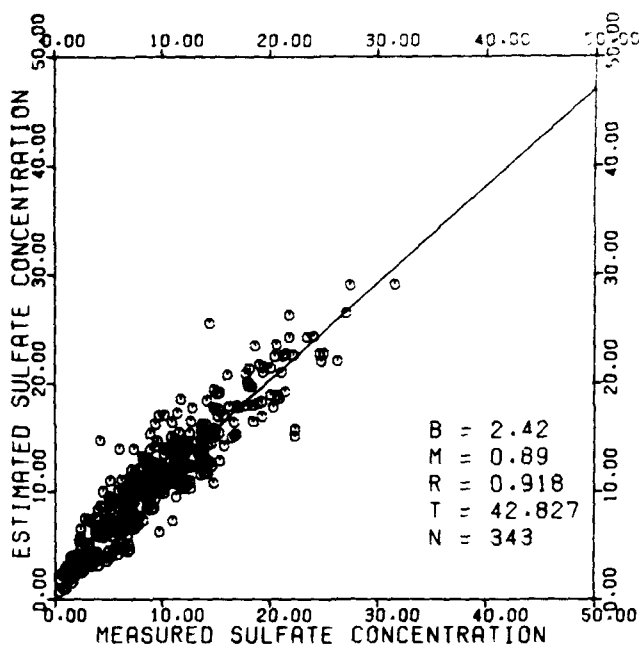
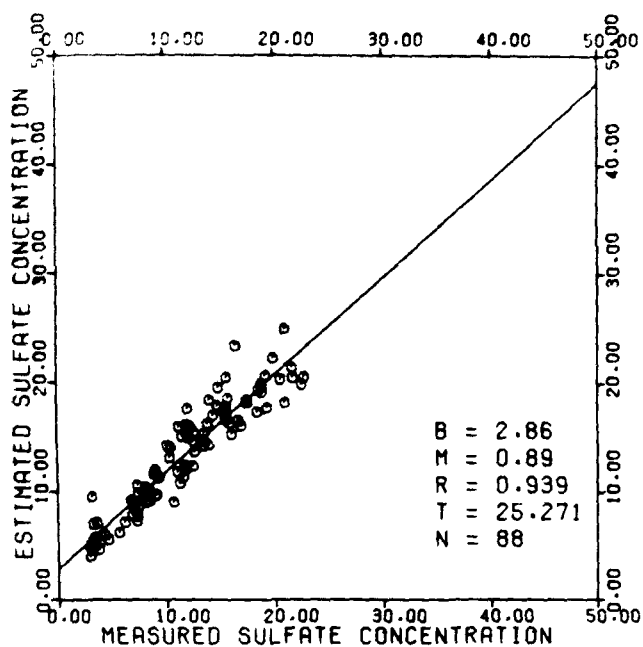


Figure 6 Sulfate concentrations in ( $\mu\text{g}/\text{m}^3$ ). B, M, R, T, N in the plots are the intercept, slope, correlation coefficient, T test, and number of data points respectively.

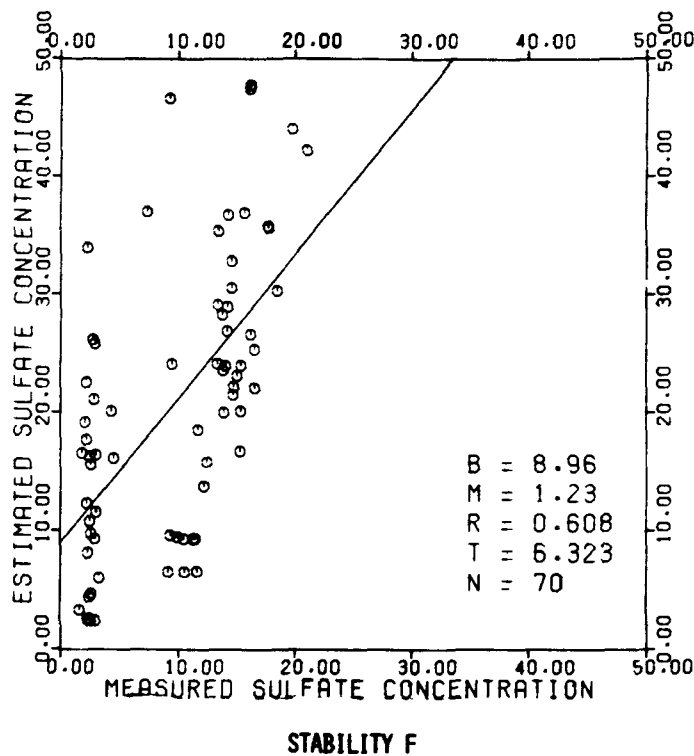


Figure 6 (con.)

level, with a range from 17 to 35  $\mu\text{g}/\text{m}^3$ .

With increasing stability, the data indicate that HIWAY fails to model concentrations accurately. At the 20- $\mu\text{g}/\text{m}^3$  level, the model estimates 30 and 34  $\mu\text{g}/\text{m}^3$  for stability E and F respectively. Precision in the model during E and F stability conditions is also less. The correlation coefficients for E and F stability are 0.81 and 0.61. The  $\text{SF}_6$  data yield the same results except that the model tends to overestimate by a factor of 2 to 3 for stabilities E and F.

#### C. Comparison of Concentrations with Height of Receptor

Figure 7 shows the measured  $\text{SO}_4$  versus estimates from HIWAY for three different receptor heights 0.5, 3.5, and 9.5 m. The largest scatter in the data occurred at the 0.5-m height, with the least at 9.5 m. The model performed about equally well for all three heights. At a measured concentration of 20  $\mu\text{g}/\text{m}^3$ , the estimated concentrations



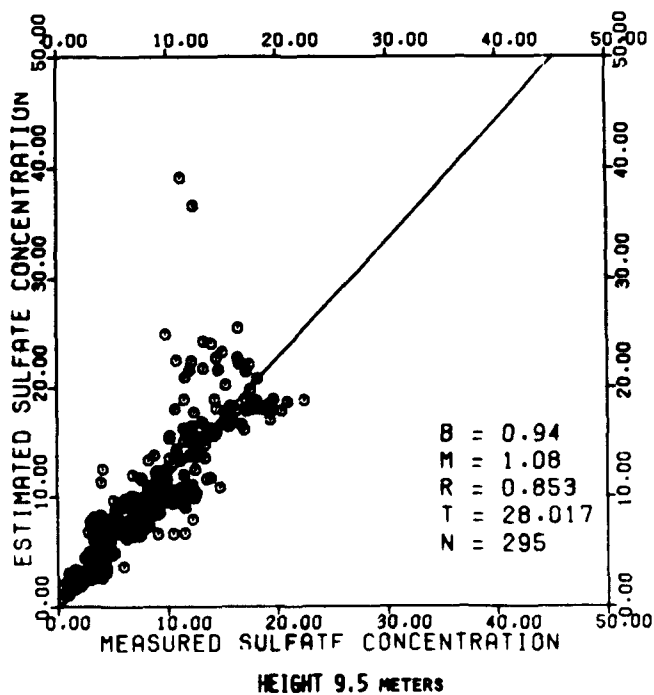
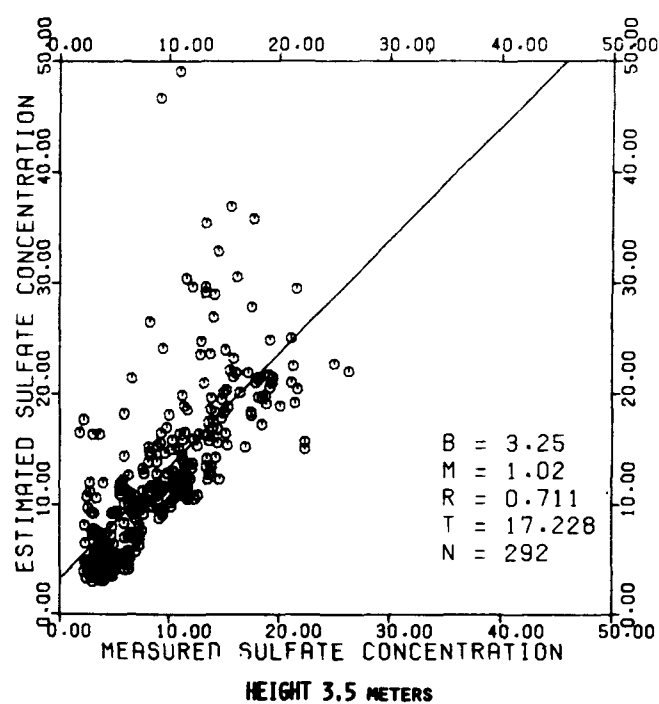
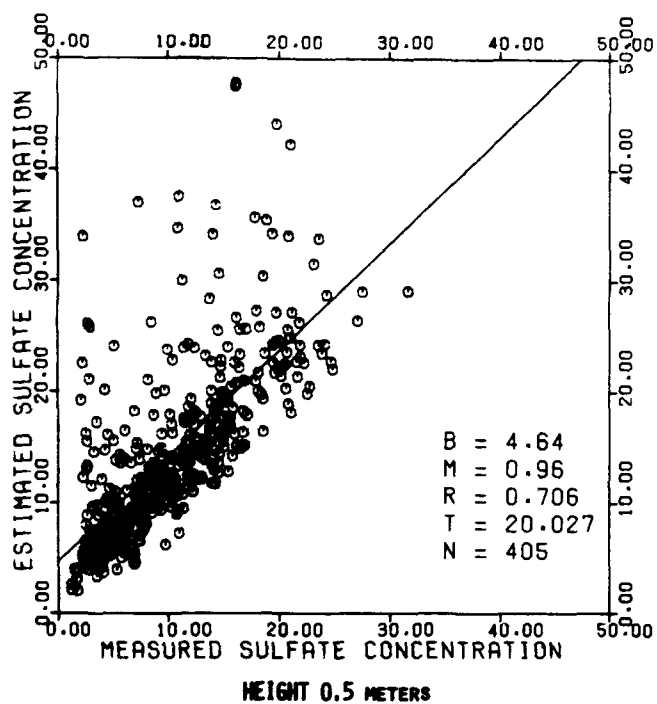


Figure 7. Sulfate concentrations in ( $\mu\text{g}/\text{m}^3$ ). B, M, R, T, N in the plots are the intercept, slope, correlation coefficient, T test, and number of data points respectively.

for the three levels from lowest to highest were 24, 24, and 23  $\mu\text{g}/\text{m}^3$ . For  $\text{SF}_6$  the estimated concentrations increased with increasing heights, with more scatter in the data at higher receptor heights.

#### D. Comparison of Concentrations with Distance

The model response with distance from the roadway is shown in figure 8. The top left graph is an analysis of data from the tower in the median of the test track (Tower 3). Also shown are analyses of the data for Towers 4, 6, and 8, which represent distances of 2, 30, and 100 m from the roadside. The data show that the model is fairly consistent through the range of distances from the roadsides. The slopes vary from 1.16 in the median down to 0.91 at Tower 8. Correlation coefficients range from 0.89 at Tower 8 to a low 0.68 at Tower 4.

The data show that the model overestimates at every tower, with the greatest overestimation occurring at Towers 3 and 4. At a measured concentration of 20  $\mu\text{g}/\text{m}^3$ , the model overestimates by 4 or 5  $\mu\text{g}/\text{m}^3$  at Towers 3 and 4, and overestimates at about 2  $\mu\text{g}/\text{m}^3$  at Towers 6 and 8.

#### E. Comparison of Concentrations with Wind Speed

In an attempt to understand how the model performs under various wind speeds, figure 9 was plotted. Measured concentrations from all samplers on the downwind side of the test track were averaged for each half-hour period. Estimated concentrations from the model plus background for the same sampling positions on the downwind side of the test track were also averaged. The differences of these averages, model plus background minus measured are plotted as a function of wind speed. Circles, triangles, and plus signs represent data when the wind direction category was parallel, oblique, or perpendicular, respectively. For the perpendicular wind case, the data show that the model is relatively invariant for wind speeds greater than 1 m/sec; data are similar with the oblique wind case.

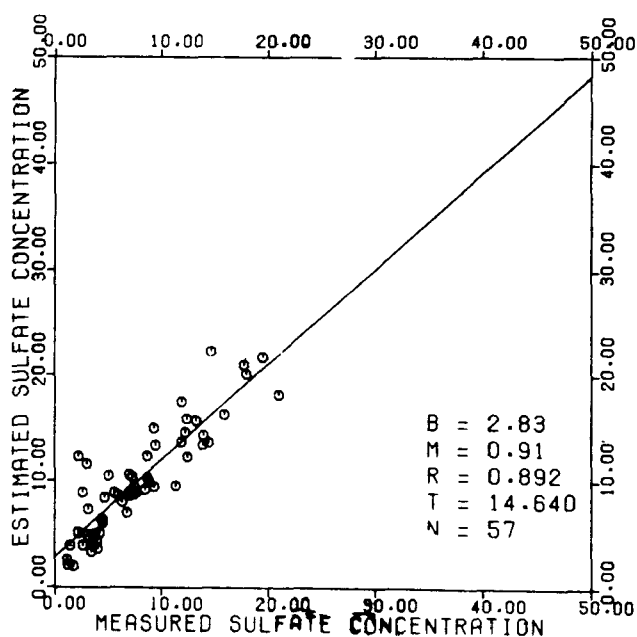
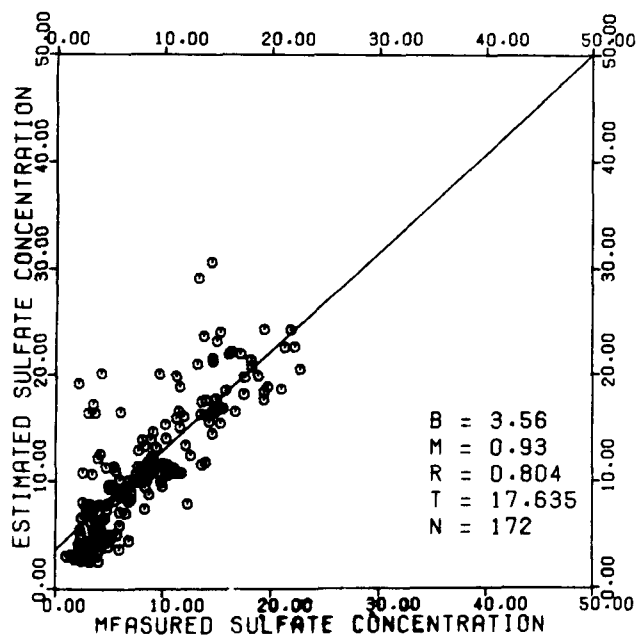
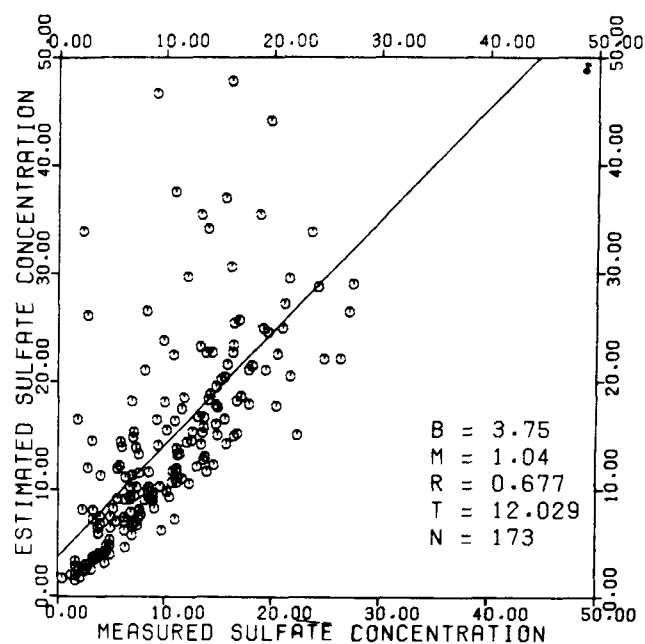
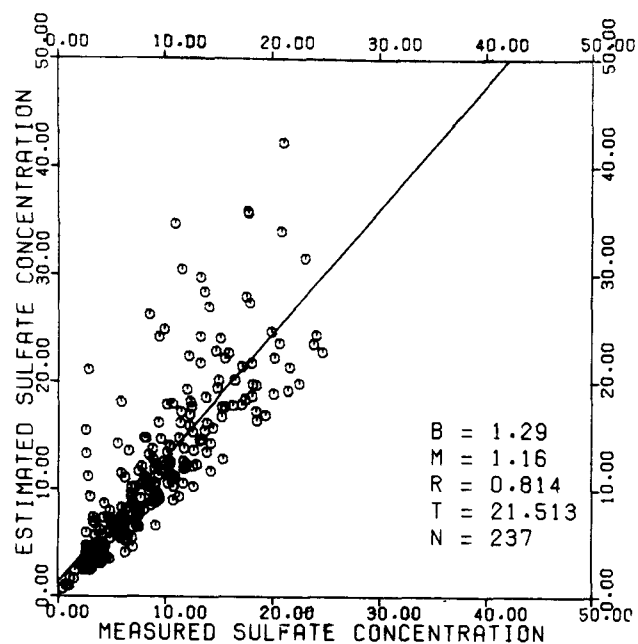


Figure 8. Sulfate concentrations in  $(\mu\text{g}/\text{m}^3)$ . B, M, R, T, N in the plots are the intercept, slope, correlation coefficient, T test, and number of data points respectively.

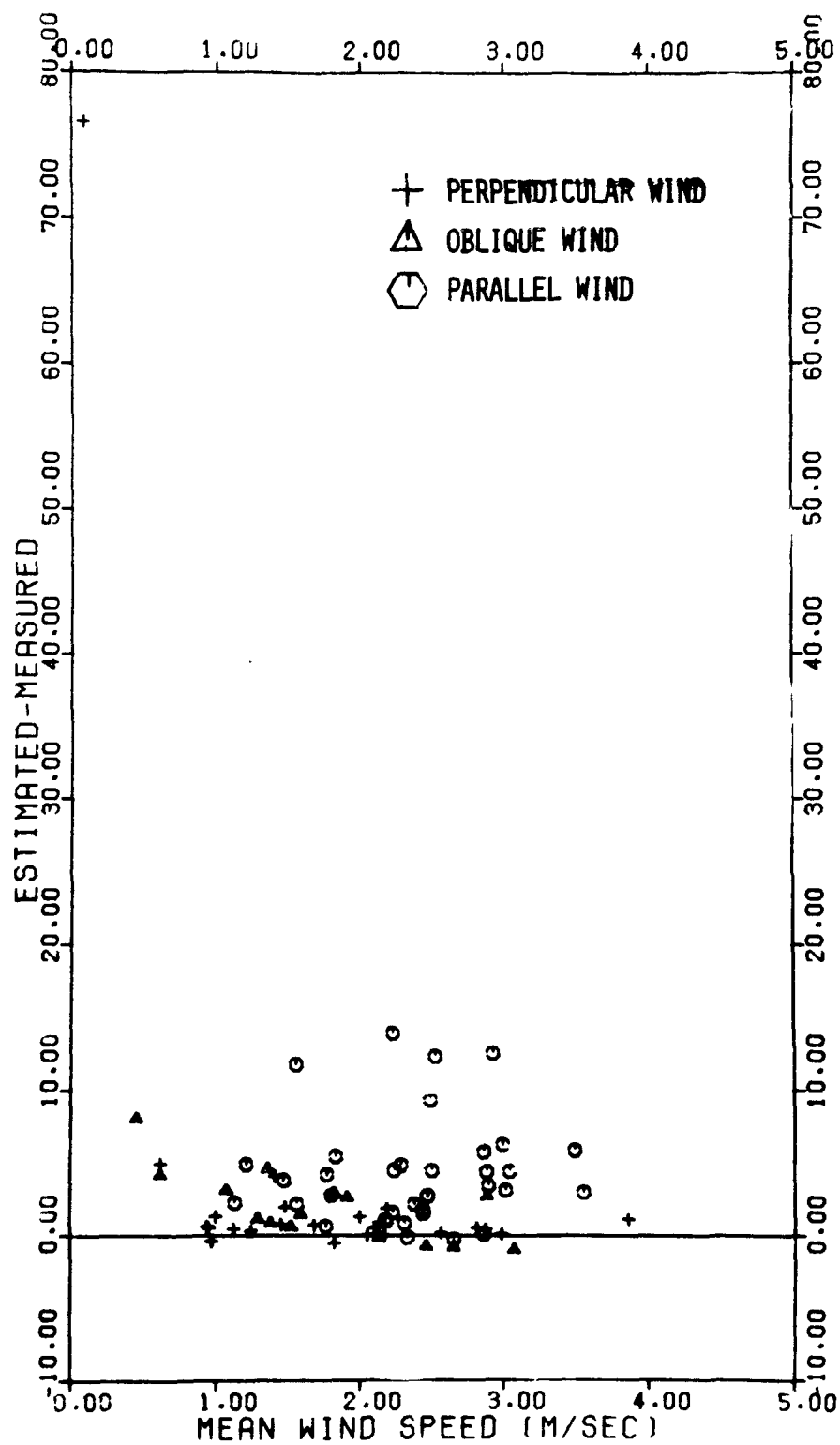


Figure 9. Estimated sulfate concentrations minus measured sulfate concentrations versus mean wind speed.

However, when the winds are within  $30^\circ$  of parallel, the model overestimates and lacks precision in the results.

#### SUMMARY

The results shown here are preliminary and represent what was accomplished during the short time period for which data were available. It should be noted that comparisons between measurements and estimates from the HIWAY dispersion model have been examined by categories based on only one parameter at a time: wind direction with the roadway, stability class, receptor height, receptor distance, and wind speed. It is desirable to group the data based upon two or more parameters. This will be attempted in the future.

Figure 3 is a plot of estimated concentrations versus measured sulfate concentrations for all the data. From the regression line HIWAY estimates a concentration of  $24 \mu\text{g}/\text{m}^3$  when  $20 \mu\text{g}/\text{m}^3$  was measured. Similarly, from figure 5 for  $\text{SF}_6$  (all data) when 2 ppb of  $\text{SF}_6$  were measured, the model estimates 3.3 ppb. Why there is such a large difference between measured and estimated concentrations for  $\text{SF}_6$  compared to  $\text{SO}_4$  is not clear. Further analysis of the data may aid our understanding of why these differences occur.

The model performed best for unstable atmospheric conditions or when the winds were near perpendicular to the test track. The model overestimated concentrations to the greatest extent during stable conditions or when the winds were near parallel to the test track. Further analysis of the data should be very helpful and should enable modifications to the model to improve performance.

#### REFERENCES

1. F. I. Badgley, A. T. Rossano, D. Lutrick, H. Alsid, *The Selection and Calibration of Air Quality Diffusion Models For Washington State Highway Line Sources*. Washington State Highway Commission Department of Highways. University of Washington, Seattle, Washington (1975).

2. D. P. Chock (1976). Personal communication.
3. General Motors Corporation, "Plans For General Motors' Sulfate Dispersion Experiment," General Motors Research Laboratories, Warren, Mich. (Sept. 1975).
4. D. Golder, "Relations Among Stability Parameters In The Surface Layer," *Boundary-Layer Meteorology*, 3:47-58 (1972).
5. K. E. Noll, T. L. Miller, R. H. Rainey, R. C. May, *Air Monitoring Program To Determine The Impact Of Highways On Ambient Air Quality*. Department of Civil Engineering-The University of Tennessee, Knoxville, Tennessee (1975).
6. F. Pasquilla, "The Estimation of the Dispersion of Windborne Material," *Meteorol.* 90:33-49, 1063 (1961).
7. D. B. Turner, *Workbook of Atmospheric Dispersion Estimates*. U. S. Environmental Protection Agency, Research Triangle Park, North Carolina. Publication No. AP-26. 1970. 84 p.
8. J. R. Zimmerman, R. S. Thompson, *User's Guide For HIWAY, A Highway Air Pollution Mode*. U. S. Environmental Protection Agency, Research Triangle Park, North Carolina. Publication EPA-650/4-74-008. (February 1975).

APPENDIX

CHEMICAL SPECIATION OF SULFATE EMISSIONS FROM  
CATALYST EQUIPPED AUTOMOBILES UNDER AMBIENT CONDITIONS

R. L. Tanner and L. Newman

Department of Applied Science  
Brookhaven National Laboratory  
Upton, New York

# CHEMICAL SPECIATION OF SULFATE EMISSIONS FROM CATALYST-EQUIPPED AUTOMOBILES UNDER AMBIENT CONDITIONS

R. L. Tanner and L. Newman\*

## ABSTRACT

*Airborne particles samples were obtained on treated quartz filters during five days of the General Motors (GM) Sulfate Dispersion Experiment and analyzed for total acidity, sulfuric acid, ammonium, soluble sulfate (two methods), total sulfur and nitrate. From the resultant data it is concluded that the immediate roadside impact from sulfate emissions by catalyst-equipped autos is of the order of 3-6  $\mu\text{g}/\text{m}^3$ , probably all in the form of sulfuric acid (in agreement with EPA and EPA contractor data). This particulate sulfuric acid emission is neutralized by ambient ammonia with a half-life of tens of seconds, the rate apparently dependent on the ambient ammonia concentration. Experimental examples of (a) sulfuric acid impact; (b) ammonia-neutralized sulfate impact; and (c) partially neutralized sulfate impact at 30 meters or 100 meters downwind from the roadway are cited.*

## INTRODUCTION

The GM Sulfate Dispersion Experiment conducted at the General Motors Proving Ground at Milford, Michigan during October 1975 was designed to elucidate the quantitative hazard from the sulfate emissions of catalytic converter-equipped automobiles under ambient roadside conditions. It provided for the participation, in addition to the GM Environmental Sciences staff, of two branches of EPA's Environmental Sciences Research Laboratory (ESRL) and their contractors, as well as independently supported groups such as Brookhaven National Laboratory

---

\*R. L. Tanner and L. Newman, Atmospheric Sciences Division, Department of Applied Science, Brookhaven National Laboratory, Associated Universities, Inc., Upton, New York 11973.



(BNL). The BNL experimental work consisted of the collection of one hour HiVol samples on treated quartz filters at two locations (2 meters and 100 meters east of the roadway) and comparison of the analytical results with those from a background sample (30 meters west of the roadway). In addition, low volume samples of ambient and diffusion-processed air (ref. 1) (single cut, 50% penetration diameter = 0.07 - 0.09  $\mu\text{m}$ ) were collected daily at one of the downwind locations.

### EXPERIMENTAL

Airborne particle samples were obtained by HiVol sampling of  $\text{H}_3\text{PO}_4$ -treated quartz fiber filters during the Sulfate Experiment on 10/6, 10/8, 10/10, 10/21, and 10/22 (days 279, 281, 283, 294, and 295, respectively), and analyzed for total acidity, sulfuric acid, ammonium, soluble sulfate (two methods), total sulfur, and nitrate as described below.

Titrateable acidity of all samples was determined by the Brosset method (ref. 2) employing Gran titration (ref. 3) and calculated as  $\mu\text{g}/\text{m}^3$  of  $\text{H}_2\text{SO}_4$ . A negative number indicates that part of the pH 4 leach solution was neutralized by the collected particulate sample. Ammonium was determined in all samples by an Autoanalyzer version of the indophenol colorimetric techniques (ref. 4). Soluble sulfate was determined by two methods: an Autoanalyzer turbidometric technique (ref. 5) (all samples); and the new flash volatilization-flame photometric detection (FVFPD) technique (ref. 6) (most samples). Total sulfur was determined in selected samples by reduction to  $\text{H}_2\text{S}$  with  $\text{HI}/\text{H}_3\text{PO}_3$ , conversion to  $\text{CdS}$  and radiochemical determination after metathesization to  $^{110}\text{Ag}_2\text{S}$  (ref. 7). Sulfuric acid was specifically analyzed by extraction of a portion of the filter with benzaldehyde (ref. 8), back leach into aqueous solution and determination as sulfate by the FVFPD method. Nitrate was determined by the hydrazine reduction-colorimetric method (ref. 9).

The summary of data from the five sampling days for which reasonably coherent sets of analyses were obtained is included as tables 1-5. Sample identification is by categories A-E: A indicates the mode of

Table 1. BNL Data for 10/6/75 Day 279 GM Sulfate Dispersion Experiment

Wind Direction = 250°      Wind Speed = 1.4 m/sec.

A	Sample Identification			E	Titratable		Ammonium $\mu\text{g}/\text{m}^3$	Turbidometric Sulfate $\mu\text{g}/\text{m}^3$	FVFPD Sulfate $\mu\text{g}/\text{m}^3$	Extracted $\text{H}_2\text{SO}_4$ $\mu\text{g}/\text{m}^3$
	B	C	D		Acidity $\mu\text{g}/\text{m}^3$ as $\text{H}_2\text{SO}_4$					
HV	30m up	(1m)		3 hr	-1.7		3.4	11.4	11	0.5
HV	2m down	(3m)	#1	1 hr	-3.1 <sup>a</sup>		3.0 <sup>a</sup>	19.7 <sup>a</sup>	22	2.5
HV	2m down	(3m)	#2	1 hr	-3.1		3.2	15.6	22	1.6
HV	100m down	(1m)	#1	1 hr	1.8		5.8	16.6	NA	1.6
HV	100m down	(1m)	#2	1 hr	0.3		4.7	15.0	E	2.2

<sup>a</sup>Value listed is mean of 2 determinations

Table 2. BNL Data for 10/8/75 Day 281 GM Sulfate Dispersion Experiment

Wind Direction = 60° Wind Speed = 1.7 m/sec.

Titratable										
Sample Identification				Acidity	Ammonium	Turbidometric		FVFPD	Extracted	Nitrate
A	B	C	D	E	g/m <sup>3</sup> as H <sub>2</sub> SO <sub>4</sub>	μg/ m <sup>3</sup>	Sulfate μg/m <sup>3</sup>	Sulfate μg/m <sup>3</sup>	H <sub>2</sub> SO <sub>4</sub> μg/m <sup>3</sup>	μg m <sup>3</sup>
HV	30m up	(1m)		3 hr	-1.0	2.87	12.6	15	0.46	7.8
HV	2m down	(3m)	#1	1 hr	L	L	L	L	L	L
HV	2m down	(3m)	#2	1 hr	-1.3	1.76	9.5	22	0	6.7
PDU	2m down	(2.5m)		2 hr	ca. 1.1	2.55	13.2	E	ND	9.4
PDU	2m down	(2.5m)		2 hr	ca. 1.6	1.37	6.4	E	ND	4.2
HV	100m down	(1m)	#1	1 hr	-2.2	2.32	10.9	E	NA	7.8
HV	100m down	(1m)	#2	1 hr	-1.9	2.56	12.5	21	0.48	7.7

Table 3. BNL Data for 10/10/75 Day 283 GM Sulfate Dispersion Experiment

Wind Direction = 240° Wind Speed = 1.3 m/sec.

Titratable						FVFPD	Extracted	Total S		
Sample Identification			Acidity	Ammonium	Turbidometric					
A	B	C	D	E	$\mu\text{g}/\text{m}^3$ as $\text{H}_2\text{SO}_4$	$\mu\text{g}/\text{m}^3$	$\text{H}_2\text{SO}_4$ $\mu\text{g}/\text{m}^3$	as sulfate $\mu\text{g}/\text{m}^3$		
HV	30m up	(1m)		3 hr	0.13	7.2	17.4	NA	0.8	15.5
HV	2m down	(1m)	#1	1 hr	-5.2	7.5	23.9	E	0.9	NA
HV	2m down	(1m)	#2	0.5 hr	L	L	L	L	L	L
HV	2m down	(1m)	#3	0.5 hr	-6.6	5.1	21.2	E	2.3	E
HV	100m down	(3m)	#1	1 hr	1.04	6.2	16.1	17	4.0	16.7
HV	100m down	(3m)	#2	1 hr	1.07	4.6	14.7	23	1.1	28
PQU	100m down	(2.5m)		2 hr	1.8	6.5	22	E	ND	ND
PQUB	100m down	(2.5m)		2 hr	0.5	4.8	12	E	ND	ND

Table 4. BNL Data for 10/21/75 Day 294 GM Sulfate Dispersion Experiment

Wind Experiment = 225° Wind Speed = 1.5 m/sec.

Sample Identification					Titratable		Total S				
A	B	C	D	E	Acidity μg/m <sup>3</sup> as H <sub>2</sub> SO <sub>4</sub>	Ammonium μg/m <sup>3</sup>	Turbidometric Sulfate μg/m <sup>3</sup>	FVFD Sulfate μg/m <sup>3</sup>	Extracted H <sub>2</sub> SO <sub>4</sub> μg/m <sup>3</sup>	as Sulfate μg/m <sup>3</sup>	Nitrate μg/m <sup>3</sup>
HV	30m up	(1m)		3 hr	-1.6	2.28	9.5	30	0	8.9	7.7
HV	2m down	(3m)	#1	1 hr	-2.8	2.02	11.9	NA	1.0	9.6	4.4
HV	2m down	(3m)	#2	1 hr	-4.2	3.25	13.9	11.0	0	12.8	4.7
HV	2m down	(3m)	#3	0.6 hr	-5.4	NA	14.3	E	0	NA	NA
HV	100m down	(1m)	#1	1 hr	-3.0	2.58	7.1	11.0	0	NA	5.8
HV	100m down	(1m)	#2	1 hr	-3.9	3.04	12.8	11.1	1.0	14.7	8.2
HV	100m down	(1m)	#3	0.6 hr	-3.4	2.54	10.1	9.2	0	NA	8.1

Table 5. BNL Data for 10/22/75 Day 295 GM Sulfate Dispersion Experiment

Wind Direction = 40° Wind Speed = 0.6 m/sec.

Titratable													
Sample Identification				Acidity	Ammonium		Turbidometric		Extracted	Total S		Nitrate	
A	B	C	D	E	$\mu\text{g}/\text{m}^3$ as $\text{H}_2\text{SO}_4$	$\frac{\mu\text{g}}{\text{m}^3}$	Sulfate $\mu\text{g}/\text{m}^3$	$\text{H}_2\text{SO}_4$ $\mu\text{g}/\text{m}^3$	As Sulfate $\mu\text{g}/\text{m}^3$			$\frac{\mu\text{g}}{\text{m}^3}$	
IV	30m up	(1m)		3 hr	-1.4	6.8	14.4	0.55	11.1	NA		NA	
HV	2m down	(3m)	#1	1 hr	-1.8	5.4	10.9	0	NA	13.6		13.6	
IV	2m down	(3m)	#2	1 hr	-3.8	4.5	11.1	0	12.9	14.7		14.7	
PQU	2m down	(2.5m)		2 hr	6.2	3.4	10.8	ND	ND	15.1		15.1	
PQDB	2m down	(2.5m)		2 hr	-1.4	3.3	E	ND	ND	12.8		12.8	
IV	100m down	(1m)	#1	1 hr	-2.3	3.6	7.3	0	NA	13.1		13.1	
HV	100m down	(1m)	#2	1 hr	-2.2	3.7	9.2	1.2	9.1	16.1		16.1	

sample collection, HV = Staplex HiVol sampling on 4 inches diameter circles of  $\text{H}_3\text{PO}_4$  - treated quartz; PQU = low volume sampling of untreated air; PQDB = low volume sampling of diffusion processed air, the latter two on 47 mm treated quartz circles. B indicates the location of filter vis-a-vis the track: 30m up corresponds to Tower 1 (GM designation), 2m down to Tower 4, and 100m down to Tower 8. C indicates the vertical distance in meters of the sampler from the ground (in parentheses). D indicates the number of the sample (in chronological order) when more than one sample was taken at a given location during an experimental run. E indicates the duration of the sampling in hours. The 30m upwind samples were always taken at Tower 1 from 0.5 hr before to 0.5 hr after the run; hence, for 10/8 and 10/22/75, when the winds were out of the eastern quadrant, the 30m upwind sample is actually downwind from the track. An example from Day 295 data table, line 3: a high volume sample was taken 2m east of the track at an elevation of 3m above ground during the second hour of the run.

All numerical values for chemical determinations are reported in units of  $\mu\text{g}/\text{m}^3$ . NA = data not yet available; ND = data which cannot be obtained from the sample collected due to experimental limitation; L = sample lost, no analyses performed; E = erroneous data obtained.

## RESULTS AND DISCUSSION

The information which we sought to obtain from these experiments was as follows. Comparison of total soluble sulfate by turbidimetry of FVFPD at the upwind and downwind sites would allow quantization of the increase in sulfate concentration due to auto emissions from the track. The results from this part of the experiments indicate an increase in sulfate at 2m downwind which varied from  $3.2 \mu\text{g}/\text{m}^3$  on 10/20 (data not tabulated) to  $6.2 \mu\text{g}/\text{m}^3$  on 10/6. During four simultaneously sampled days, data obtained by GM at the same location indicated an average of  $0.9 \mu\text{g}/\text{m}^3$  greater sulfate increase while during 2 of those days, EPA observed an equal sulfate increase.

Secondly, comparison of total sulfur concentrations at downwind sites versus background with soluble sulfate levels at the same sites would reveal whether all the increase in sulfur is ascribable to sulfate - presumably sulfuric acid and its neutralization products. The data show that the average difference between soluble sulfate by turbidimetry and total sulfur (as sulfate) for nine determinations at all sampling locations was  $1.8 \mu\text{g}/\text{m}^3$  and the difference in mean values by the 2 methods is 4%. Clearly the water-extracted sulfate and total sulfur methods are equivalent and the increase in sulfur is with high probability in the form of sulfate.

We compared data for total acidity and sulfuric acid by the specific benzaldehyde extraction-FVFPD method to determine if increases in acidity matched increases in sulfate at two downwind locations relative to background, and to see if the increased acidity was attributable to  $\text{H}_2\text{SO}_4$ . The acidity data obtained at 2m downwind of track were complicated by the presence of large, basic particles apparently generated by the vehicular traffic on the roadway and by the fact that background aerosol particles on four of six sampling days were basic, *i.e.*, neutralized part or all of the pH 4 leach solution. The increase in total acidity and sulfuric acid documented by the Brosset-Gran titration and benzaldehyde extraction - FVFPD methods, respectively, was comparable for samples taken 30m or 100m from the roadway: 100m from roadway, 10/6,  $\Delta(\text{Acidity}) = 2.8 \mu\text{g}/\text{m}^3$ ,  $\Delta(\text{H}_2\text{SO}_4) = 1.4$ ; 30 m from roadway, 10/22,  $\Delta(\text{Acidity}) = 0.8$ ,  $\Delta(\text{H}_2\text{SO}_4) = 0.55$ . The benzaldehyde extraction technique was superior to total acidity determinations for the roadside samples (2m down) although the observed  $\text{H}_2\text{SO}_4$  increase was 25% or less of the sulfate increase on a molar basis.

No influence of the roadway traffic on the ambient nitrate levels was observed.

Determinations of ammonium concentrations at downwind sites and background led to the following observations: No ammonium increases over background were observed at the roadside site (2m from track) except for a marginally significant increase on 10/22 when the NE



winds placed this site 2m upwind from the track. Significant ammonium increases were observed at downwind sites on 10/6 (100m) and 10/22 (30m) with marginally significant increases on 10/8 (30m) and 10/21 (100m). Furthermore, the ammonium increases appear to be positively correlated with the combination of "larger than average" sulfate increases and the ambient ammonia concentration.

Close examination of our data led to the identification of three sampling days which illustrate the apparent correlation outlined above. On sampling day 283 (10/10), a substantial increase in sulfate over background at the 2m down site was observed (BNL =  $5.2 \mu\text{g}/\text{m}^3$ , mean of BNL, GM, EPA data =  $6.1 \mu\text{g}/\text{m}^3$ ), but the ambient ammonia concentration was low (EPA: <2ppb  $\text{NH}_3$ ). No significant increase in ammonium at the 100m downwind site was observed, but there was a downwind increase in sulfate ( $1.2 \mu\text{g}/\text{m}^3$  by reduction- $^{110}\text{Ag}_2\text{S}$ ), acidity by Gran titration ( $1.0 \mu\text{g}/\text{m}^3$ ) and  $\text{H}_2\text{SO}_4$  by extraction ( $1.7 \mu\text{g}/\text{m}^3$ ). This indicates that on this day, the emitted sulfuric acid was being diluted, but not significantly neutralized, during transit of the first 100m from the roadway.

A different situation was observed on 10/21 when a moderate increase of  $4\text{--}5 \mu\text{g}/\text{m}^3$  of sulfate at 2m downwind was observed and an increase of 0.5 to 0.7 persisted at the 100m downwind site. No acidity increase and probably no  $\text{H}_2\text{SO}_4$  increase was observed at the latter site, but an increase in ammonium  $\geq$ , the molar amount needed to neutralize the increased sulfate was observed. Unfortunately, no ambient ammonia data are available for the 10/21 date, but we would estimate a value of 2-3 ppb to be sufficient for the observed  $\text{H}_2\text{SO}_4$ -particle neutralization effect.

A situation intermediate between those for 10/10 and 10/21 was observed on 10/6. A large increase in sulfate at the 2m downwind site was observed (BNL =  $6.2 \mu\text{g}/\text{m}^3$ ; mean of BNL, GM, EPA data =  $6.2 \mu\text{g}/\text{m}^3$ ) which, according to BNL data, persisted at the 100m downwind site ( $4.4 \mu\text{g}/\text{m}^3$ ). An increase in both acidity by Gran titration (2.8) and sulfuric acid by extraction (1.4) was observed at the latter location, but an increase in ammonium was also observed which,

when combined with the acid increase, more than accounts for the sulfate increase. It should be noted that a relatively high gaseous ammonia concentration of 3.3 ppb was measured by EPA during this experiment. It is tempting to conclude that the relatively high sulfate increase from  $\text{H}_2\text{SO}_4$  emissions was partially neutralized (ca. 70%) by ambient  $\text{NH}_3$  during passage from the roadway to the 100m downwind location.

Sufficient data to determine if ambient ammonia concentrations are significantly depleted and become the limiting reagent before the sulfate plume reaches the 100m downwind location are not available from BNL data. However, one may calculate a mean lifetime for emitted sulfuric acid particles under the conditions of the 10/6 experiment (increase in  $[\text{H}_2\text{SO}_4] = 1.4$  ppb, and ambient  $[\text{NH}_3] = 3.3$  ppb) based on the transit time from the roadway to the 100m downwind site:

Mean wind direction =  $250^\circ$

Mean wind speed = 1.31 m/sec

Mean distance upwind to roadway =  $\frac{100\text{m}}{\cos 20^\circ} = 106\text{m}$

Mean transit time to sampler =  $\frac{100\text{m}}{1.31\text{m/sec}} = 81 \text{ sec.}$

Mean  $\text{H}_2\text{SO}_4$  particle lifetime (assume 50% conversion and linear chemistry) = ca. 1 min.

The observation of partially or wholly ammonia-neutralized sulfuric acid at the 100m downwind site on some experimental days is not inconsistent with the observation by EPA of unneutralized  $\text{H}_2\text{SO}_4$  at the 15m down location. The methodology is insufficiently precise to exclude 10 or 20% neutralization at the latter location, and overall the agreement between BNL and EPA sulfate impact data is exceptionally good.

Additional data (acidity, sulfate, ammonium, nitrate) were obtained using low volume sampling of ambient and diffusion-processed air (ref. 1). The diffusion battery was arranged and operated at conditions giving 50% penetration for particles of diameter 0.07 -

0.09  $\mu\text{m}$ , e.g., above the expected size range of the emitted sulfuric acid, but lower than the size of most of the mass of ambient sulfate. The sampling rate for the diffusion battery configuration available was necessarily only about  $1\text{m}^3/\text{hr}$  and the sample size was thus insufficient to yield reliable data on the size distribution of the emitted acid sulfate. It should be noted that there is no inherent limit on sampling rate and that new diffusion batteries soon to be available in our laboratories will be able to give 4-cut size discrimination and chemical composition information at sampling rates to  $6\text{m}^3/\text{hr}$  on 47mm diameter filters.

### CONCLUSIONS

A. Sulfate emissions from the fleet of catalyst-equipped vehicles at the GM Sulfate Dispersion Experiment resulted in increased sulfate burdens of 3.2 to  $6.2\text{ }\mu\text{g}/\text{m}^3$  at the immediate roadside.

B. Comparison of total sulfur and sulfate data indicates that the auto emission of sulfur is in the form of sulfate.

C. Increases in total acidity and sulfuric acid concentrations downwind of the track strongly infer that the sulfate emission is in the form of sulfuric acid.

D. Ammonium increases downwind of the track, when coupled with acidity and  $\text{H}_2\text{SO}_4$  data, strongly indicate that the emitted sulfuric acid is neutralized by ammonia with a resultant mean half-life for sulfuric acid particles of on the order of tens of seconds. This lifetime is not unexpectedly dependent on the ambient ammonia concentration.

### REFERENCES

1. W. H. Marlow and R. L. Tanner "Aerosol size discrimination with determination of chemical composition by diffusion sampling," submitted to *Science*, December 1975.
2. C. Askne, C. Brossnet and M. Fermm Swedish Water and Air Pollution Research Laboratory, Bothenburg, Sweden, IVL Report B 157, August 1973; C. Askne and C. Brosset, *Atmos. Environ.* 6, 695 (1972).

3. G. Gran, *Analyst* (London), 77, 661 (1952).
4. W. T. Bolleter, C. J. Bushman and P. W. Tidwell "Ammonia in water and seawater," Industrial Method No. 154-71w/Tentative, Technicon Industrial Systems, Tarrytown, N. Y., February 1973, *Anal. Chem.* 33, 592 (1961).
5. Technicon Industrial Systems, *Sulfate Method VIb via Turbidimetry*, Tarrytown, N. Y., 1959.
6. J. D. Husar, R. B. Husar and P. K. Stubits, *Anal. Chem.* 47, 2062 (1975).
7. J. Forrest and L. Newman "Sampling and analysis of atmospheric sulfur compounds for isotope ratio studies," *Atmos. Environ.* 7, 561 (1973).
8. D. Leahy, R. Siegel, P. Klotz and L. Newman "The separation and characterization of sulfate aerosol," *Atmos. Environ.* 9, 219 (1975).
9. A modification of the method described in: J. B. Mullin, and J. P. Riley, *Anal. Chem. Acta* 12, 476 (1955).

#### ACKNOWLEDGMENT

Support by the Division of Biomedical and Environmental Research, ERDA is acknowledged. We thank R. Garber and W. Marlow for many helpful discussions and M. Phillips of our Analytical Group for performing the analyses.

**TECHNICAL REPORT DATA**  
(Please read Instructions on the reverse before completing)

1. REPORT NO. EPA-600/3-76-035		2.		3. RECIPIENT'S ACCESSION NO.	
4. TITLE AND SUBTITLE THE GENERAL MOTORS/ENVIRONMENTAL PROTECTION AGENCY SULFATE DISPERSION EXPERIMENT Selected EPA Research Papers				5. REPORT DATE April 1976	
				6. PERFORMING ORGANIZATION CODE	
7. AUTHOR(S) Edited by: R. K. Stevens, P. J. Lamothe, T. G. Dzubay W. E. Wilson and J. L. Durham				8. PERFORMING ORGANIZATION REPORT NO.	
9. PERFORMING ORGANIZATION NAME AND ADDRESS Environmental Sciences Research Laboratory Office of Research and Development U. S. Environmental Protection Agency Research Triangle Park, North Carolina 27711				10. PROGRAM ELEMENT NO. 1AA601	
				11. CONTRACT/GRANT NO.	
12. SPONSORING AGENCY NAME AND ADDRESS Environmental Sciences Research Laboratory Office of Research and Development U. S. Environmental Protection Agency Research Triangle Park, North Carolina 27711				13. TYPE OF REPORT AND PERIOD COVERED In-house	
				14. SPONSORING AGENCY CODE EPA-ORD	
15. SUPPLEMENTARY NOTES					
16. ABSTRACT  In the fall of 1975, General Motors conducted an extensive field experiment at the GM proving grounds in Milford, Michigan. The purpose of the experiment was to measure the concentrations and assess characteristics of aerosols, especially sulfates and sulfuric acid, emitted by a fleet of catalyst-equipped cars operated under simulated freeway conditions. In addition, emissions dispersion and meteorological parameters were measured; this data served as input for developing a plume dispersion model.  At the invitation of General Motors, EPA, along with their contractors and grantees, participated in this experiment. This report consists of several important research papers that discuss and present the results of studies carried out by EPA during the GM experiment.					
17. KEY WORDS AND DOCUMENT ANALYSIS					
a. DESCRIPTORS		b. IDENTIFIERS/OPEN ENDED TERMS		c. COSATI Field/Group	
*Air pollution Field tests *Automobiles *Catalytic converters *Exhaust emissions *Aerosols		particles *sulfates *sulfuric acid ammonia atmospheric diffusion models		13 B 14 B 13 F 07 A 07 D 07 B 04 A	
18. DISTRIBUTION STATEMENT  RELEASE TO PUBLIC		19. SECURITY CLASS (This Report) UNCLASSIFIED		21. NO. OF PAGES 149	
		20. SECURITY CLASS (This page) UNCLASSIFIED		22. PRICE	